

Identification of Potential Biomarkers for Depressive Disorders

Dissertation

zur

Erlangung des Doktorgrades (Dr. rer. nat.)

der

Mathematisch-Naturwissenschaftlichen Fakultät

der

Rheinischen Friedrich-Wilhelms-Universität Bonn

vorgelegt von

Jörg Breinfeld

aus Karl-Marx-Stadt

Bonn 2017

Angefertigt mit Genehmigung der Mathematisch-Naturwissenschaftlichen Fakultät der Rheinischen
Friedrich-Wilhelms-Universität Bonn

Tag der Promotion:

Erstgutachter: Prof. Julia Stingl

Zweitgutachter: Prof. Klaus Mohr

Erscheinungsjahr: 2017

Die vorliegende Arbeit wurde in der Forschungsabteilung des Bundesinstitutes für Arzneimittel und Medizinprodukte (BfArM) unter Leitung von Frau Prof. Dr. Julia Stingl angefertigt.

Diese Dissertation ist auf dem Hochschulschriftenserver der ULB Bonn http://hss.ulb.uni-bonn.de/diss_online elektronisch publiziert.

“Eureka!”

Archimedes von Syrakus

Table of Contents

Chapter I - Introduction	1
1. Pharmacogenomics and Personalized Medicine	1
2. Depressive Disorders	2
2.1. Pathogenesis.....	2
2.2. Diagnosis and Prognosis	3
2.3. Treatment	4
2.3.1. Antidepressant Response Biomarkers.....	6
3. Drug- and Disease-induced Depressions	7
4. Personalized Medicine of Depressive Disorders - Novel Approaches.....	9
4.1. Cell Based Approaches	9
4.2. Neuroimaging Approaches	9
Chapter II - Aims of the Project.....	11
Chapter III - Material and Methods.....	13
1. Cell-based Methods.....	13
1.1. Human Lymphoblastoid Cell Lines.....	13
1.1.1. Origin and Patient's Characteristics	13
1.1.2. Generation.....	14
1.1.3. Mycoplasma Testing.....	15
1.1.4. Cryopreservation	15
1.1.5. Cell Counting.....	16
1.1.6. Cultivation.....	16
1.1.7. Treatment with Antidepressants.....	16
1.2. Determination of Proliferation Rates	17
1.3. Gene Expression Analyses	19
1.3.1. RNA extraction.....	19
1.3.2. Synthesis of Complementary DNA	19

1.3.3.	Primer Design and Validation	19
1.3.4.	Quantitative Real-Time Polymerase Chain Reaction	20
1.3.5.	Determination of RNA quality	21
1.3.6.	Genome-wide Gene Expression Profiling	22
1.4.	Statistical Analysis.....	24
2.	Neuroimaging	25
2.1.	Clinical Study Design	25
2.1.1.	Overview	25
2.1.2.	Participants	25
2.1.3.	Investigational Medicinal Product	26
2.1.4.	Psychiatric Evaluation	26
2.2.	Magnetic Resonance Imaging	27
2.2.1.	Functional Principle	27
2.2.2.	Paradigms	27
2.2.3.	Data Acquisition.....	29
2.2.4.	Data Analysis.....	30
3.	Software.....	31

Chapter IV - Results.....32

1.	Identification of Potential Gene Expression Biomarkers for Antidepressant Response	32
1.1.	Results from the MARS Cohort.....	32
1.1.1.	Screening Experiments	32
1.1.2.	Proliferation Phenotyping.....	35
1.1.3.	Identification of Potential Gene Expression Markers.....	40
1.2.	Results from the STAR*D Cohort.....	52
1.2.1.	Proliferation Phenotyping.....	52
1.2.2.	Gene Expression Analyses of Candidate Genes.....	58
2.	Neuroimaging of Interferon-induced Depressive-like Behavior.....	60
2.1.	Psychometric Testing	61
2.2.	Functional Magnetic Resonance Imaging	63
2.2.1.	Foraging	63
2.2.2.	Faces	67

Chapter V - Discussion	69
1. Previous Findings from MARS and STAR*D	69
2. Lymphoblastoid Cell Lines in Pharmacogenomical Research.....	70
3. Peripheral Proliferation as Surrogate Marker for Antidepressant Response.....	72
4. Microarray-based Identification of Tentative Gene Expression Biomarkers	76
4.1. Role of EGF Signaling in Depression	77
4.2. Role of WNT Signaling in Depression	77
4.3. Role of Drug Metabolizing Enzymes in Depression	78
4.4. Role of Drug Transporters in Depression	79
5. Validation of Tentative Gene Expression Biomarkers	80
6. Interferon beta, Sickness Behavior and Depression.....	81
7. Functional Neuroimaging	84
7.1. Responses to Emotional Faces after Interferon Administration	84
7.2. Responses to Monetary Reward after Interferon Administration	86
8. Outlook / Future Perspectives.....	87
Chapter VI - Summary	90
Abbreviations	93
List of Figures	98
List of Tables	100
References	101
Appendix	139
List of Publications	144
Curriculum Vitae	146
Acknowledgements.....	147

Chapter I - Introduction

1. Pharmacogenomics and Personalized Medicine

As long ago as 1959, the German pediatrician Friedrich Vogel suspected our genes being responsible for the individual effects of drugs and coined the term of pharmacogenetics ¹. Previously, there was no logical explanation to the observation that some people benefit from a pharmacotherapy while others do not. Researchers advanced the field by extending our knowledge about pharmacological processes influencing individual drug effects: Between-patient differences in genes involved in pharmacodynamics (*e.g.* drug targets) or pharmacokinetics (*e.g.* drug metabolizing enzymes, drug transporters) might explain the observed individuality in drug efficacy and drug safety. With the deciphering of the human deoxyribonucleic acid (DNA) sequence and the development of genetic high-throughput methods, pharmacogenetics transformed more and more to pharmacogenomics where the interaction between single drugs and the whole genome is in the focus of attention. The results of the human genome project - which finished in 2001 - led to a rapid development of the new research area of pharmacogenomics ². Since then, the most astonishing progress was done in the field of oncology where many new experimental results found their application in clinical routine (*e.g.* cobas[®] epidermal growth factor receptor (EGFR) mutation test kit ³). Recently, the therapy individualization of other indications like mental disorders became a greater focus of attention and it is widely assumed that personalized medicine - consisting of diagnosis and therapy based on individual environmental, phenotypic and genetic requirements - will be the future of psychiatric medical practice ⁴.

2. Depressive Disorders

Depressive disorders are well-known since the times of the ancient Greeks - then named melancholia - and was attributed to an imbalance of the basic bodily fluids (blood, phlegm, yellow and black bile) ⁵. In modern times, according to the Diagnostic and Statistical Manual of Mental Disorders (DSM-5), depression is defined by sad mood, loss of interest, appetite and concentration, sleep disturbances, fatigue, irritability, negative self-image and suicidal ideation ⁶. This group of diseases is characterized by a neurobiological pathology of the monoaminergic system, over-reactivity of the hypothalamic-pituitary-adrenal (HPA) axis, dysfunction of amygdala and hippocampus and decreased levels of BDNF ⁷. Depressive disorders belong to the most prevalent mental illnesses in the world affecting over 350 million people with resulting deaths by suicide of approximately one million people per year ⁸. Furthermore, recent analyses predict that depressive disorders will account for the largest part of the economic burden within the next 20 years ⁹. The heritability for depression is reported at up to 40% and an early onset, presence of psychosis as well as a high degree of recurrence seem to be at least partially heritable ^{10,11}. However, the mode of inheritance is complex with multiple gene sets being involved and it is further complicated by the impact of environmental factors ^{12, 13}. The connection between candidate genes and depressions has been analyzed recently ¹⁴, but so far no genetic alterations that specifically lead to the development of depressions have been identified ¹⁵.

2.1. Pathogenesis

Even after decades of intensive research efforts the complex pathology of depressions still remains not completely understood. However, the previous investigations led to different theories that explain single aspects of the pathogenesis of depressions. The chemical hypothesis states there is an imbalance of mood-regulating neurotransmitters - especially serotonin, noradrenaline and dopamine - within the brain due to an increased clearance of these neurotransmitters from the synaptic cleft. The decreased activity of these neurotransmitters at the key sites in the brain is believed to be one of the leading causes of depressions. This was supported by the fact that the majority of antidepressant drugs are known to modify the neurotransmitter levels within the synaptic cleft (see chapter 2.3). Another hypothesis - the so called neurotrophic hypothesis - implies there are restructuring processes within the brain: Depressive patients show a volumetric decrease in mood-associated brain parts accompanied by a loss of activity ¹⁶. The most affected areas are the cortex (prefrontal and orbitofrontal), the amygdala and the hippocampus ¹⁷ amongst others such as the ventral striatum or the subgenual and anterior cingulate cortex ¹⁶. All these brain

parts obtain a role in depression-related functions like processing of emotions and feelings, reward system, mood control as well as anxiety, stress and fear reactions.

Based on the fact that women are more affected than men ^{18, 19}, the hormone-based hypothesis emerged as well. Changes in levels of corticotropin-releasing hormone (CRH), cortisol and estrogen were associated with a higher risk of depression ²⁰ and symptomatic improvement due to antidepressants therapy is more effective after restoration of these hormones ²¹. At least partially, depressions seem to be caused by a chronic hyperactivity of the HPA axis leading to various neuro-endocrine responses. Further investigations identified pro-inflammatory cytokines as potential mediators for depression (immunological hypothesis). Immune responses and neurodegeneration are tightly connected ²² and for instance higher concentrations of interleukin 6 and tumor necrosis factor (TNF) alpha were found in blood of depressed patients relative to healthy controls ²³. Inflammation increasing factors such as obesity or smoking have been linked to depression as well ²⁴. Probably, cytokine effects in combination with a maladaptation to immune responses may lead to a chronification of symptoms of sickness behavior and therefore to depressions ²⁵. Some of these hypotheses may partially overlap and still none of the mentioned hypotheses alone is able to fully cover the ontology of the complex disease of depression.

2.2. Diagnosis and Prognosis

In Germany, approximately twelve percent of the patients visiting a general practitioner suffer from depressive disorders and in approximately 25% of these cases no proper diagnosis is made ²⁶. One reason for this is a variety of unspecific, co-occurring side symptoms (*e.g.* insomnia, weight changes, lack of concentration, libido disorder or pain). Furthermore, the differential diagnosis remains difficult and the method of choice to detect depressions is the usage of depression-specific questionnaires like Hamilton Depression Rating Scale (HDRS) or Beck Depression Inventory (BDI) ²⁷, ²⁸. These questionnaires assign diagnosis based on symptoms of patient behavior (*e.g.* mood, feelings of guilt, suicide ideation, insomnia, *etc.*) interpreted by the physician or the patient itself. The disadvantages of the mentioned questionnaire based diagnostic systems are their inaccuracy and subjectivity. There are no objective, diagnostic biomarkers available to reliably predict the individual risk of the development of a depression. However, a serum based diagnostic laboratory test (MDDScore, Ridge Diagnostics) - based on activation of the HPA axis, metabolic, inflammatory and neurochemical pathways - was launched recently and is now commercially available but not yet well established and proven as a significant improvement in clinical practice ²⁹. Although this is the first step to an objectification of diagnosis of depressive disorders, depression-specific questionnaires are still the methods of choice to detect depressions and to evaluate the progress of an antidepressant therapy.

Another promising and innovative approach is radiologic imaging of the brain because it has the potential to identify markers associated with underlying pathophysiologic processes in psychiatric disorders³⁰. According to recent research it could be able to support the differential diagnosis between Alzheimer's disease and depression in elderly people³¹. Similar applications are conceivable to distinguish unipolar from bipolar depression or schizophrenia from depression and particular research efforts are done³²⁻³⁴. Furthermore, individuals at high risk for depression and patients with chronic treatment-resistant depression have been reported with lower cortical thickness³⁵ and increased resting cerebral blood flow (CBF) in the medial prefrontal regions³⁶, respectively. Such parameters might become eventually useful as diagnostic or prognostic biomarkers in the future. In clinical practice depressive inpatients usually receive magnetic resonance imaging (MRI) measurements during the course of the disease³⁷. This is routinely performed to exclude cancerous, inflammatory, vascular or degenerative processes, but can be easily expanded to the mentioned applications. Such neuropsychological MRI measurements basically seem suitable as biomarkers for diagnosis of depression and however, will probably hardly replace the established rating scales, but might be useful as supplementary method to objectify and improve the diagnosis of depressions (see also chapter 4.2).

2.3. Treatment

The first two specific antidepressive drugs were the tricyclic antidepressant (TCA) imipramine and the monoamine oxidase (MAO) inhibitor iproniazid which were both discovered in the 1950s over the search of new antischizophrenic and antitubercotic drugs, respectively³⁸. Pharmacodynamic studies revealed that TCAs reduce the presynaptic reuptake of neurotransmitters (*e.g.* serotonin, dopamine, acetylcholine, histamine, *etc.*) while MAO inhibitors (MAOI) reduce the degradation of monoamine neurotransmitters. During the following decades these groups were further developed which led to various similar antidepressants such as chlorpromazine or chlordiazepoxide and extended treatment opportunities. Only with the introduction of fluoxetine in 1987 the next crucial milestone of antidepressant drug development was achieved. Fluoxetine is the lead substance of the innovative drug family of selective neurotransmitter reuptake inhibitors that - in comparison to TCAs - excel by a superior side effect profile. Nowadays, these selectively acting drugs have largely replaced TCAs and MAOIs as the drug class of choice in the treatment of depressions due to a higher specificity, tolerability, safety and convenience³⁹. Selective serotonin reuptake inhibitors (SSRI) usually are considered the first-line drugs, although other selective neurotransmitter reuptake inhibitors such as serotonin-norepinephrine reuptake inhibitors (SNRIs) or noradrenergic and specific serotonergic antidepressants (NaSSAs) are available. An overview on the most important antidepressant drug classes including some representatives and their proposed

mechanism of action is given in Table 1. Typical side effects of antidepressants are weight changes, insomnia, increased suicidal risk, libido loss and erectile dysfunction.

Table 1: Overview on antidepressant drug classes.

class	lead drugs	proposed mechanism of action
TCA	Amitriptyline	inhibition of transporters for serotonin and norepinephrine
	Imipramine	modulation of serotonergic, adrenergic, glutamatergic, cholinergic and histaminic receptors
	Nortriptyline	
MAOI	Selegiline	inhibition of monoamine oxidase
SSRI	Citalopram	inhibition of serotonin reuptake transporters
	Fluoxetine	
SNRI	Venlafaxine	inhibition serotonin and norepinephrine reuptake transporters
NaSSA	Mirtazapine	modulation of adrenergic and serotonergic receptors
NRIs	Reboxetine	inhibition of norepinephrine reuptake transporters

TCA - tricyclic antidepressants, TeCAs - tetracyclic antidepressants, MAOI - monoamine oxidase inhibitors, SSRI - selective serotonin reuptake inhibitors, SNRI - Serotonin-norepinephrine reuptake inhibitors, NaSSA - noradrenergic and specific serotonergic antidepressant, NRIs - norepinephrine reuptake inhibitors

Although there are several mechanisms of action, all antidepressive drugs are believed to modify neurotransmitter levels by one means or another. However, this does not explain the delay in clinical improvement which is observed three weeks at the earliest after beginning of an antidepressant therapy because the pharmacological modulation of neurotransmitter systems occurs rapidly within a few hours. Thus, this mechanism might be only an initial event of antidepressant effects followed by a series of intraneuronal events such as changes in neural gene expression, functional adaptation, neurotrophic processes and synaptogenesis. Effective antidepressant treatments seem to normalize the structural and functional abnormalities found in the brains of depressive patients^{40, 41}. For instance, chronic treatment with antidepressants leads to an increased proliferation in the hippocampus⁴² and mood stabilizers such as valproate or lithium are thought to increase proliferation and survival of hippocampal neurons^{43, 44}. Interestingly, electroconvulsive therapy^{1 45, 46} also increases hippocampal neurogenesis⁴⁷. Thus, neural proliferation and neuroplasticity modulated by antidepressive therapy probably leading to a reversal of hippocampal atrophy^{48, 49}. Further, the treatment of patients with smaller hippocampi is

¹ Electroconvulsive therapy is an alternative approach for the last-line treatment of depression where seizures are electrically applied to the brain. The efficacy is comparable to antidepressants but it requires comedication with anesthetics and muscle relaxants as well as expensive device, and may have adverse effects like confusion and memory loss.

prolonged over weeks⁵⁰. One of the key players in this proliferative action seems to be the brain-derived neurotrophic factor (BDNF) whose gene expression is significantly upregulated in the hippocampi of animals treated with antidepressant drugs such as citalopram or imipramine^{51, 52}.

2.3.1. Antidepressant Response Biomarkers

The latest S3 guideline for unipolar depression lists ten drug classes with 27 antidepressants (including more than 3,000 licensed medications in varying dosage, administration ways, technological modifications, different producers *etc.*) that are recommended for the treatment of moderate and severe forms of depressions⁵³. Despite (or because of) the given variety of antidepressive drugs the individual therapy success is still in need of improvement due to low response rates. Up to 50% of patients show no adequate improvement in their clinical state after treatment with first-line antidepressant medication⁵⁴. An early symptomatic evaluation of individual therapy success is complicated by a delay in clinical improvement of several weeks up to months and the applicability of biomarkers in psychiatry is still in its infancy^{55, 56}. Approximately a third of the initial non-responders to antidepressant drugs will achieve remission over the following course of the treatment regimen (without switch of medication)⁵⁷. During this period of non-response the compliance might decrease and the clinical conditions could decline which also may cause an increase in suicidal risk. To improve the treatment efficacy pre-therapeutic knowledge about the expected clinical success would be highly beneficial. However, so far it is impossible to predict the individual treatment outcome of depressive patients due to a lack of predictive biomarkers and convincing pharmacogenomical studies (*e.g.* reviewed by Narasimhan & Lohoff⁵⁸). The main reason for this lack might be the high heterogeneity of psychiatric diseases and the complexity of the CNS aggravating the study of the underlying mechanism of individual therapy effects as well as a lack of basic knowledge due to the absence of adequate animal models. On this account, both choice and dosage of antidepressant drugs is still dependent on trial and error prescription and are routinely administered by clinical knowledge of the particular physician⁵⁹.

3. Drug- and Disease-induced Depressions

Depressions frequently occur as concomitant diseases in a variety of psychological and non-psychological disorders. A higher prevalence of depression was observed in patients suffering from chronic inflammation like cardiovascular diseases, type 2 diabetes or rheumatoid arthritis^{60, 61} and for instance, the prevalence of depression in patients with coronary heart disease is three times higher compared to the general population⁶². In addition, levels of inflammatory blood markers such as cytokines, chemokines or acute phase proteins are increased in patients with severe depression inferring a relationship between inflammation (*i.e.* immune system activation) and depression^{23, 63-65}. According to Dantzer *et al.* inflammation might increase the risk to developing depression more than the traditional psychosocial factors (*e.g.* negative life events, chronic stress or lack of social contacts)²⁵.

Depressions belong to the most important psychiatric comorbid conditions in neurological disorders like multiple sclerosis (MS)⁶⁶ which accompanies with a decrease in quality of life and an increase in disability⁶⁷. In comparison to other chronic, non-neurological diseases, depressions have a higher incidence in MS⁶⁸⁻⁷⁰ and the highest rate beneath other neurological diseases like epilepsy or amyotrophic lateral sclerosis⁷¹. Depressions occur in approximately 30% of patients with MS in an early phase of disease progression^{72, 73} and the more severe the MS the higher the likelihood of depressiveness⁷⁴. Therefore it is recommended to screen MS patients for depression during follow-up visits^{75, 76}. MS and depressive disorders share elevated serum concentrations of cytokines and decreased hippocampal volumes^{77, 78}. Additionally, depressed MS patients show greater atrophy of anterior temporal regions and more hyperintense lesions in medial frontal regions⁷⁹. The diagnosis of depression in MS is challenging due to overlapping symptoms (*e.g.* fatigue, insomnia, altered appetite, cognitive dysfunction, memory and concentration impairment)⁸⁰ and therefore, depression frequently remains undiagnosed and untreated⁸¹. Based on the rate of depression in MS, numerous suicides are recorded in MS patients^{82, 83}, with a 7.5 higher risk compared to the healthy population⁸⁴. MS is the most common autoimmune disorder affecting the central nervous system (CNS) and the most common progressive disorder of young adulthood⁸⁵. It is characterized by chronic inflammations of the brain resulting in axon demyelination and breakdown of the blood-brain-barrier (BBB) causing the typical symptoms (*e.g.* ataxia, tremor, nystagmus *etc.*). Neurochemical, structural and immunological aberrations seem to have a fundamental impact on the pathogenesis of depression in MS, although the underlying mechanisms remain controversial and seem to be a multifactorial response to this chronic progressive disease⁸⁶. One hypothesis implies humoral responses to inflammation or stress being responsible for the development of sickness behavior which in turn might become chronic and therefore abets the pathogenesis of depression²⁵. Psychosocial reasons based on stress reactions to diagnosis,

uncertain prognosis, impending disability and missing social support are known to further worsen the depressive symptoms in MS⁸⁷. The most commonly used disease-modifying drugs are interferon beta, glatiramer acetate, mitoxantrone, natalizumab, fingolimod and dimethyl fumarate with a high variability in treatment response⁸⁸. Interferons are able to decelerate the progression of disability and to reduce the rate of MS relapses^{89,90} through immunomodulatory their properties⁹¹. Unfortunately, interferons are also reported to be able to induce depression and depression-like behavior: Treatment with interferon alpha leads to depression in approximately a third of patients⁹²⁻⁹⁵ while interferon beta is also thought to be causative for depressive side effects with varying occurrence rates⁹⁶⁻⁹⁹. These symptoms might be based on effects on serotonergic pathways because they can be prevented by pretreatment with SSRIs¹⁰⁰ and patients with genetic serotonin transporter (SERT) variants are more likely to develop a depression during interferon administration^{101,102}. However, drug-induced depression is not limited to a particular group of drugs, but has been associated with cardiovascular agents, anti-infectives, CNS drugs, dermatologic agents, hormonal treatments and chemotherapeutic drugs^{103, 104}. Some possible molecular mechanisms are postulated in the literature suggesting an impaired functionality of neurotransmitter systems - especially norepinephrine, dopamine, serotonin and gamma-aminobutyric acid - as a consequence of drug intake¹⁰⁵. For instance, a decrease of blood tryptophan (a serotonin precursor) levels was reported due to an immunotherapy-induced activation of the tryptophan metabolizing enzymes tryptophan 2,3-dioxygenase and indoleamine-pyrrole 2,3-dioxygenase^{106, 107}. Hence, depressions might also be induced by drugs targeting the immune system whereby patients with physiological (*e.g.* over-reactive HPA)¹⁰⁸ or psychological (*e.g.* higher depressiveness scores before initial therapy with drug-inducing agents) risk factors are more likely to develop severe depressions¹⁰⁹. Furthermore, isotretinoin - a drug used for the treatment of cystic and therapy resistant acne - is suspected to induce depressions^{110, 111} as well as the anticonvulsant primidone¹¹² and in general, corticosteroids¹¹³ and oral contraceptives¹¹⁴. Summarizing, drug-induced depression is a frequently observed phenomenon - including a variety of different drug classes and indications - which has an extensive impact on therapy compliance, individual well-being and the economics of the health care system. A better understanding of the mechanism behind drug-induced depressions is required.

4. Personalized Medicine of Depressive Disorders - Novel Approaches

4.1. Cell Based Approaches

Recent research focuses on integrating latest neurobiological findings of depressions to help guiding individual treatment more efficiently and the search for genetic biomarkers predicting individual clinical response has become the main focus of biomedical research in the area of psychiatric diseases. Numerous studies have investigated genetic characteristics such as mutations or SNPs (single nucleotide polymorphisms) for associations with antidepressant drug response, but the majority of the outcomes missed replication or even showed opposite results in subsequent studies^{58, 115}. For that reason, other approaches away from simple DNA characteristics towards RNA or protein properties are needed to study the individual clinical response to antidepressants, *i.e.* focusing on the more complex inter-individual variability in gene expression¹¹⁶. One promising approach is the usage of lymphoblastoid cell lines (LCLs) to study individual antidepressant drug effects on gene expression under well-controlled, laboratory conditions. This was recently employed by several working groups¹¹⁷⁻¹¹⁹ and further, will be within the devoted attention of the present work. LCLs are B-lymphocytes immortalized by Epstein-Barr-virus (EBV) transformation and due to their broad availability and potency to reflect individual patient's features they are promising models in biomarker research in psychiatry. More than 4,100 brain transcripts are expressed in blood cells and gene expression between B-lymphocytes and LCLs is strongly correlated within same individuals¹²⁰. This and the fact that LCLs express more than 50% of all human genes in general make them suitable models to study antidepressant-induced changes in gene expression.

4.2. Neuroimaging Approaches

As already stated in chapter 2.2, radiologic imaging of the brain has the potential to identify markers associated with underlying pathophysiologic processes in psychiatric disorders and MRI measurements probably will be useful tools to detect diagnostic or prognostic biomarkers in the future. MRI is a non-invasive imaging technique used for a wide range of medical applications like diagnosis of diseases or injuries (*e.g.* neurological cancers, joint diseases) as well as for medical research. In contrast to X-ray computed tomography, the main advantage of MRI is the absence of ionizing, mutagenic radiation. In the past, the primary aim of MRI in psychiatry was to measure neural correlates of mental disorders in order to identify changes in locations and magnitudes of neuronal structure and function under pathological conditions. Nowadays, neuroimaging focusses on the application of these parameters as biomarkers to support diagnosis, assess potential risk

factors and to predict the efficacy of psychotropic drugs ¹²¹. By improving our understanding of individual pathogenic mechanisms of neuronal diseases, MRI allows the development of new drug therapies and potentially provides high sensitive measurements of treatment response in genetically defined cohorts ¹²².

We differ between two main types of MRI: structural imaging (sMRI) and functional imaging (fMRI). Structural and functional alterations in the brain are strongly connected in psychiatric disorders and hence, fMRI is a promising neuroimaging tool to analyze neural activity associated with psychotropic drug effects like attention, emotional processing or reward-related reactions ^{123, 124}. Thus, fMRI provides additional neuroimaging phenotypes for pharmacogenomical research. The advantages of fMRI perfusion imaging are its quantifiable results and the high level of repeatability rendering it a powerful tool to visualize drug effects in clinical studies ¹²⁵. Changes in CBF and therefore in neural activity during psychological tasks and processes can be visualized. Consequently, specific brain structures can be addressed depending on the chosen paradigm ¹²⁶. To date, there are only a few neuroimaging studies available investigating the impact of the relationship between cerebral properties and genetics on psychiatric treatment. However, the impact of MRI to our knowledge acquisition regarding psychiatric diseases has been huge in the past decades and so it is not surprising that many of the described abnormalities of the depressed brain (see chapter 2.1) are based on findings from MRI studies. Further, manifold results support the applicability of MRI measurements in the context of personalized medicine of depressive disorders, especially in the field of diagnosis and monitoring depressions ¹²⁷. The main challenge is to transfer the findings from clinical research into clinical practice. Therefore, it is required to better understand the individual variability of functional brain level connectivity underlying depressive disorders by MRI methods in order to improve the personalized medicine approach of depressive disorders.

Chapter II - Aims of the Project

Since the mechanisms and molecular backgrounds of the high individual variability of depressive disorders and the particular treatment efficacy has not been sufficiently understood so far, we focus on the identification of potential biomarkers by application of different approaches - cell based (I) and neuroimaging based (II) - to further advance the field of personalized medicine of depressive disorders.

(I) The current therapy success of depressive disorders remains in need of improvement due to low response rates and a delay in symptomatic improvement. Whereas depressions are associated with decreased hippocampal neurogenesis, antidepressant treatments seem to have the opposite action. They stimulate cell proliferation as well as the survival and maturation of neurons and therefore, modulate neuroplasticity. A link between hippocampal neurogenesis and the therapeutic action of antidepressants was suggested based on animal studies ¹²⁸. It is hypothesized that irreconcilable hippocampal neurogenesis deficits cause non-response to antidepressant therapy ¹²⁹. Thus, a connection between hippocampal neurogenesis (*i.e.* neuronal proliferation) and individual clinical effectiveness of antidepressants in patients suffering from depressive disorders is proposed ¹³⁰. Here, we want to study the effects of antidepressants on cellular proliferation rates by usage of human LCLs derived from depressed patients as model systems. The main focus of this project is to investigate the relationship between individual clinical response and the peripheral, antidepressant-modulated proliferation in patient-derived LCLs. Further, we are aiming at the identification of tentative neuroplasticity-associated gene expression biomarkers for the treatment individualization of depressive disorders. To this end a hypothesis-free approach using genome-wide gene expression profiling helps us to further improve our understanding on the individuality of antidepressant effects on both a molecular and a genetic level as well as of the underlying mechanisms of action of antidepressants.

(II) In a clinical study we focus on the affective side effects of the cytokine interferon beta which is a potent drug for the treatment of MS. Interferons are widely suspected to trigger depression-like behavior after long-term administration: Approximately one third of patients treated with interferon alpha develops symptoms of depressions ⁹². Similar effects of interferon beta were reported ¹³¹, but are not well researched until now. The neurobiological correlates and pathogenic

mechanisms of these affective symptoms remain unknown. One open issue concerns the mechanisms at system level through which interferon may produce psychological symptoms because it is unclear whether these symptoms arise from interferon beta treatment itself or as a side symptom from the progressing disease of MS. In the absence of clinical studies in healthy cohorts, the roles of interferon medication and those of the underlying diseases cannot be distinguished¹³². Here, we want to identify evidence for the depression-inducing effect of the cytokine interferon beta by psychometric testing and by measuring changes of brain activation patterns in depression-related brain areas. To this end, we will investigate interferon beta mediated change in brief functional neuroimaging probes of emotional function such as amygdala reactivity on viewing emotionally arousing stimuli¹³³ or neural correlates of reward anticipation¹³⁴. These two aspects of information processing were chosen as representative of well-known, important features of depressive functioning: lack of sensitivity to reward (anhedonic symptoms)¹³⁵ and hyperreactivity to negative emotional stimuli¹³⁶. The functional imaging aims at assessing change in intermediate phenotypes related to interferon beta mediated psychotropic side effects and so this study will help to clarify if typical neural correlates of depressive mood are detectable in individuals receiving interferon beta treatment.

Chapter III - Material and Methods

1. Cell-based Methods

A register of the used lab equipment, disposables, chemicals, solutions, media and kits including the names of the manufacturers and their particular office is listed in the Supplement (pp. 139).

1.1. Human Lymphoblastoid Cell Lines

1.1.1. Origin and Patient's Characteristics

LCLs were derived from two different antidepressant studies: the Munich Antidepressant Response Signature (MARS) project and the Sequenced Treatment Alternatives to Relieve Depression (STAR*D) study. The studies were approved by respective Ethical Committees. Participating patients gave verbal and written informed consent to provide biomaterial for the study of antidepressant response biomarkers also including transformation of blood lymphocytes into cell lines. An overview on the study population used in the presented work is given in Table 2. Complete patient's characteristics and drug profiles are listed in the Supplement (pp. 142).

Table 2: Characteristics of the MARS and STAR*D LCL study cohort.

		MARS			STAR*D		
		total	NR	R	total	NR	R
gender	male	24	10	14	24	14	10
	female	26	15	11	26	11	15
age	years	49.9 ± 11.8	51.6 ± 11.4	48.3 ± 12.2	48.5 ± 11.8	48.8 ± 9.5	48.3 ± 13.9
depression scale*	initial	27.0 ± 7.4	25.5 ± 8.2	28.6 ± 6.3	17.9 ± 3.2	18.9 ± 3.1	16.9 ± 3.0
	final	11.8 ± 8.7	18.7 ± 5.1	4.8 ± 5.0	9.0 ± 7.2	15.5 ± 3.9	2.6 ± 1.9
different antidepressants	number	4.0 ± 1.6	2.3 ± 0.9	1.6 ± 0.6	1.0 ± 0.0	1.0 ± 0.0	1.0 ± 0.0

* MARS: Hamilton Depression Rating Scale; STAR*D: Quick Inventory of Depressive Symptomatology
NR - non-responder, R - responder

The MARS study was a naturalistic clinical study on antidepressant drug response designed for pharmacogenetics analyses of antidepressant drug response biomarkers¹³⁷⁻¹³⁹. EBV transformed LCLs were generated in a subset of patients from the MARS project. LCLs were gained by EBV transformation from full EDTA-blood samples provided by the MARS patients that have been

admitted for depression treatment to the hospital of the Max Planck Institute of Psychiatry in Munich, Germany ¹³⁷. MARS was an observational study of depressed patients being treated according to the attending physician's choice. Depressive symptoms were rated by the 21-item HDRS at weeks 0, 5 and 8 after study inclusion ²⁷. Response was defined as HDRS reduction of at least 50% (compared to initial values at study inclusion) and remission was achieved after a total reduction of HDRS to values smaller than eight ¹⁴⁰. STAR*D was an open label, randomized, multicenter, controlled clinical study aiming on the definition of effective subsequent treatment strategies after a first unsuccessful antidepressant therapy ¹⁴¹. All patients were diagnosed with unipolar depression and were treated with a citalopram monotherapy at the initial phase of this study. A total of n=50 cell lines were obtained, derived from patients with Caucasian origin that have been treated with citalopram in defined doses. Depressive symptoms were rated by Quick Inventory of Depressive Symptomatology (QIDS) ¹⁴² over the course of up to 14 weeks. LCLs were purchased from the NIMH Center for Collaborative Genetic Studies. They were chosen to cover n=25 first-line therapy responders to citalopram (with more than 50% decline of depressive symptoms during the first month) and n=25 treatment resistant patients (with no response or remission during the whole treatment algorithm of the STAR*D study).

1.1.2. Generation

LCLs were generated from lymphocytes isolated from blood samples through EBV transformation ^{143, 144}. Peripheral blood mononuclear cells (PBMCs) were isolated by density gradient centrifugation using Ficoll. The cell pellet was resuspended in 800 µl EBV-supernatant from B95-8 cell line and 100 µl each were seeded into eight wells of a 48-well cell culture plate. After addition of 200 µl RPMI (Roswell Park Memorial Institute) medium containing 20% fetal calf serum (FCS) per well, cells were incubated at 37°C in a humidified CO₂ incubator (with 5% CO₂). After five days, one volume of fresh RPMI medium (containing 20% FCS) and cyclosporine A (in ethanol) were added to a final concentration of 1 µg/ml. On day 23 to 26 after isolation, cells were further cultivated in T25 cell culture flasks with exchange of the medium (containing 15% FCS) every second day. To control the process of LCL generation (*i.e.* the accumulation of B lymphocytes and the non-accumulation of T lymphocytes), cell identity was tested regularly using the T- and B-cell specific antibodies CD3, CD19 and CD45 (Tritest™ Kit): 100 µl of cell suspension was incubated with 10 µl of Tritest™ solution for 30min at 4°C. After erythrocytes cell lysis using 5ml of FACS (fluorescence-activated cell sorting) lysis buffer and centrifugation (4000rpm, 2min, Pico centrifuge), the cell pellet was washed with 1ml of NaCl solution (0.9% w/v), resuspended in 250 µl of NaCl solution (0.9% w/v) and transferred to a FACS tube. Subsequently, flow-cytometry measurements were carried out (Figure 1).

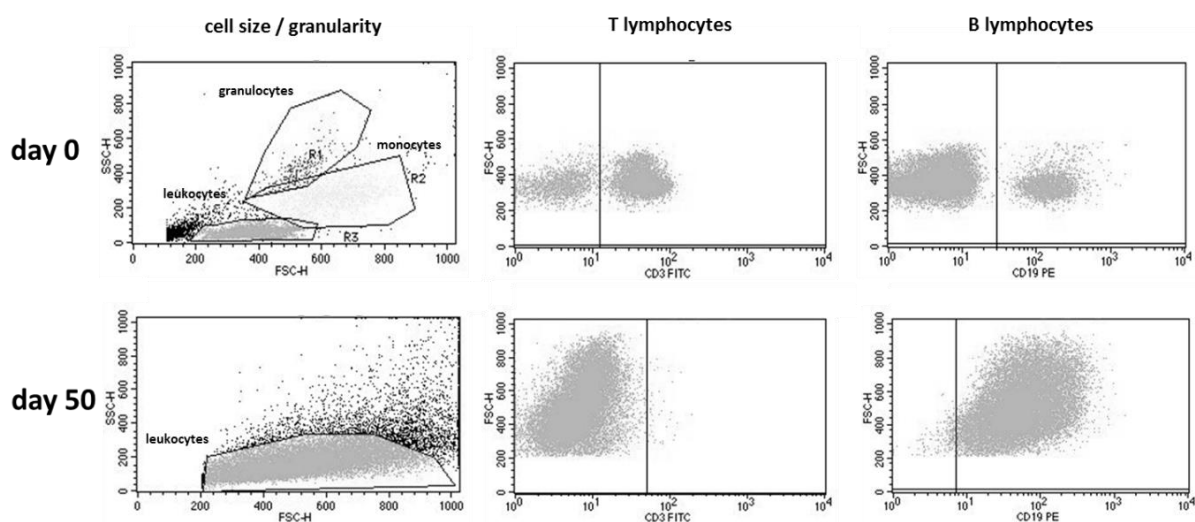


Figure 1: Cell identity before (day 0) and after (day 50) EBV transfection measured by cell specific antibody based flow cytometry. Over the time the cellular distribution shifts to B lymphocytes whereby T lymphocytes disappear from the culture constitution.

1.1.3. Mycoplasma Testing

Since mycoplasma infections are not detectable microscopically, enzyme-linked immunosorbent assays, *i.e.* MycoAlert™ Plus Mycoplasma Detection Kit, were used according to the manufacturer's instruction. The presence of mycoplasmal enzymes is exploited by a selective biochemical test based on the conversion of ADP (adenosine diphosphate) to ATP (adenosine triphosphate). A cell suspension aliquot is transferred to a sterile microcentrifuge reaction tube and pelleted at 200 x g for 5 min. To 100 µl of the supernatant in a sterile 96-well plate, 100 µl of MycoAlert™ Plus Reagent is given to each sample. After an incubation time of 5 min, the luminescence was measured in a Safire² multi-functional plate reader. To each sample 100 µl of MycoAlert™ Plus Substrate was added and incubated for 10 min at room temperature. Subsequently, the luminescence was determined again and the ratio between the values obtained from the first and from the second read was calculated. If mycoplasmal enzymes are not present, this ratio equals to one.

1.1.4. Cryopreservation

After successful generation and negative tests for mycoplasma infections LCLs were stored as cryopreserved aliquots until needed for experiments. Cell density was determined and cells were transferred in a 15ml Falcon tube in the desired number (usually between 1×10^6 and 1×10^7 cells) and centrifuged at 300 x g. The pellet was washed with preheated PBS (phosphate buffered saline), resuspended in 1ml of a preheated mixture of FCS and DMSO (9:1). DMSO is a cryoprotective additive reducing the formation of ice crystals which would destroy the cell membranes during the

freezing process. After transfer of the cell suspension into a cryotube, they were put immediately into a Mr. Frosty™ Freezing Container filled with ice-cold isopropyl alcohol and stored in a -80°C freezer for one day. Subsequently, the cryotubes were transferred to a liquid nitrogen container for long-term storage.

1.1.5. Cell Counting

From the appropriate cell suspension, 10 µl were transferred to a 0.5ml reaction tube and mixed with 10 µl of trypan blue solution. Trypan blue is a diazo dye used to distinguish living cells from dead cells through permeability differences (dead cells are stained due to decreased cell membrane integrity). After careful mixing, cell counts were determined using TC20™ Automated Cell Counter. Growth curves were generated by cumulative population doubling level (CPDL) method according to the following formula¹⁴⁵:

$$CPDL = \sum \frac{\ln N_f / N_i}{\ln 2}$$

N_f ... final cell number
 N_i ... initial cell number

1.1.6. Cultivation

All cell culture work was carried out under aseptic conditions using laminar flow. All applied media and solutions were preheated to 37°C before contact with cells. FCS was heat-inactivated (30min, 56°C) and stored in aliquots at -20°C. LCLs were cultured in RPMI medium supplemented with 15% heat-inactivated FCS, antibiotics (100 µg/ml penicillin, 100 µg/ml streptomycin) and a final concentration of 4 mM L-glutamine for at least two weeks before experiments were carried out. Culture media were stored at 4°C. To re-culture cryopreserved cells, one aliquot was rapidly thawed at 37°C and transferred to 9 ml of preheated medium in a 15ml Falcon Tube and then centrifuged at 300 x g for 3 min. Medium exchanging was done three times a week. Cells were incubated at 37°C in a humidified CO₂ incubator (with 5% CO₂) in cell culture flasks (either T25 or T75) in upright position and used within two months from thawing.

1.1.7. Treatment with Antidepressants

LCLs were treated with different concentrations of SSRI antidepressant drugs for up to three weeks in T25 cell culture flasks. Stock solutions containing fluoxetine or citalopram were prepared in

DMSO at a concentration of 0.25 mg/ml and were stored as 1.5ml aliquots in glass vials at -20°C . Prior to use, stock solutions were sterile filtered by using a DMSO safe 0.2 μm nylon membrane syringe filter, a 1.5 ml syringe and a cannula. Cell culture media containing antidepressants were always freshly prepared before adding to the cells. Cells were treated with antidepressants while MOCK treated control cultures were grown in parallel. Every second day cell density was determined and set to 3×10^5 cells per milliliter.

1.2. Determination of Proliferation Rates

To determine individual proliferation rates, 5-ethynyl-2'-deoxyuridine (EdU) incorporation assays (Life technologies) were used. Experiments were carried out after continuous incubation with antidepressants for a maximum of three weeks. Cells were treated with a final concentration of 10 μM EdU for two hours and detection of EdU incorporation was performed according to the manufacturer's protocol using a FACS Calibur flow cytometer. EdU is a nucleoside analog to thymidine which is incorporated into newly synthesized DNA strands. Due to an artificial ethynyl moiety, a fluorescence dye (Alexa Fluor[®] 647) can be attached in a click reaction^{146, 147}, where the alkyne group of the EdU compound reacts in a copper catalyzed manner with the azide group of the fluorescence dye to a stable triazole (Figure 2, A). The fluorescence intensity of each cell can be determined by basic flow cytometry methods (Figure 2, B and C).

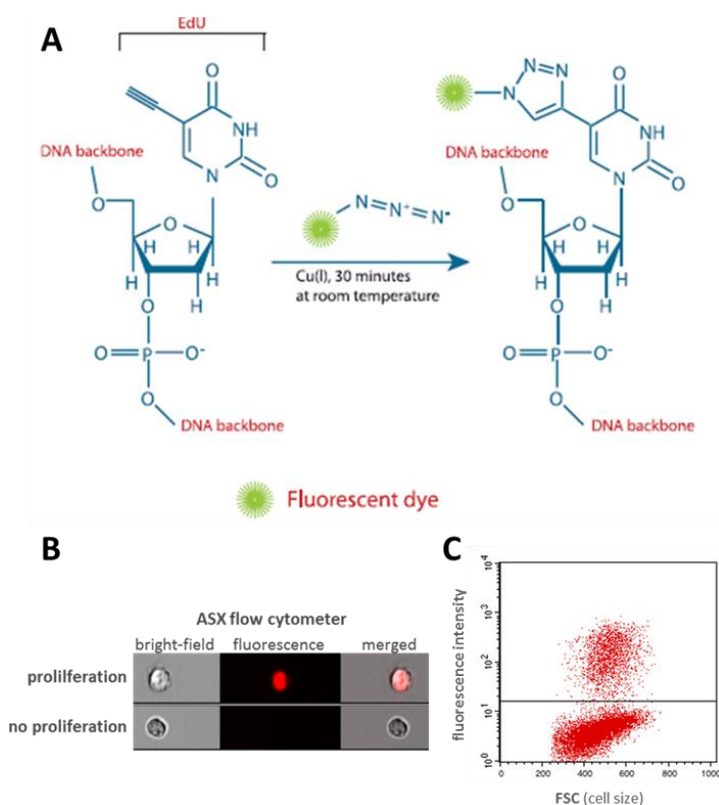


Figure 2: Basic principle of the EdU proliferation assay. In a copper catalyzed reaction, a fluorescence dye is attached to newly synthesized DNA strands. Modified according to Invitrogen Handbook¹⁴⁸ (A). Fluorescence intensity is measured by flow cytometry (B). Discrimination of proliferating and non-proliferating cells by fluorescence analysis (C).

EdU-Workflow

Sample preparation was done according to the manufacturer instructions in technical and biological duplicates. Cultured cells were transferred from cell culture flasks into cell culture multi-well plates and incubated with EdU solution at a final concentration of 10 μ M for two hours (37°C, 5% CO₂). Afterwards, cells were harvested by centrifugation (5 min, 7000 rpm) and the pellet was washed once with 750 μ l of BSA (bovine serum albumin) solution (1% w/v in PBS). Cells were fixed by 25 μ l of Click-iT[®] fixative containing paraformaldehyde for 15 min under light-free conditions followed by a further washing step with 900 μ l of BSA solution (1% w/v in PBS). Before cell staining with 250 μ l Click-iT[®] reaction cocktail (218.75 μ l PBS, 5 μ l CuSO₄, 25 μ l reaction buffer additive, 1.25 μ l Alexa Fluor[®] 647 fluorescence dye azide) for 45 min under light-free conditions, they were permeabilized through 100 μ l Click-iT[®] saponin-based permeabilization and wash reagent. After a final washing step, cell pellets were resuspended in 600 μ l Click-iT[®] saponin-based permeabilization and wash reagent and analyzed by flow cytometry.

Flow Cytometry Measurements

Cellular fluorescence was measured by FACS Calibur flow cytometer. Gates were set to exclude both cell debris and cell aggregates. Measurements were performed until 10,000 events were reported. The detector parameters are shown in Table 3, primary threshold was channel FL2 with a value of 21. No secondary threshold or compensation was applied. Data analyses were performed using CellQuest Pro software.

Table 3: Detector parameters of the FACS Calibur flow cytometer measurements of the EdU proliferation assays.

parameter	Voltage	AmpGain	Mode
forward scatter	E-1	3.52	Linear
sideward scatter	300	1.10	Linear
fluorescence channel FL1	670	1.00	Logarithmic
fluorescence channel FL2	366	1.49	Linear
fluorescence channel FL2 - Amplitude	-	1.00	Linear
fluorescence channel FL2 - Width	-	1.00	Linear
fluorescence channel FL3	650	1.00	Logarithmic

1.3. Gene Expression Analyses

1.3.1. RNA extraction

Cells were pelleted and resuspended in 350 μ l lysis buffer (containing 1% v/v β -mercaptoethanol). Prior to nucleic acid extraction, cell lysates were homogenized via QiaShredder to reduce viscosity and to remove insoluble material. RNA was extracted using the NucleoSpin[®] RNA Kit according to the manufacturer instructions. After addition of 350 μ l of 70% ethanol to the lysate, the sample was transferred to an RNeasy Mini spin column and centrifuged for 15 s at 13,000 x g. RNA was washed once with 700 μ l Buffer RW1, twice with Buffer RPE, dried through centrifugation (2min, 13,000 x g) and eluted in 30 μ l RNase free water. Nucleic acid concentrations were quantified using a NanoDrop[®] Spectrophotometer.

1.3.2. Synthesis of Complementary DNA

From 1 μ g of RNA, cDNA was prepared using Transcriptor First Strand cDNA Synthesis Kit in a thermal cycler over three steps (25°C for 10 min, 55°C for 30 min, 85°C for 5 min). RNA concentrations were adjusted to 100 ng/ml using RNase free water in a volume of 10 μ l followed by addition of 30 μ l of Mastermix (12 μ l ddH₂O, 8 μ l transcriptase buffer, 4 μ l random hexamer primer, 4 μ l dNTPs, 1 μ l protector RNase inhibitor, 1 μ l reverse transcriptase). PCRs (polymerase chain reactions) were carried out in a 0.2 ml collection tube and a total reaction volume of 40 μ l.

1.3.3. Primer Design and Validation

Primers for desired nucleotide sequences were designed using the Primer-BLAST primer design tool (design parameters are shown in Table 4). Suggested primer pairs were checked for salt-adjusted melting temperature as well as potential formation of secondary structures and gene specificity using Oligonucleotide Properties Calculator¹⁴⁹ and UCSC Genome Bioinformatics BLAT alignment tool¹⁵⁰, respectively. Custom made, lyophilized primers were purchased from Eurofins Genomics (Ebersberg, Germany) and rehydrated in RNase free water to a concentration of 100 μ M. Primers were validated by RT-PCR including evaluation of specificity through melting curve analysis (Figure 3, A). Afterwards, PCR products (5 μ l mixed with 1 μ l of 6x loading dye) were separated by agarose gel (1%) electrophoresis for 45 min at 100 V (Figure 3, B). As a standard GeneRuler 50 bp DNA Ladder was used. Detection was performed after 30min incubation in ethidium bromide solution (200 ml TAE buffer with 2 μ g/ml ethidium bromide) in a chemiluminescence detection system using Diana Software.

Table 4: Design parameters and specifications for custom made primers.

Design parameter	specification
PCR product size	150nt -250nt
primer melting temperature	58-60°C
Maximum T _m difference	1°C
intron inclusion	yes
intron length range	1,000nt - 1,000,000nt
organism	Homo sapiens

T_m - melting temperature, nt - nucleotides

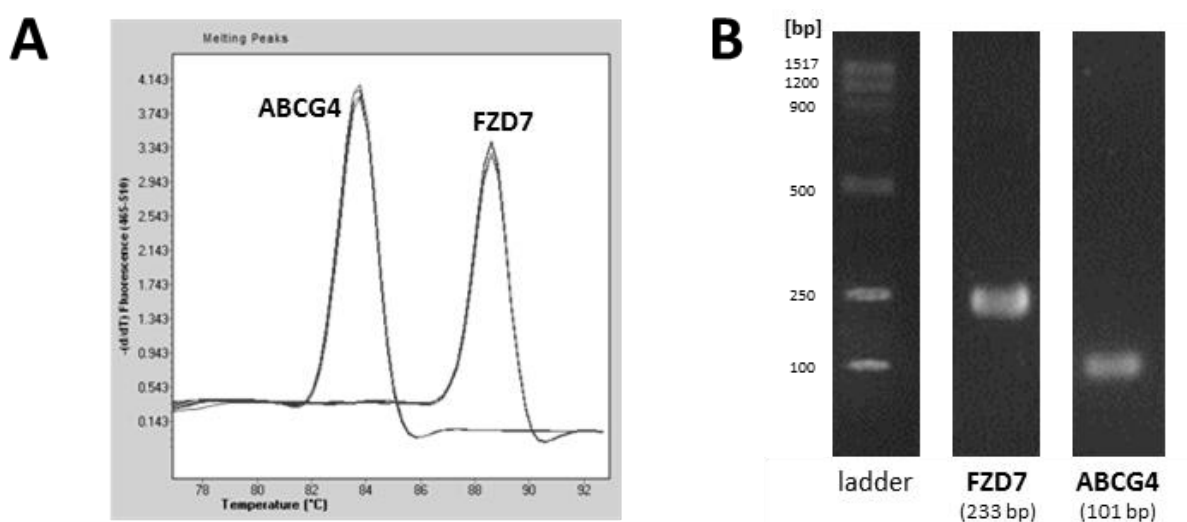


Figure 3: Validation of custom-made primers was performed via melting curve analyse (A) and agarose gel electrophoresis (B).

1.3.4. Quantitative Real-Time Polymerase Chain Reaction

Real-time PCR experiments were conducted using QuantiTect SYBR Green PCR Kit. QuantiTect and primers were purchased from Qiagen (Hilden, Germany) (Table 5).

Experiments were carried out using white 96-well plates in a LightCycler® 480 II system in technical and biological duplicates. After addition of 17 μ l Mastermix (consisting of 55 μ l ddH₂O, 40 μ l cDNA, 125 μ l SYBR green Mastermix) to each well, 3 μ l of primer solution was given to each well. Cycle conditions are shown in Table 6. Data was analyzed using LightCycler® 480 Software Version 1.5.1.62 SP2. Basal gene expression was indicated as Δ CT values. Gene expression fold change (FC) was calculated by $\Delta\Delta$ CT method using *GAPDH* as reference gene¹⁵¹.

Table 5: Primers used for RT-PCR experiments.

gene	full gene name	assay name or sequence
<i>ABCB1</i>	ATP-binding cassette sub-family B member 1 (P-glycoprotein)	Hs_ABCB1_1_SG
<i>ABCG4</i>	ATP-binding cassette sub-family G member 4	Fwd: CCTGGAGTTCAGGAACCAAC Rev: GTGAAGATGCCAGCATGGAG
<i>BTC</i>	betacellulin	Hs_BTC_1_SG
<i>CACNA2D3</i>	calcium channel, voltage-dependent, alpha 2/delta subunit 3	Hs_CACNA2D3_1_SG
<i>CYP3A43</i>	cytochrome P450 3A43	HS_CYP3A43_1_SG
<i>EGFR</i>	epidermal growth factor receptor	Hs_EGFR_vb.1_SG
<i>ERBB3</i>	epidermal growth factor receptor 3	Hs_ERBB3_vb.1_SG
<i>FZD7</i>	frizzled homolog 7	Fwd: CCTTCCCCTTCTCATGCC Rev: CAGCCCGACAGGAAGATGAT
<i>GAPDH</i>	Glyceraldehyde 3-phosphate dehydrogenase	Hs_CACNA2D3_1_SG
<i>HBEGF</i>	heparin-binding EGF-like growth factor	HS_HBEGF_1_SG
<i>KI67</i>	Marker of proliferation Ki-67	Fwd: AGGGAAAGGAGAAGCAGGAAATTCAGAC Rev: GAGGACATAGGCAAACAAACGACGACA
<i>MAPK9</i>	mitogen-activated protein kinase 9	Hs_MAPK9_va.1_SG
<i>PIK3R5</i>	phosphoinositide-3-kinase, regulatory subunit 5	HS_PIK3R5_1_SG
<i>SULT4A1</i>	sulfotransferase family 4A, member 1	Hs_SULT4A1_1_SG
<i>TCF7</i>	transcription factor 7	Hs_TCF7_va.1_SG
<i>TCF7L2</i>	transcription factor 7-like 2	Hs_TCF7L2_1_SG
<i>WNT2B</i>	wingless-type MMTV integration site family, member 2B	Hs_WNT2B_va.1_SG

fwd - forward, rev - reverse

Table 6: RT-PCR cycle conditions.

cycle numbers	temperature	duration
1	95°C	10min
60	95°C	10s
	58°C	15s
	72°C	20s
1	4°C	-

1.3.5. Determination of RNA quality

Since degraded RNA affects down-stream experiments such as gene expression analysis, prior to microarray experiments the quality of RNA was evaluated using the Agilent 2100 Bioanalyzer system. This is a high sensitive standard method to assess RNA integrity and ribosomal ratios using electrophoretic separation of the samples and fluorescence based detection. With proceeding degradation of the RNA, the ratio between 18S and 28S ribosomal subunits band intensity

decreases. The Bioanalyzer software generates gel-like images and electropherograms (Figure 4) and calculates the RNA integrity number (RIN) - a standardized, user-independent scale reaching from values 1 (most degraded RNA) to 10 (most intact RNA) ¹⁵².

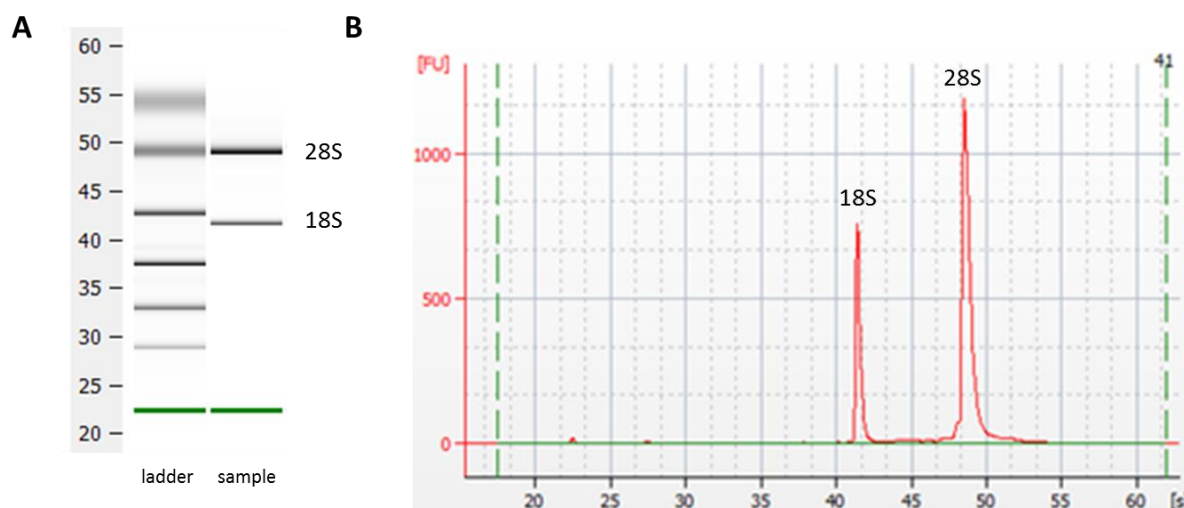


Figure 4: Gel-like images (A) and electropherogram (B) of a successful Bioanalyzer run. The bands and peaks of the ribosomal 18S and 28S compounds are clearly visible. Impurities would generate additional signals. Only RNA samples with high purity were used for further experiments.

Workflow

First, the gel and gel-dye mix were prepared: After placing 550 μ l of Agilent RNA 6000 Nano gel matrix in a spin filter, the filter was centrifuged for 10min at 1500 x g. To a 65 μ l aliquot of filtered gel, 1 μ l of RNA 6000 Nano dye concentrate was added and centrifuged for 10min at 13,000 x g. After transferring 9 μ l of the gel-dye mix to the chip, 5 μ l of markers as well as 1 μ l of heat-inactivated (70°C, 2 min) samples and RNA 6000 Nano ladder solution were pipetted into the particular wells. Measurement of the chips was done using the Agilent 2100 Bioanalyzer instrument. Data analysis was performed using Agilent 2100 Bioanalyzer Expert Software. Only RNA samples with RIN values larger than eight were used for subsequent down-stream experiments.

1.3.6. Genome-wide Gene Expression Profiling

A microarray-based gene expression analysis allows simultaneous quantification of gene products. Here, the SurePrint G3 Human Gene Expression 8x60K Microarray Kit (Agilent One Color Microarray Technology) containing more than 27,000 biological features was used. A feature consists of picomoles of immobilized probes which are gene specific DNA sequences. After fluorescence labeling of sample cRNA (complementary to probes) and probe-target-hybridization, fluorescence intensity as a measure of gene product amounts is determined, followed by gene chip quality control and data analysis.

Workflow

After positive evaluation of RNA quality, microarray analyses were performed in ten cell lines (untreated and after 21 days of incubation with 0.5 µg/ml fluoxetine) according to the manufacturer's instructions. A total of 100 ng mRNA extracted from LCL cell cultures was used for reverse transcription and labelling. The generation of cDNA was conducted with T7 promoter primers and AffinityScript reverse transcriptase in a total reaction volume of 10 µl incubating for two hours at 40°C followed by 15 min at 70°C. Fluorescence labelling was performed for two hours at 40°C after addition of NTP mix, T7 RNA polymerase and cyanin-3-cytidine triphosphate (CY3). After column-based purification of CY3-labelled cRNA, 600ng of CY3-labelled cRNA (specific activity >10.0 pmol Cy3/µg cRNA) was fragmented at 60°C for 30 minutes in a reaction volume of 25 µl containing 1x Agilent fragmentation buffer and 2x Agilent blocking agent. On completion of the fragmentation reaction, 25 µl of 2x Agilent hybridization buffer was added to the fragmentation mixture and hybridized to the microarrays slides for 17 hours at 65°C in a rotating hybridization oven. Subsequently, microarrays were washed 1 min at room temperature with GE Wash Buffer 1 (Agilent) and 1 min with 37°C GE Wash buffer 2 (Agilent), then dried immediately by brief centrifugation. Fluorescence intensities were measured by SureScan Microarray Scanner after a final washing step to remove non-specific bound cRNA.

Quality Control and Data Analysis

Quality control was performed using Feature Extraction V 10 Software and included analysis of various physical quality parameters such as spike-in signals, outlier analysis, spot finding algorithms or spatial distribution of signals. Further, features with low-intensity or poor quality were removed. Data analysis was conducted using GeneSpring (Agilent) and data pre-processing includes normalization, flagging and filtering. After background subtraction and determination of raw spot intensities, normalization was performed using the multiaverage method which is necessary to adjust data sets for technical variations such as efficacy of dye incorporation, heat and light exposition, hybridization conditions and scanning conditions. Thus, relative abundance is reduced focusing exclusively on biologically relevant changes. To reduce artifacts, signal intensities below a defined cut-off point were removed from the dataset. The probeset was filtered on data files (control type 0) with the condition that at least 100% of the values in any one out of one condition are within the range.

Pathway analyses identify specific gene networks affected by *in vitro* treatment relative to untreated controls. Single experiment pathway analysis was performed using the imported pathway database from GenMAPP Pathway Markup Language and 0.05 as an uncorrected p-value cut-off. Hierarchical cluster analysis is a technique grouping samples and genes with similar

expression patterns. Non-significant genes were removed by fold-change analysis. Differential gene expression was rated in pairs (treated vs. untreated) with a significance level of $p < 0.05$ (uncorrected) where value limits for under- and overexpressed genes were set to -2 and 2, respectively. To functionally characterize the remaining genes, gene ontology (GO) analyses and protein interaction analyses were carried out using the web-based STRING (Search Tool for the Retrieval of Interacting Genes/Proteins) database¹⁵³. A GO study extracts information about the biological function of a given gene set by identifying genes being involved in particular GO terms. Systematic search of CNS annotations were carried out using the gene names and one of the following terms: brain, neuron, neurogenesis, neural plasticity, proliferation, depression or antidepressant.

1.4. Statistical Analyses

Statistical analyses were carried out using IBM SPSS Statistics 21. All p-values are reported as nominal p-values and are unadjusted for multiples testing unless stated otherwise. In dependence of the nature of the data types either parametric (Student's t-tests, Pearson correlation) or non-parametric tests (Wilcoxon-Mann-Whitney rank-sum test, Spearman's rank correlation) were used when analyzed with respect to the proliferation rates and gene expression data. To test for differences between antidepressant treated and untreated proliferation rates in the same cell lines the paired t-test was used. Between the groups of responders and non-responders the proliferation rates were compared with unpaired Student's t-tests. To measure the strength of the relationship between the proliferation rates of different treated cells Pearson's correlation coefficient (ρ) was calculated. Unpaired Student's t-tests were used to analyze basal gene expression differences between non-proliferating and proliferating cell lines and to analyze basal gene expression differences between clinical subgroups (*e.g.* response after five and eight weeks and remission after five and eight weeks). Data of gene expression FCs was analyzed by Wilcoxon-Mann-Whitney rank-sum test. Associations between proliferation vs. age and proliferation vs. gender were calculated using Pearson's correlation and Student's t-test for equal variances (tested by Levene's test), respectively. For all remaining applications, implemented statistic programs of the specific software (GeneSpring, STRING) were used.

2. Neuroimaging

2.1. Clinical Study Design

2.1.1. Overview

This prospective, open label, non-randomized, single center, phase I trial was approved by the Federal Institute for Drugs and Medical Devices (BfArM) and the ethics commission of the Medical Faculty of the University Bonn. The full study's title reads "Immune- and miRNA-response to recombinant interferon beta in healthy volunteers and patients with relapsing remitting multiple sclerosis" (trial short title: RESI) and is listed under EudraCT-number "2012-005475-13" in the EU Clinical Trials Register database. Before and after a nine-day standard therapy with recombinant interferon beta, psychometric testing as well as MRI measurements were conducted. A total number of 17 healthy volunteers were enrolled in this study. The trial was conducted at the dedicated phase I unit of the clinical study center of the university hospital Bonn in accordance with the ICH Guideline for Good Clinical Practice, the relevant national regulations and the Declaration of Helsinki.

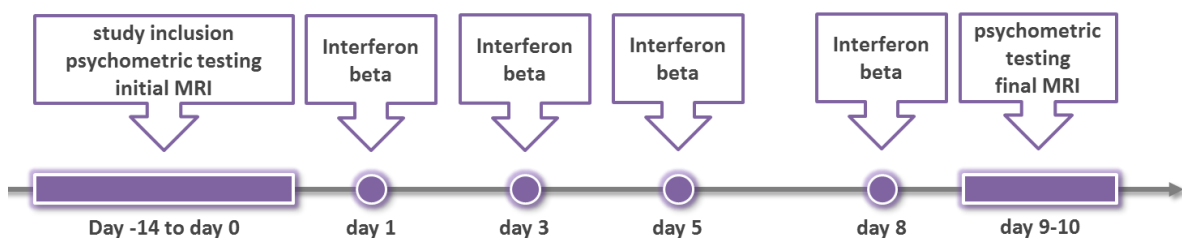


Figure 5: Overview of the study procedure. Before and after a nine-day standard therapy with interferon beta, psychometric testing as well as MRI measurements were performed.

2.1.2. Participants

Participants were healthy volunteers between 18 and 65 years who were recruited by the Clinical Study Center of the University Hospital in Bonn, Germany. Inclusion criteria were adequate function of liver (bilirubin, alanine transaminase, aspartate transaminase), kidney (creatinine), thyroid gland (thyroid-stimulating hormone), bone marrow (white blood cells, granulocytes, platelets, hemoglobin) and blood clotting (prothrombin time, partial thromboplastin time). Additionally, females needed to obtain a negative serum pregnancy test prior to treatment start and were instructed to use an approved contraceptive method (Pearl index < 1%) during and for 3 months after the trial. Exclusion criteria were abuse of alcohol, drugs or medication as well as a present co-

medication with corticosteroids and a pronounced fear of blood drawings. Furthermore, potential subjects with a known allergy/hypersensitivity to interferon beta or any other ingredient of the injection solution, a history of malignant, cardiac, psychiatric disorders (including suicidal behavior) and particular infective diseases (*e.g.* acquired immunodeficiency syndrome, Hepatitis B or C) were excluded from this study. MRI-specific exclusion criteria were metal implants (*e.g.* pacemaker, inner-ear prosthesis, nerve stimulator, implanted defibrillator, infusion pump, artificial joints), magnetic or metallic objects that cannot be removed from the body (*e.g.* body piercing, dental prosthesis, implanted electrodes, contraceptive coil, acupuncture needle), claustrophobia, persistent tinnitus and tattoos or permanent makeup of a particular size (more than 10% of the body surface). Participants were not allowed to take part in other clinical trials with therapeutic intervention during this trial or within one month before enrolment. Mental health was evaluated by Mini-international neuropsychiatric interview (MINI). Inclusion was performed after the subjects gave written informed consents.

2.1.3. Investigational Medicinal Product

Interferon beta-1a received its marketing authorization in Germany in 1998. Prefilled syringes containing 44 µg of interferon beta-1a (Rebif®, Merck) were subcutaneously injected by trained personnel on days 1, 3, 5 and 8. Other ingredients are mannitol, poloxamer 188, L-methionine, benzyl alcohol, sodium acetate, acetic acid, sodium hydroxide and *aqua ad injectabilia*. No dose adjustments are intended by the trial protocol. In case of severe side effects (*e.g.* fever, head and body aches or chills) concomitant medication was allowed after consultation with the attending physician.

2.1.4. Psychiatric Evaluation

To assess change of psychiatric parameters after treatment with Interferon beta, depression and anxiety symptoms were examined with HDRS and STAI (State-Trait Anxiety Inventory) questionnaires, respectively. The interview-based HDRS was firstly developed by Max Hamilton in 1966 and consists of multiple items aiming on depression-specific psychological parameters. Otherwise, the STAI bases on a self-report consisting of 40 questions with a four-pointed scale and measures the two main forms of anxiety (current and general anxiety). Higher scores are positively associated with more severe levels of depression or anxiety in both questionnaires. Paired t-tests by SPSS12 were used to statistically evaluate pre/post-changes in psychometric parameters.

2.2. Magnetic Resonance Imaging

2.2.1. Functional Principle

MRI scanners are able to use strong, uniform magnetic fields and radio waves to produce images of the human brain. Since the human body is largely composed of water molecules, tissue specific differences in the magnetic moment of the proton spin can be used to generate contrast pictures. Functional MRI allows determining brain activity while doing different tasks. The brain activity can be measured by detecting changes associated with blood flow because neuronal activation and CBF are tightly connected (hemodynamic response). An activation of a particular brain area leads to an increased metabolic activity and oxygen consumption. In consequence, oxygenated hemoglobin decreases and a disproportionate increase in perfusion emerges that stays at constant levels for the duration of the stimulation. The change in signal magnitude of the magnetic properties can be detected by MRI. The underlying mechanism is called blood-oxygen-level dependent (BOLD) contrast which describes the proportion of hemoglobin magnetization (oxygenated hemoglobin is diamagnetic and deoxygenated hemoglobin is paramagnetic) in the magnetic field ¹⁵⁴. The higher the magnetic field strength, the higher the observed BOLD contrast and the signal-to-noise ratio ¹⁵⁵. The localization of activated brain areas is possible through modelling differences in the BOLD signal following the contrast between task execution and resting-state (control condition). Statistical modelling allows the processing of test statistics of these contrast effects in each voxel which can be visualized as statistical parametric maps.

2.2.2. Paradigms

To measure specific brain activation patterns of depression-associated areas, all individuals had completed two tasks in functional brain imaging. Different paradigms were used to cover both the reward system and brain circuits of emotion. To probe sensitivity to reward cues in the ventral striatum and brain stem, a paradigm was employed - based on the work of Knutson *et al.* ¹⁵⁶ - in which participants could collect money at different amounts (high and low), anticipated by appropriate cues ¹⁵⁷. Participants were instructed to view the images and to press a button with their thumbs depending on the horizontal position of an appearing dot on the screen (see Figure 6). The total scan length of this paradigm was 8:07 minutes. Each correct response was rewarded by appropriate monetary amounts (0.01 € or 0.20 €) and money was paid off in cash after the scan, if the total amount was over 20.00 € - ensuring a high motivational status of the volunteers (maximal reward: 20.37 €).

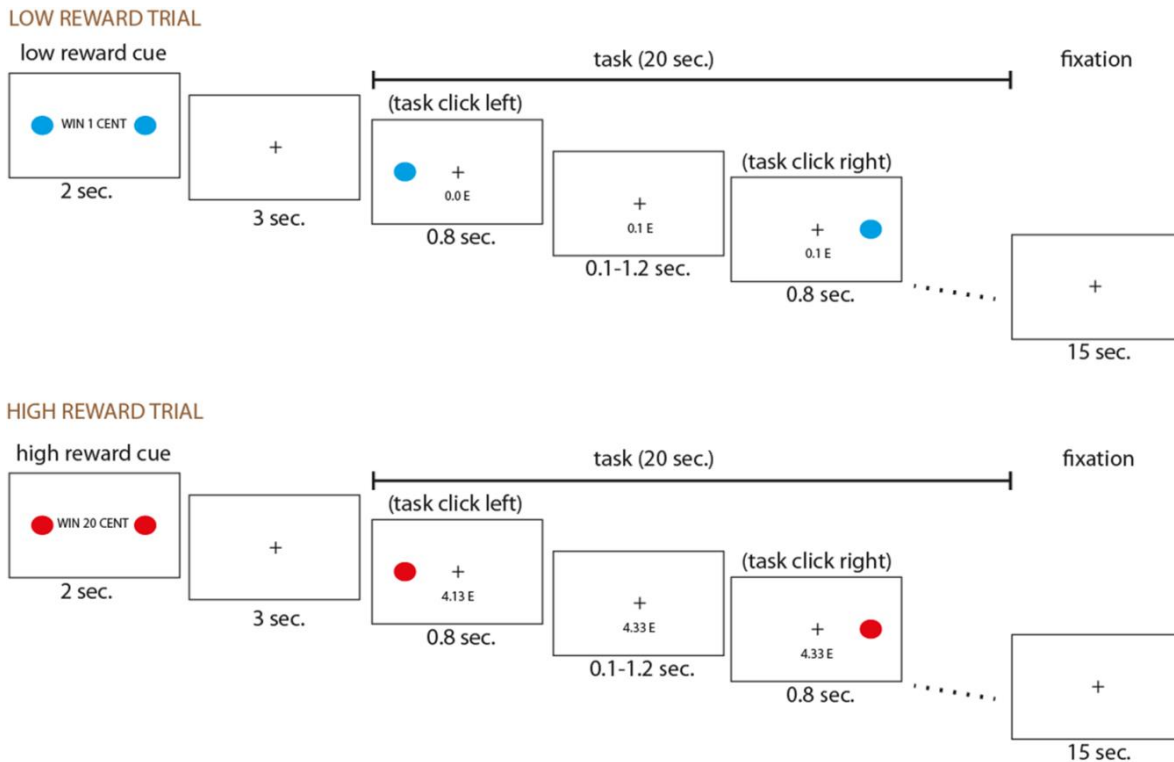


Figure 6: Principle of the “reward” paradigm. Subjects are instructed press the left or right button of the keypad depending on the horizontal position of an appearing dot on the screen. Correct responses were rewarded according to the displayed monetary value. According to Viviani *et al.*¹⁵⁷.

To target the amygdala and to evaluate reactivity to emotional stimuli, blocks of faces displaying the emotion of anger, sadness and disgust were displayed in a passive exposure paradigm^{158, 159}. In alternation, blocks of faces and geometric forms were presented (Figure 7) resulting in a total scan length of 3:17 minutes. Social images were taken from a set of standardized facial expressions provided by the Swedish Karolinska Institute¹⁶⁰.

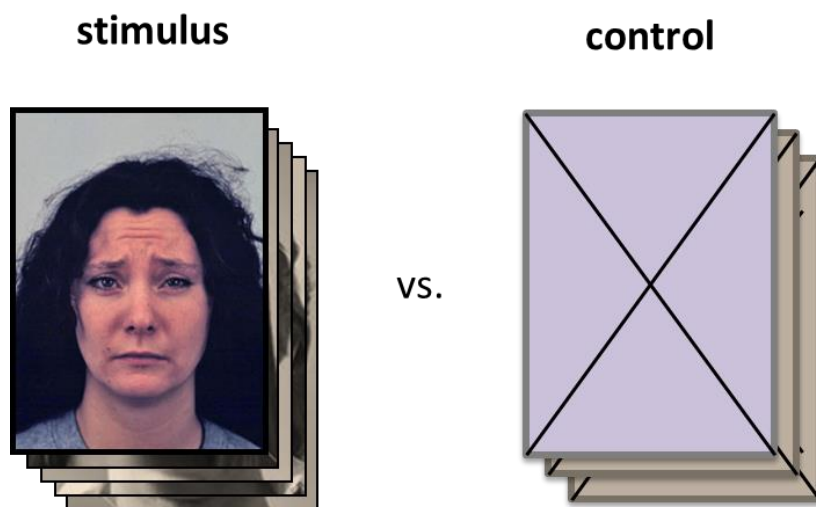


Figure 7: Principle of the faces paradigm. Subjects are instructed to focus on the alternating appearing blocks of images consisting of emotional faces (stimulus condition) and neutral geometric forms (control condition)¹⁶⁰.

2.2.3. Data Acquisition

Data were acquired on a Skyra 3T MRI scanner (Siemens Healthcare, Erlangen, GER) by trained personnel. Scan sequences were controlled by manufacturer's software. To ensure safety, metal detector analyses were conducted prior to entering the scan room. Subject wellbeing was continuously monitored by video camera, intercom and manual alarm system during the scan. To avoid subject's hearing damages, foam earplugs were applied. Subject head movements were restrained with foam padding inside the 32 channel head coil. Paradigm pictures were presented on a monitor located behind the scanner and were displayed to the subjects via mirrors. Task responses were recorded by a button-box.

To determine the exact brain position, overview scans (Head Scout Localizer) were conducted at the beginning of the scan procedure. Functional scans were acquired by echo planar imaging (T2-weighted gradient-echo). An overview on measurement parameters is given in Table 7.

Table 7: Overview on fMRI measurement parameters

parameter	functional imaging	additional information
AutoAlign	Head>Brain	
Concatenations	1	slice distribution over multiple measurements
Distance factor	20%	gap between single slices expressed as percentage of slice thickness
Echo time	30 ms	time between the radiofrequency pulse and MR signal sampling
Filter	none	corrections for non-uniform receiver coil profiles
Flip angle	90°	
FoV read	192 mm	size of the spatial encoding area of the image
FoV phase	100%	
Matrix size	64x64	
PAT	off	
Phase encoding direction	A>>P	direction of the pulsed magnetic field gradient
Phase oversampling	0%	artifact reduction technique for field-of-view exceeding objects
Repetition time	2460 ms	time between excitations pulses
Slices	30	number of recorded planar regions
Slice thickness	2.5 mm	
Voxel size	3.0x3.0x2.5	parameter for spatial resolution

FoV - field of view, PAT - parallel acquisition technique

The measurement window of fMRI was adjusted to achieve maximal coverage of the brain including the regions of interest such as the amygdala and the ventral striatum (Figure 8). The tilting angle of the measurement window was adjusted to the interface between the fourth ventricle and the brain stem (blue line) for each individual participant ensuring a constant coverage of all relevant brain areas over the course of this study.

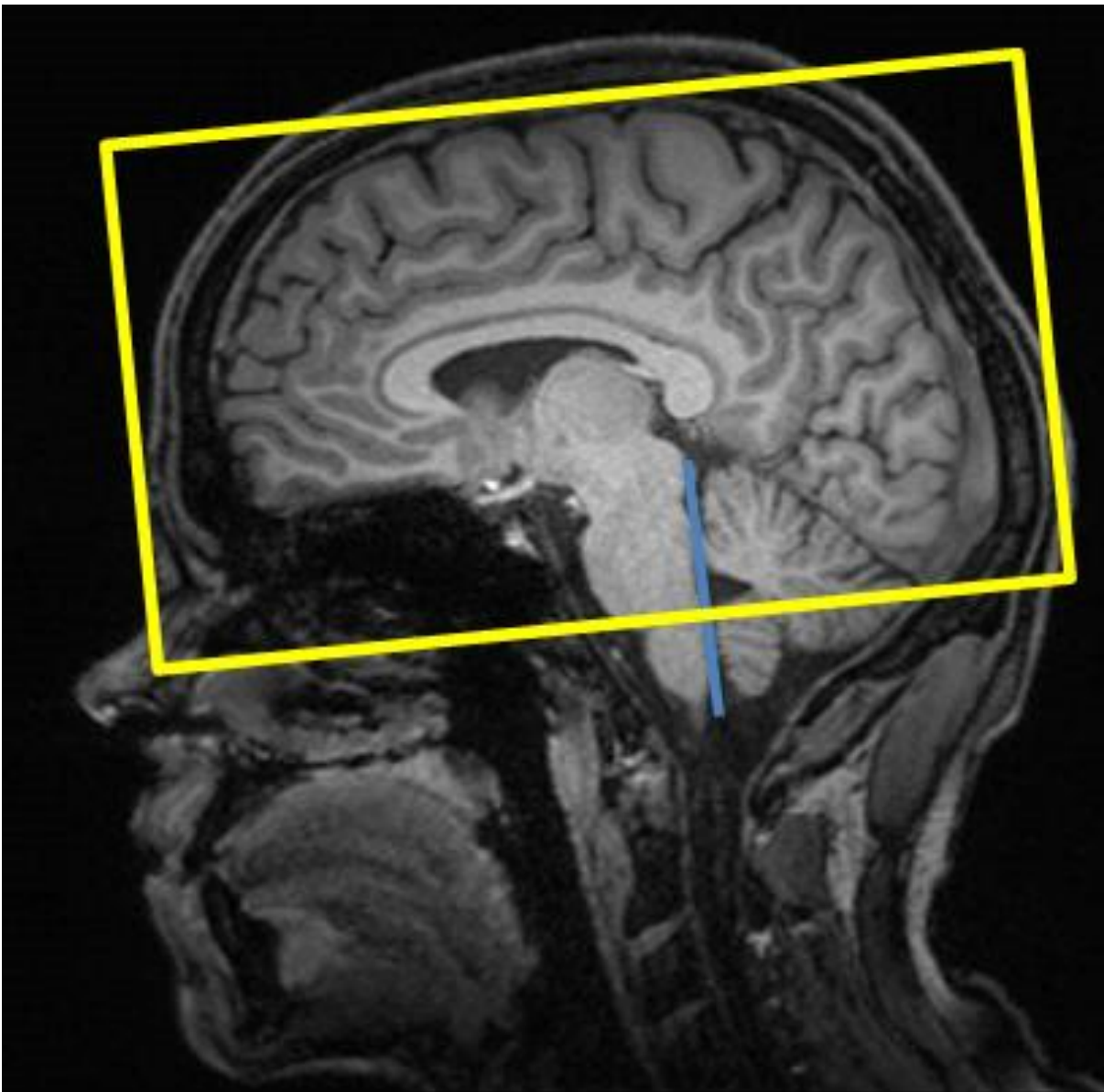


Figure 8: Orientation of the measurement window. The tilting angle is adjusted to the interface between the fourth ventricle and the brain stem (blue line) to achieve maximal coverage.

2.2.4. Data Analysis

The imaging data were analyzed using SPM12 software which is a collection of specialized statistical techniques for the examination of brain activity differences in fMRI ¹⁶¹. Images for each subject were preprocessed including realignment to correct for head motion, normalization into a standard stereotactic space of an anatomical reference (by transformation of the images through translation, rotation, scaling and nonlinear warping) to allow comparisons between different subjects and smoothing with an 8 mm Gaussian kernel to increase signal-to-noise ratio. Regressors for faces paradigm were “pictures vs. control” (geometrical forms) and for foraging paradigm were “cue high

vs. cue low". Contrasts were embedded into a design matrix that generates linear models with parameter estimates to compare fMRI data before and after interferon therapy. Statistical analyses were based on classical T-statistics and include calculations on peak level, cluster level and set level with FDR (false discovery rate) adjusted p-values by usage of height and spatial extent thresholds. Set level inferences are based on activated brain regions, *i.e.* the number of connected clusters above the threshold and are usually more powerful compared to cluster level analyses¹⁶². Cluster level inferences consider the spatial extent (*i.e.* the volume or the number of activated and connected voxels that comprise the subset) and the peak height of the cluster when calculating significance. They are more sensitive than set level analyses but at the expense of localizing power¹⁶². The peak inference only takes the maxima height of single voxels into account and therefore is the less powerful method to detect brain activation differences. The repeated testing of the model in each voxel is accounted for by a correction for the multiple testing. Subsequently, the obtained p-values are visualized as statistical parametric maps using a p-value threshold of 0.001.

3. Software

Bioanalyzer 2100 Expert Software	Agilent (Santa Clara, CA, USA)
CellQuest Pro	BD Bioscience (Franklin Lakes, NJ, USA)
Feature Extraction V 10 Software	Agilent (Santa Clara, CA, USA)
GeneSpring X12	Agilent (Santa Clara, CA, USA)
MATLAB	The MathWorks (Natick, MA, USA)
Microsoft Office 2010	Microsoft Corporation (Redmond, WA, USA)
MRI console software	Siemens Healthcare (Erlangen, GER)
LightCycler® 480 Software	Roche (Basel, CH)
DIANA	raytest GmbH (Straubenhardt, GER)
Presentation	Neurobehavioral Systems Inc. (Berkeley, CA, USA)
Primer-BLAST design tool	NCBI (Rockville Pike, MD, USA)
BLAT alignment tool	UCSC Genome Bioinformatics (Santa Cruz, CA, USA)
Oligonucleotide Properties Calculator	Northwestern University (Chicago, IL, USA)
SPSS Statistics 21	IBM (Armonk, NY, USA)
Statistical Parametric Mapping	Karl Friston (University College London, GB)

Chapter IV - Results

1. Identification of Potential Gene Expression Biomarkers for Antidepressant Response

1.1. Results from the MARS Cohort

The MARS study is a naturalistic clinical study on antidepressant drug response designed for pharmacogenetics analyses of antidepressant drug response biomarkers. LCLs were generated in a subset of patients from the MARS project and were used as model systems to study individual proliferation and gene expression between fluoxetine-treated and untreated samples aiming on the identification of potential biomarkers for the pre-treatment prediction of individual antidepressant drug effects (experimental overview in Figure 9). Initially, screening experiments were carried out to identify a suitable experimental setup and as prove of concept verification. Subsequently, microarray experiments were carried out to find potential gene expression biomarkers. Proliferation phenotyping experiments of 50 MARS cell lines were conducted contemporaneously to study the differences of antidepressant-induced changes in proliferation behavior between non-responder and responder derived cell lines. Finally, results of both arms were combined in an edge-group approach as a further validation method to reduce the amount of potential biomarkers for remaining validation experiments.

1.1.1. Screening Experiments

To identify the most suitable experimental setup and method for measurement of individual proliferation rates, screening experiments were carried out using ten LCLs (derived from n=6 responders and n=4 non-responders representing the average patient population with different medication profiles) from MARS study and fluoxetine as indicator drug. During the long-term incubation with different concentrations (0.0, 0.1, 0.5, 10.0 µg/ml) of fluoxetine, cell counts were recorded (three times a week) as well as EdU proliferation assays (weekly) and *MKI67* gene expression (end point measurements after 21 days of *in-vitro* treatment with fluoxetine). On this

occasion, significant proliferative effects were measurable after three weeks of *in-vitro* treatment with therapeutical concentrations of fluoxetine using the EdU assay (Figure 10, A). Between treated and untreated samples no significant differences were detectable by cell counting (Figure 10, B). Very small significant effects were observable by *KI67* gene expression analysis (Figure 10, C).

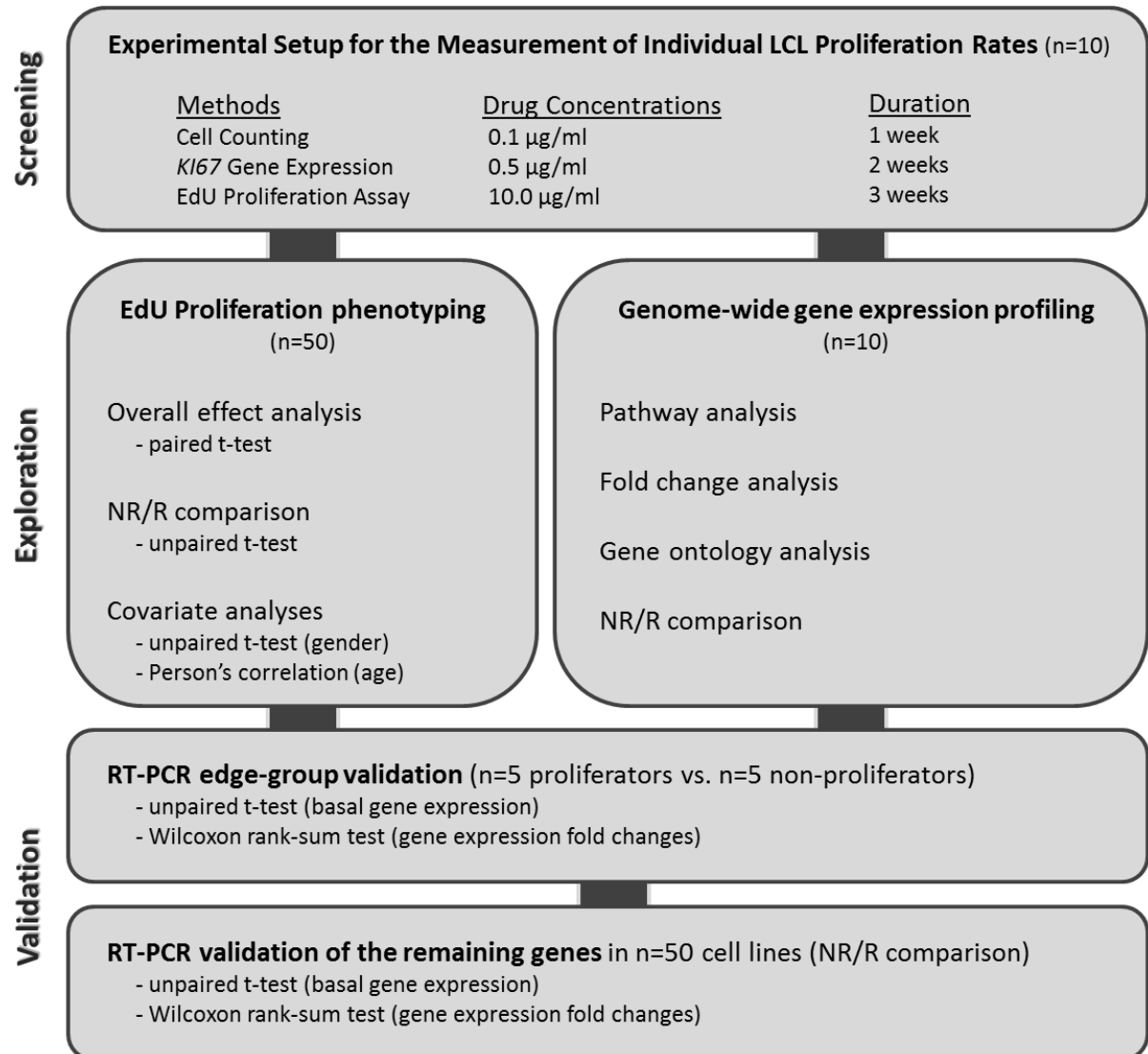


Figure 9: Overview of the three phased project (screening, exploration and validation). After prove-of concept screening experiments which aimed on the identification of suitable experimental conditions, genome-wide gene expression and EdU phenotyping experiments were carried out to identify potential gene expression biomarkers and to explore the association between antidepressant induced LCL proliferation and donor's clinical response status, respectively. Potential biomarkers were characterized in an edge-group approach followed by further RT-PCR validation experiments.

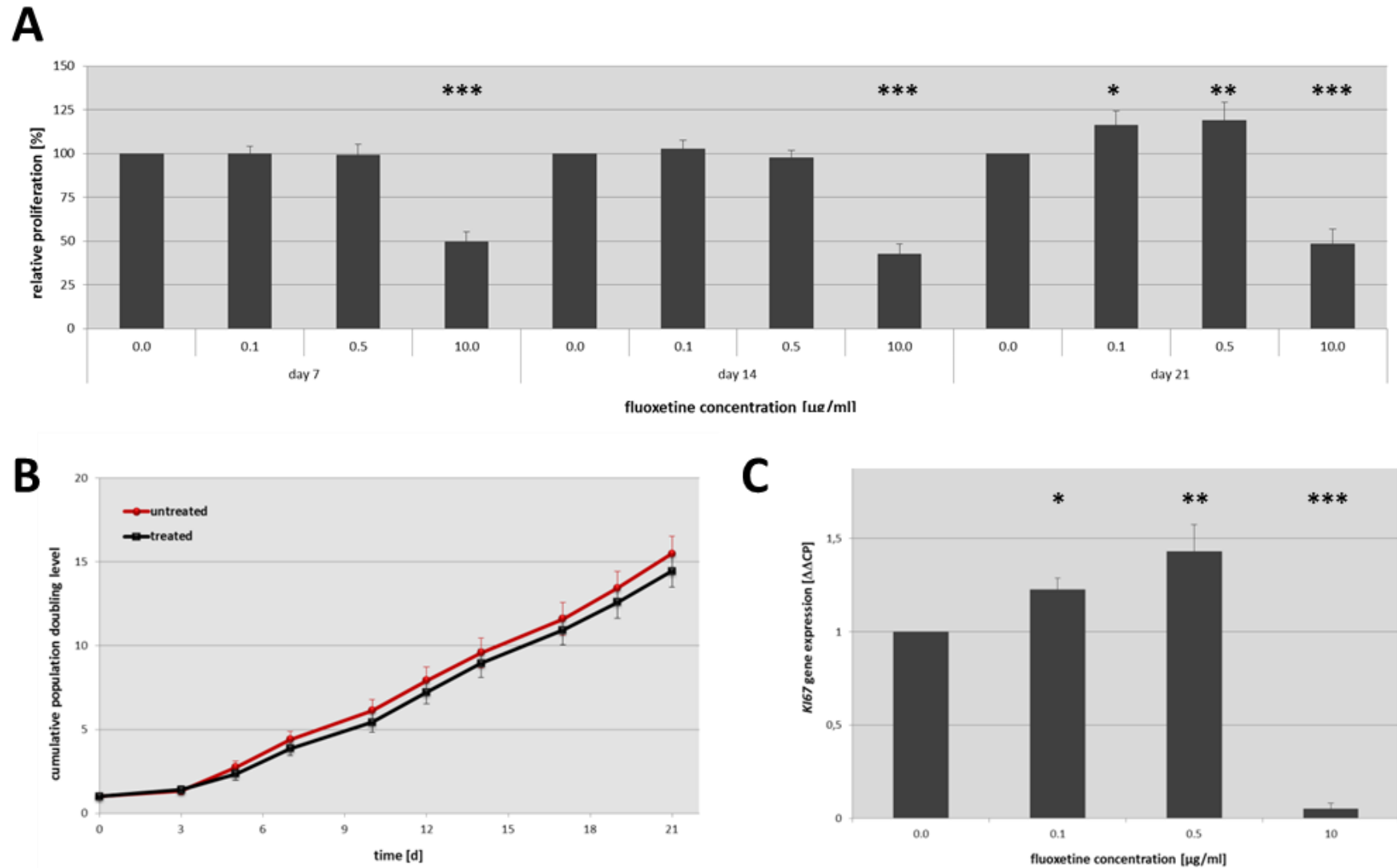


Figure 10: Result of the screening experiments using $n=10$ LCLs derived from the MARS study (values are indicated as means of these $n=10$ samples). Significant proliferative effects were observable by EdU proliferation assays after three weeks of incubation with fluoxetine but not after one or two weeks (A). No significant differences between treated and untreated samples were detectable via cell counting (B). Statistical but no biological significant effects ($FC < 2$) were reported through K167 gene expression experiments (C). Statistical analyses included Student's t tests with p -values: * < 0.05 , ** < 0.01 , *** < 0.001 .

Detection of proliferation by EdU is the only method that directly measures proliferation and that allows a single cell evaluation. Individual differences between cell lines were detectable and most distinct proliferative effects occurred after three weeks of incubation with fluoxetine in therapeutical concentrations (0.1 $\mu\text{g/ml}$ and 0.5 $\mu\text{g/ml}$) (Figure 11). Occasional proliferative effects were reported after one or two weeks of incubation with fluoxetine. Fluoxetine at a final concentration of 10.0 $\mu\text{g/ml}$ show decreased proliferation rates in most of the cell lines.

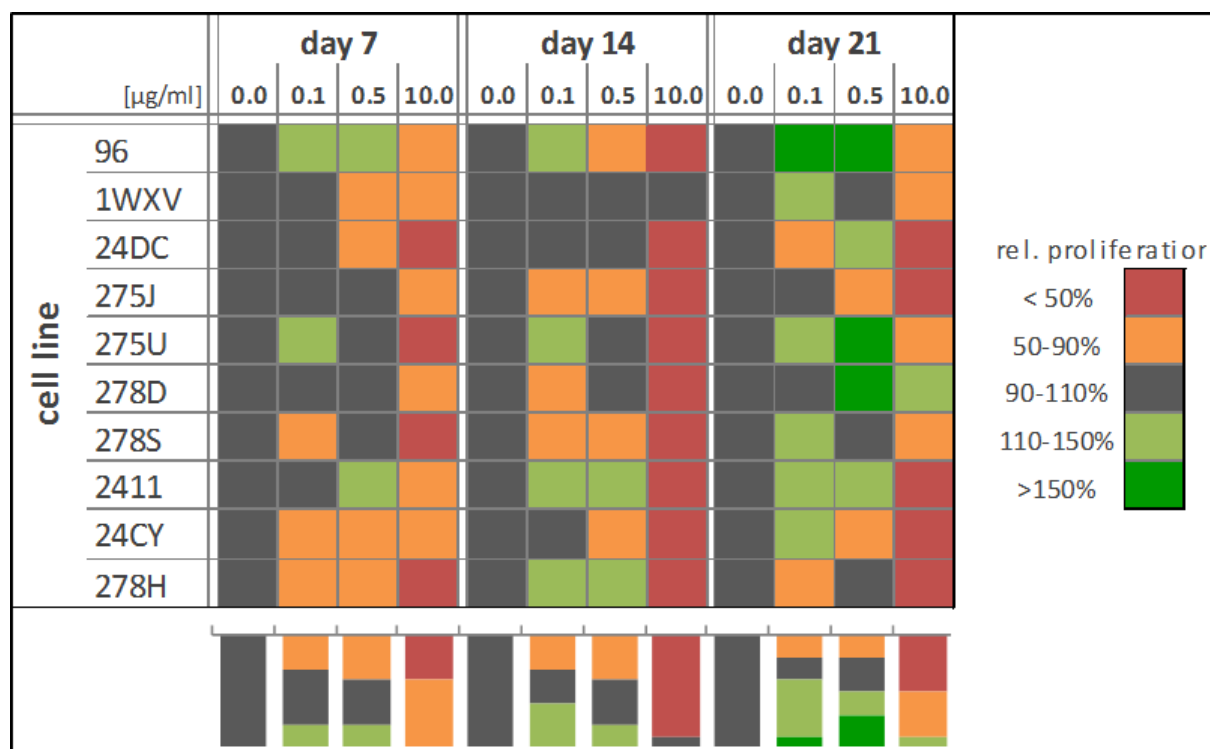


Figure 11: Heat-Map of EdU screening experiments. Ten cell lines were treated with different concentrations of fluoxetine over a time period of three weeks. After one, two and three weeks EdU proliferation assays were carried out. Different colors represent ranges of relative proliferation rates (ratio between fluoxetine treated and untreated controls of the same cell line): Reddish shades indicate a decreased proliferation and different green shades indicate an increase of relative proliferation rates; unchanged proliferation is indicated by black coloring. The occurrence frequency of each color (representing a defined range of relative proliferation) is shown in the bar graphs at the bottom of the figure. Strongest proliferative signals were detectable after three weeks of incubation with therapeutical concentrations of fluoxetine (0.1 $\mu\text{g/ml}$ and 0.5 $\mu\text{g/ml}$).

1.1.2. Proliferation Phenotyping

To assess individual differences in cell proliferative effects of fluoxetine in LCLs from patients with documented clinical response status, we conducted long-term cell incubation with fluoxetine (21 days) revealing a large variability in relative proliferation rates ranging from 54.7 to 155.2% in comparison to untreated cells from the same donor (Figure 12) indicating there are both pro- and anti-proliferative effects of fluoxetine in LCLs. Averaged over all 50 cell lines no significant overall effects were observable ($100.00 \pm 0.0\%$ control vs. 97.25 ± 3.02 ; $p=0.367$).

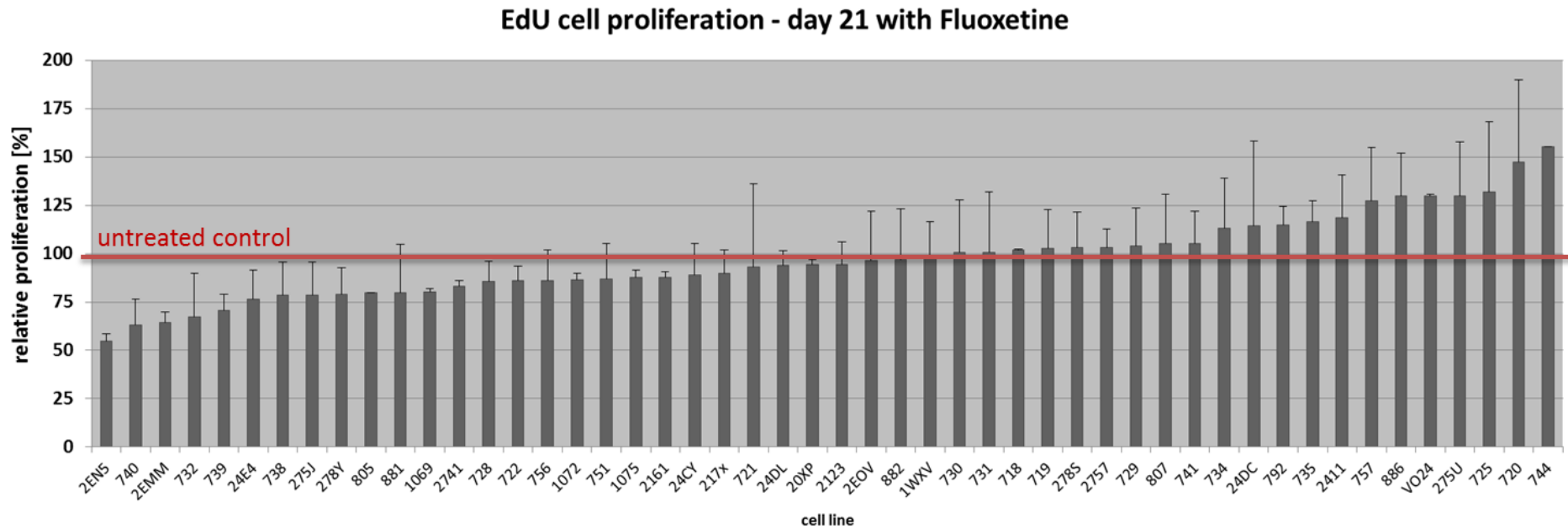


Figure 12: EdU phenotyping of MARS cell lines. A total of n=50 cell lines (n=25 non-responder and n=25 responder derived cell lines) were treated for 21 days with therapeutical concentrations of fluoxetine (0.5 µg/ml). Proliferation rates were measured by EdU proliferation assay and are indicated as values relative to untreated control samples of the same cell lines (relative proliferation values of > 100% mean increased proliferation after fluoxetine treatment). Strong interindividual differences are detectable between the different cell lines ranging from 55% to 155% of relative proliferation rates.

Although there are inter-individual differences, when grouping the cell lines according to their clinical status no significant differences between the proliferation rates of the single groups (non-responder vs. responder) were detectable (Figure 13, A). Basal proliferation, *i.e.* LCL proliferation without fluoxetine, is not associated with clinical response as well (Figure 13, B).

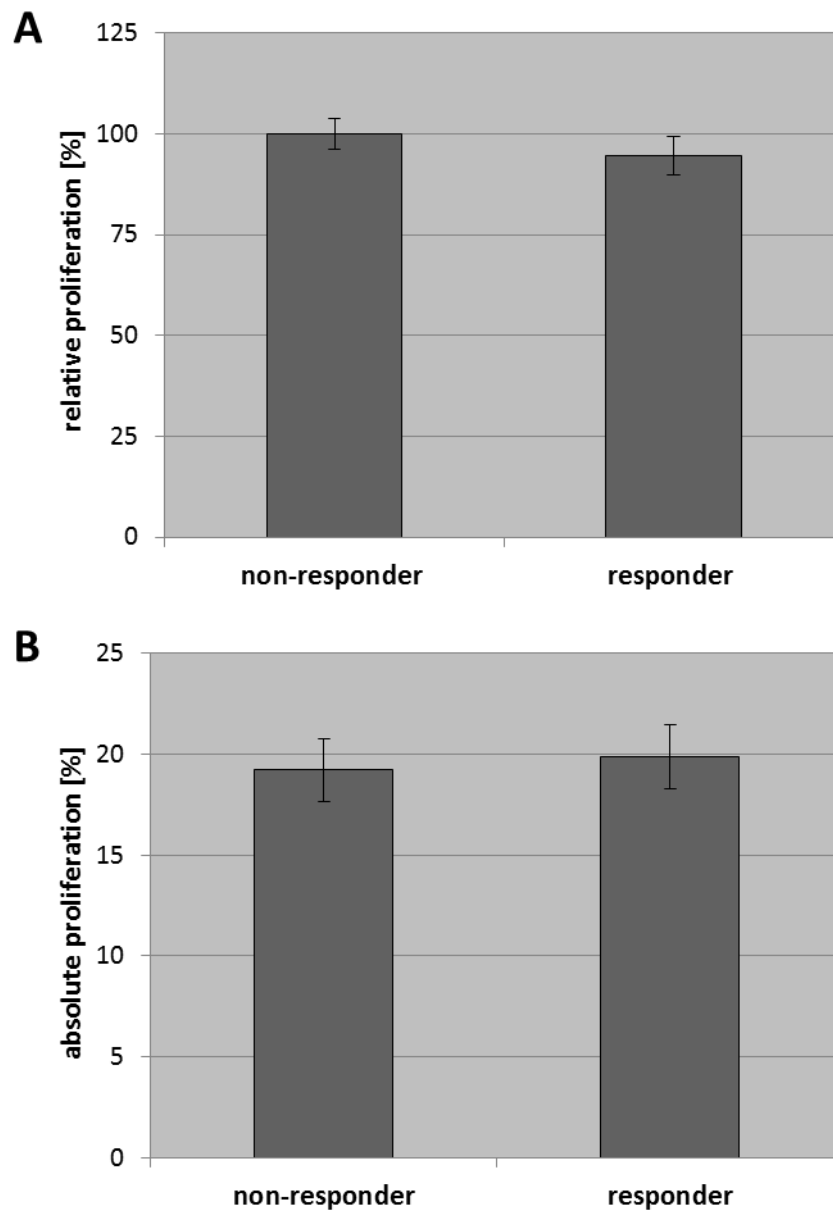


Figure 13: Comparison of relative proliferation (after *in-vitro* treatment with fluoxetine relative to untreated samples from the same donor) between non-responder (n=25) and responder (n=25) derived LCLs (A) and between absolute, basal proliferation (untreated samples from the same donor) of non-responder (n=25) and responder (n=25) derived cell lines (B). Deviations are indicated as standard errors. No significant differences between responder and non-responder derived cell lines are detectable.

Furthermore, we performed a trend analysis to identify a possible relation between individual response and individual LCL proliferation. No significant association was detected by Pearson's correlation analysis ($r=0.082$, $p=0.57$) between proliferation rates and clinical response measured as percentage change in Hamilton-score compared between weeks 0 and 8 (Figure 14).

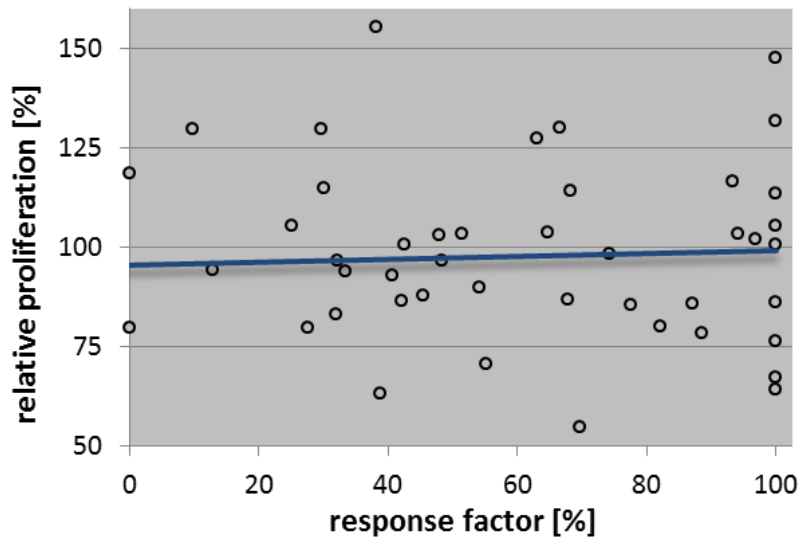


Figure 14: Correlation plot between response factor and relative proliferation. The response factor is defined as percentage change in Hamilton scoring calculated for each participant between values at study inclusion (week 0) and at study end (week 8). Consequently, a cell line with a response factor > 50% is classified as responder. Individual relative LCL proliferation after three weeks of incubation with therapeutical concentrations of fluoxetine (0.5 $\mu\text{g}/\text{ml}$) is indicated as ratio to the untreated sample of the same cell line. By Pearson's correlation analysis no association between response factor and relative proliferation is detectable ($r=0.082$ with $p=0.57$).

The covariates gender (Figure 15, A) and age (Figure 15, B) showed no significant impact on individual proliferation rates by unpaired Student's t-test ($p_{\text{gender}}=0.513$) and Pearson's correlation analysis ($r_{\text{age}}=0.071$ with $p_{\text{age}}=0.622$). The same applies for donor's underlying diseases, *i.e.* bipolar disorder, single episode major depressive disorders and recurrent major depressive disorders where no significant differences were detectable (Figure 16).

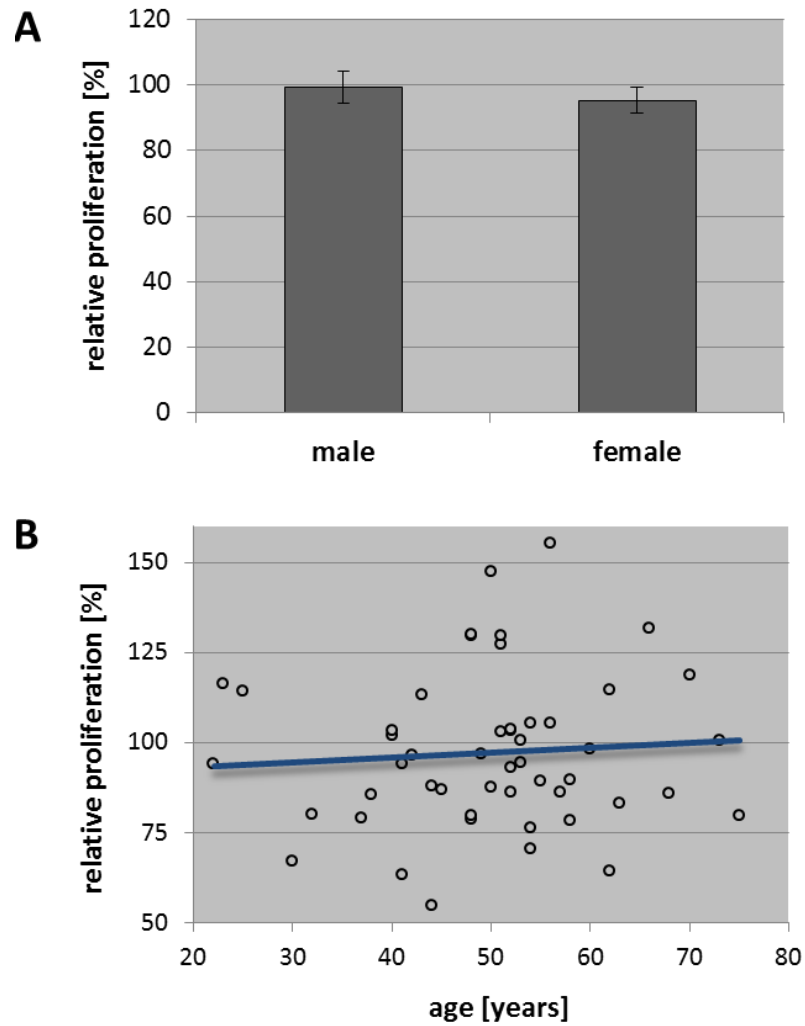


Figure 15: Analyses of the covariates gender (A) and age (B) and their impact on relative proliferation rates (after 21 days of continuous treatment of $n=50$ LCLs with therapeutical concentrations of fluoxetine compared to untreated controls from the same cell lines). No significant impact of gender or age on relative proliferation rates was observable by Student's t-test ($p_{\text{gender}}=0.513$) or Pearson's correlation analysis ($r_{\text{age}}=0.071$ with $p_{\text{age}}=0.622$). Deviations are indicated as standard errors.

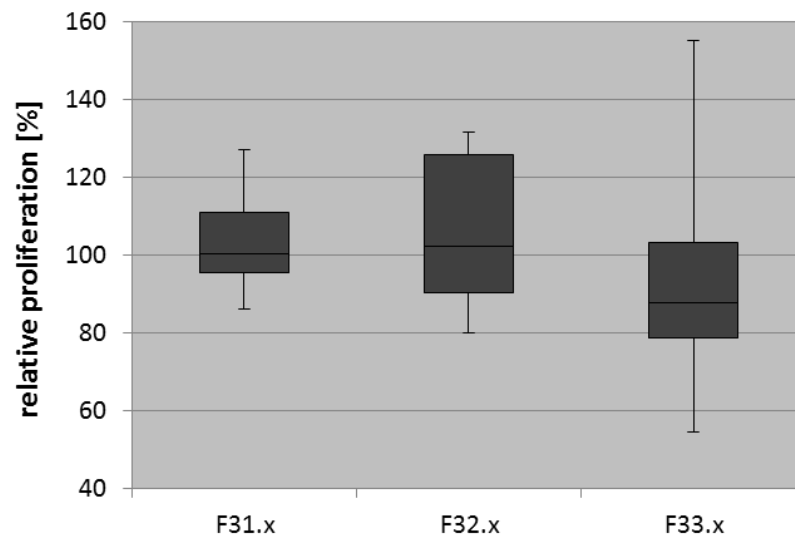


Figure 16: Box plot of relative proliferation and donor's underlying diseases indicated as International Statistical Classification (ICD) codes: F31.x - bipolar disorder ($n=7$); F32.x - single episode major depressive disorders ($n=10$); F33.x - recurrent major depressive disorders ($n=33$). No significant differences were detectable ($p=0.799$; $p=0.237$; $p=0.889$).

1.1.3. Identification of Potential Gene Expression Markers

The gene expression changes of $n=10$ LCLs (identical to those used in the screening experiments) was measured in a genome-wide approach to characterize gene expression changes by long-term fluoxetine and to identify potential gene expression biomarkers. Gene expression profiles were compared between untreated samples and samples treated for 21 days with $0.5 \mu\text{g/ml}$ of fluoxetine which is similar to the range in plasma concentrations in patients. Microarray data were deposited in NCBI's Gene Expression Omnibus (GEO) database^{163, 164} and are accessible through GEO Series accession number GSE83386.

From 27,000 available genetic features, up to 15,241 were differentially regulated ($\text{FC} > 2$) in cell line 275U whereby only 3,501 genes were affected in cell line 278S indicating vast inter-individual differences in fluoxetine-induced gene expression profiles (Figure 17). Averaged over all ten cell lines they differentially expressed $7,715 \pm 1,271$ genes ($\text{FC} > 2$), 960 ± 164 genes ($\text{FC} > 5$) and 282 ± 41 ($\text{FC} > 10$) genes.

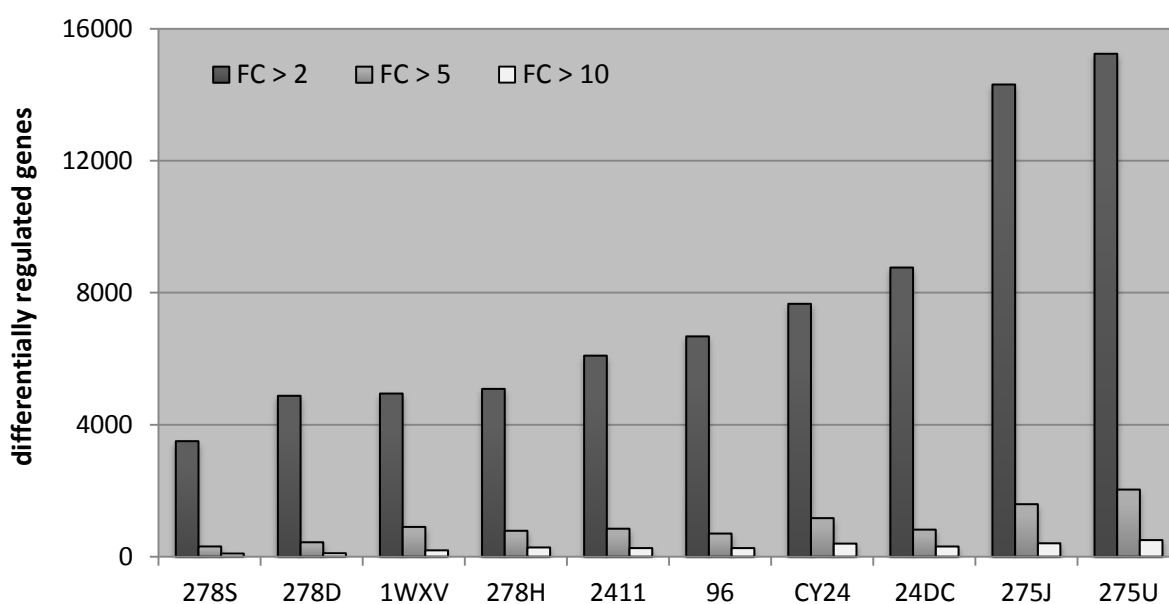


Figure 17: Quantities of differentially regulated genes ($\text{FC} > 2$, $\text{FC} > 5$ and $\text{FC} > 10$) in ten LCLs after three-week incubation with fluoxetine compared to untreated controls of the same samples and measuring gene expression profiles by Agilent microarray system with approximately 27,000 biological features.

From this huge number of genes, potential genetic expression biomarkers, *i.e.* genes differentially regulated in non-responder and responder derived cell lines, need to be detected. To this end, various filtering techniques which are implemented in the microarray analysis software were applied (briefly summarized in Table 8 together with a short explanation of the techniques and the number of remaining genes after application of the appropriate filter) in order to successively

decrease the number of genes and therefore, to identify potential gene expression biomarkers. The results from each method will be described in detail in the following sections of this work.

Table 8: Overview of different filtering methods for the identification of potential gene expression biomarkers out of the whole-genome gene expression data and their particular impact of remaining number of genes (n).

filter technique	Additional information	n
Cluster analysis	Identification of cell lines clusters with different gene expression profiles (compared between untreated and fluoxetine-treated samples)	3,501 - 15,241
Pathway analysis	Identification of pathways inversely regulated in NR and R derived indicator cell lines	390
Fold change analysis	Filtering of genes obtained from pathway analysis according to their FCs after <i>in-vitro</i> treatment of the cell lines with fluoxetine	127
Gene ontology analysis	Functional check point analysis	127
NR/R-comparison	Filtering of inversely regulated genes between NR and R derived cell lines	15
edge-group analysis	Comparison of gene expression between cell lines with most distinct anti- and pro-proliferative effects from EdU phenotyping	5

NR - non-responder, R - responder

The first method applied was a cluster analysis that aims on the identification of cell line clusters with different gene expression profiles compared between fluoxetine-treated and mock-treated samples of the same cell lines. Figure 18 shows the hierarchical clustering tree of the used cell lines that have been treated with fluoxetine for 21 days versus untreated control samples of the same cell lines. Except of cell lines 275U, 275J and 24DC, all samples of the same cell lines are located within the same cluster. This means these three cell lines showed great gene expression changes after *in-vitro* treatment with fluoxetine. The remaining cell lines (278S, 278D, 278H, 2411, 96, CY24 and 1WXV) experienced no substantial differences in gene expression after fluoxetine incubation on gene cluster level.

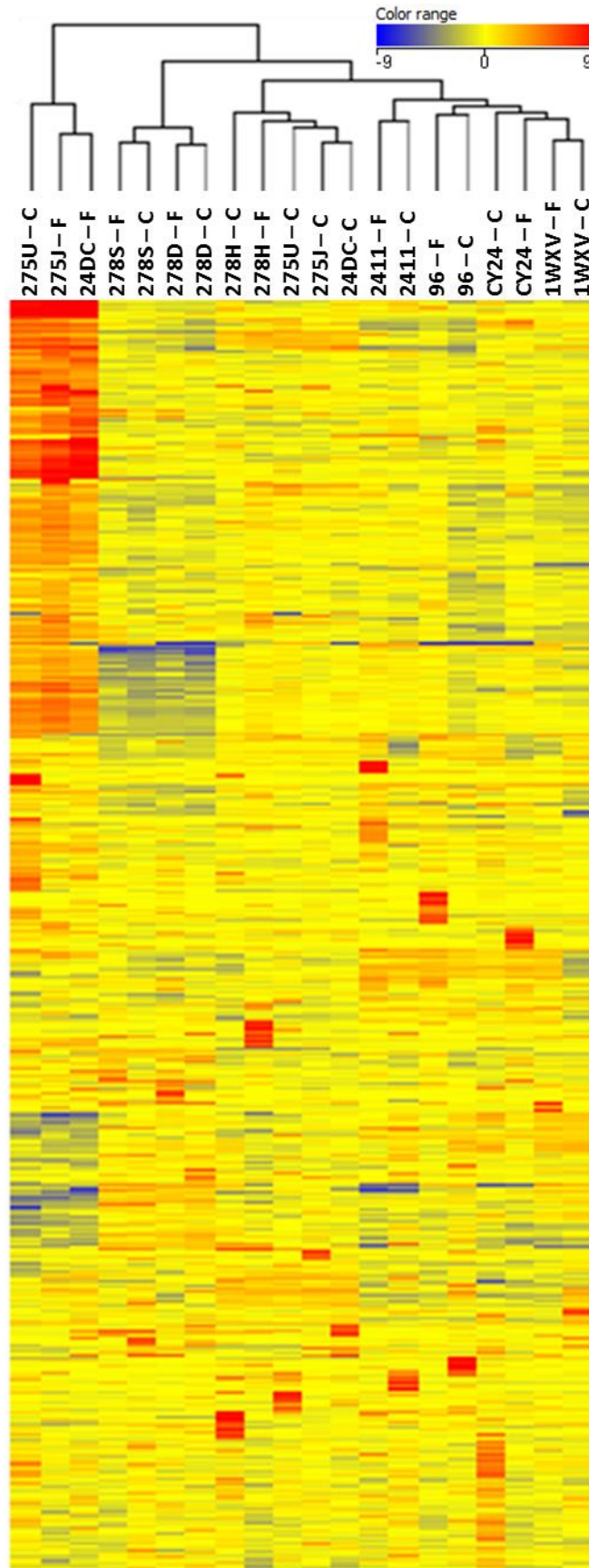
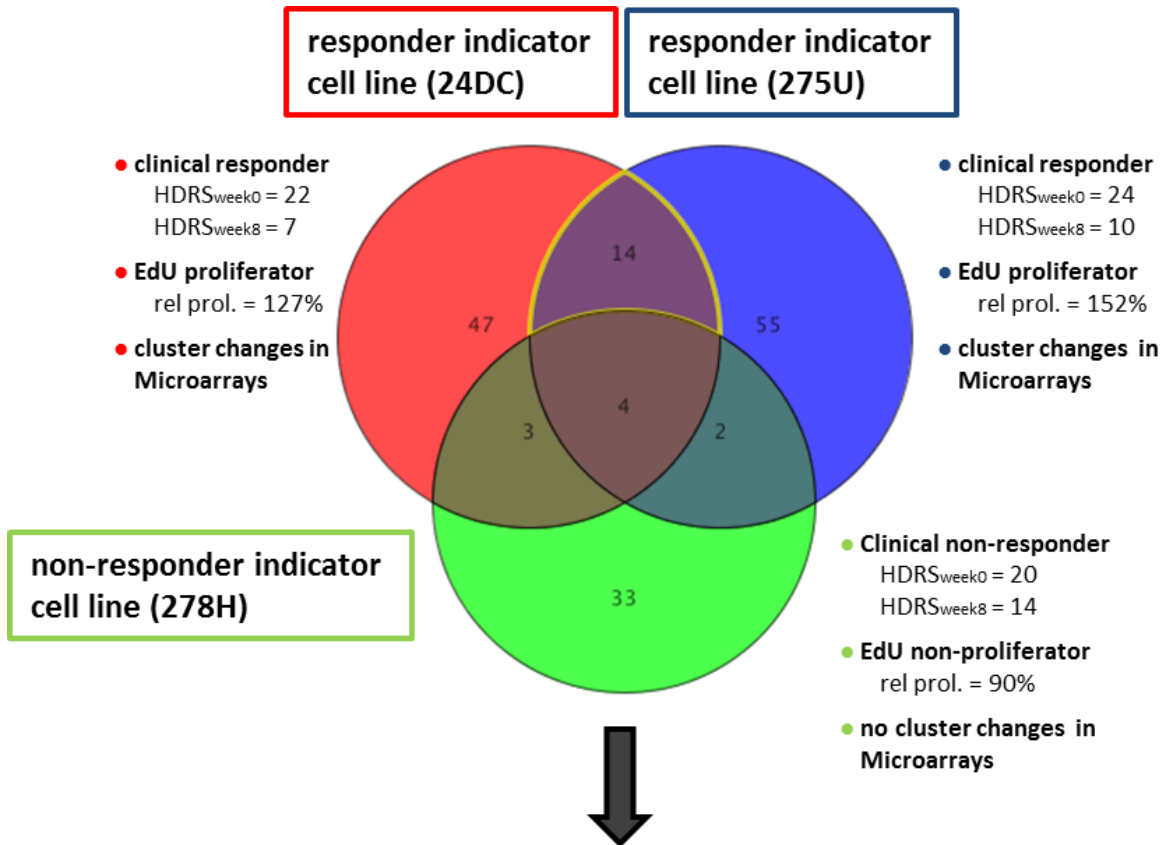


Figure 18: Dendrogram of the hierarchical clustering analysis of the ten LCLs after three weeks of incubation with fluoxetine compared to untreated samples of the same cell lines. Up- and down-regulated genes are indicated by blue and red coloring, respectively. The most distinct changes in gene expression were recorded for the cell lines 275U, 275J and 24DC.

Secondly, a pathway analysis was carried out in three indicator cell lines (characterized by rectified clinical response status, experimental EdU proliferation status and hierarchical clustering status obtained from microarray experiments) to identify pathways that are involved in individual fluoxetine action and that possibly contain potential gene expression biomarkers. The pathway analysis revealed different amounts of significantly activated pathways by fluoxetine in the cell lines 24DC (67 pathways), 275U (75 pathways) and 278H (42 pathways). Compared between responder and non-responder indicator cell lines (24DC and 275U vs. 278H), 14 inversely-regulated pathways were highlighted by Venn-analysis (Figure 19) that contain a total of 192 differentially expressed genes after incubation with fluoxetine ($FC > 2$, $p < 0.05$). The functions of this gene set were characterized by STRING-based GO analysis (Table 9). A total of 127 genes were reported to be involved in GO terms associated with brain remodeling processes such as neurogenesis (generation of neurons), axonogenesis (generation of axons), neuron differentiation (specialization of neural progenitor cells to neurons) or neuron projection (prolongation of nerve cells like axon or dendrite formation).

Gene expression differences of these genes between non-responder and responder derived cell lines as measured by microarray experiments were evaluated. After consideration of individual cell line donor's response status, 15 genes showed differences (FC difference > 2) in gene expression between responder ($n=6$) and non-responder ($n=4$) derived cell lines. The gene names, mean fold change differences as well as their annotated CNS functions are listed in Table 10. Gene expression differences between responder and non-responder fold changes by fluoxetine range from 40.3 for *BTC* to 2.0 for *ERBB3* (epidermal growth factor receptor 3). All these genes can be assigned to either WNT signaling pathways (e.g. *WNT2B*, *FZD7*, *TCF7L2*) or EGF signaling pathways (e.g. *BTC*, *EGFR*, *HBEGF*) or to a group of pharmacokinetic genes (e.g. *CYP3A43*, *SULT4A1*, *ABCB1*, *ABCG4*). According to literature, most of these genes can be associated with brain-specific functions such as neuroplasticity, neural cell proliferation or stem cell regulation. Consequently, these genes were appointed as candidate gene expression biomarker genes and were used for further investigation.



Pathways	p-value	
Wnt Signaling Pathway and Pluripotency	WP399_54212	2.1e-4
	WP399_45007	3.4e-4
	WP399_74897	8.1e-4
Polyol Pathway	WP690_45266	8.7e-4
Arrhythmogenic Right Ventricular Cardiomyopathy	WP2118_47057	1.0e-3
	WP2118_71265	1.0e-3
ErbB Signaling Pathway	WP673_29836	9.9e-3
	WP673_41091	1.7e-2
	WP673_69914	1.7e-2
Sulfation Biotransformation Reaction	WP692_48223	1.7e-2
TCA Cycle	WP78_47741	2.4e-2
RaiA Downstream Regulated Genes	WP2290_53118	5.3e-2
	WP2290_51121	5.3e-2
	WP2290_69039	5.3e-2

Figure 19: Pathway analysis combined with Venn analysis revealed 14 pathways (yellow frame) differentially regulated between responder and non-responder indicator cell lines (24DC and 275U vs. 278H). Indicator cell lines are characterized by rectified LCL donor’s clinical response status, proliferation status and hierarchical clustering status. Due to different pathway versions with nearly identical pathways, only seven really different pathways remained (left column). P-values were calculated by GeneSpring X12 microarray software (Agilent) and are adjusted for multiple testing.

Table 9: Overview of the 30 most significant GO terms from the genes identified by Venn analysis. Brain and neuron specific GO terms are bold. P-values were calculated by STRING web-tool and indicated as uncorrected p-values and Benjamini-Hochberg corrected p-values (n is the number of identified genes being involved in particular GO terms).

GO Term	p-value	corrected p-value	n
Neuron differentiation (GO:0030182)	5.98e-27	7.54e-23	44
Generation of neurons (GO:0048699)	2.03e-25	8.22e-22	47
Neuron projection development (GO:0031175)	2.24e-25	8.22e-22	37
Axon development (GO:0061564)	3.00e-25	8.22e-22	34
Response to chemicals (GO:0042221)	3.26e-25	8.22e-22	76
Cell development (GO:0048468)	6.83e-25	1.43e-21	50
Neuron projection morphogenesis (GO:0048812)	1.08e-24	1.94e-21	34
Cellular response to chemical stimulus (GO:0070887)	1.47e-23	2.32e-20	57
Axonogenesis (GO:0007409)	1.91e-23	2.68e-20	32
Positive regulation of signal transduction (GO:0009967)	3.29e-23	4.14e-20	43
Fc receptor signaling pathway (GO:0038093)	6.87e-23	7.27e-20	27
Neuron development (GO:0048666)	6.92e-23	7.27e-20	37
Cell projection morphogenesis (GO:0048858)	8.93e-23	8.66e-20	35
Canonical Wnt signaling pathway (GO:0060070)	1.04e-22	9.41e-20	18
Response to wounding (GO:0009611)	1.51e-22	1.27e-19	42
Positive regulation of signaling (GO:0023056)	1.93e-22	1.52e-19	43
Neurogenesis (GO:0022008)	2.10e-22	1.53e-19	45
Cell part morphogenesis (GO:0032990)	2.18e-22	1.53e-19	35
Cell morphogenesis (GO:0000902)	1.27e-21	8.42e-19	37
Regulation of signal transduction (GO:0009966)	1.52e-21	9.079e-19	57
Cell morphogenesis involved in neuron differentiation (GO:0048667)	1.54e-21	9.079e-19	31
Cell projection organization (GO:0030030)	1.58e-21	9.079e-19	38
Positive regulation of cell communication (GO:0010647)	2.02e-21	1.11e-18	42
Wound healing (GO:0042060)	2.25e-21	1.18e-18	34
Positive regulation of protein metabolic process (GO:0032270)	2.45e-21	1.21e-18	41
Cell morphogenesis involved in differentiation (GO:0000904)	2.49e-21	1.21e-18	33
Response to growth factor (GO:0070848)	4.32e-21	2.02e-18	32
Immune response-regulating cell surface receptors (GO:0002768)	4.74e-21	2.12e-18	28
Cellular response to organic substance (GO:0071310)	4.88e-21	2.12e-18	49
Regulation of signaling (GO:0023051)	9.04e-21	3.80e-18	59

Table 10: Comparison of mean gene expression levels between responder and non-responder cell lines (n=10) and their annotated gene functions. Gene names are arranged by decreasing FC differences. CNS functions were systematically searched using the gene names and one of the following terms: brain, neuron, neurogenesis, neural plasticity, proliferation, depression or antidepressant.

gene (Entrez ID)	mean FC difference (Responder vs. Non-Responder)	CNS function
<i>BTC</i> (685)	40.30	Stimulation of cell proliferation and neurogenesis ¹⁶⁵
<i>WNT2B</i> (7482)	26.20	Regulation of pro-neural genes ¹⁶⁶
<i>EGFR</i> (1956)	18.40	neural progenitor cells proliferation and migration ¹⁶⁷
<i>CYP3A43</i> (64816)	6.90	antipsychotic metabolism ¹⁶⁸
<i>PIK3R5</i> (23533)	6.70	risk factor for insomnia and suicides ¹⁶⁹⁻¹⁷¹
<i>SULT4A1</i> (25830)	6.20	brain-specific sulfate conjugation of drugs and neurotransmitters ¹⁷²
<i>FZD7</i> (8324)	5.40	receptor for Wnt proteins in brain ¹⁷³
<i>CACNA2D3</i> (55799)	5.30	possible role in long-term antidepressants action ¹⁷⁴
<i>TCF7L2</i> (6934)	4.73	transcription factor in Wnt pathway ¹⁷³
<i>ABCG4</i> (64137)	4.10	regulation of lipid homeostasis in neurons and astrocytes ^{175, 176}
<i>TCF7</i> (6932)	3.60	transcription factor in Wnt pathway ¹⁷³
<i>HBEGF</i> (1839)	3.50	Neurogenesis and astrocytes proliferation ¹⁷⁷
<i>MAPK9</i> (5601)	2.50	mediates apoptosis in dopaminergic brain areas ¹⁷⁸
<i>ABCB1</i> (5243)	2.45	export of neurotoxic agents in BBB ¹⁷⁹
<i>ERBB3</i> (2065)	2.00	nervous system development ¹⁸⁰

To further characterize the candidate genes in an *in-silico* approach, possible interactions of these identified candidate genes were investigated: The prediction of protein interactions based on physical (direct) and functional (indirect) connections by STRING functional protein association's network revealed some interactions between the 15 top-hit genes (Figure 20). As expected, the strongest interactions were observable for the proteins of the WNT and EGF pathways and interestingly, both of these pathways show interactions with each other as well (*e.g.* WNT2B with EGFR or TCF7L2 with ERBB3). No associations were detectable for SULT4A1, CYP3A43, ABCG4 and CACNA2D3.

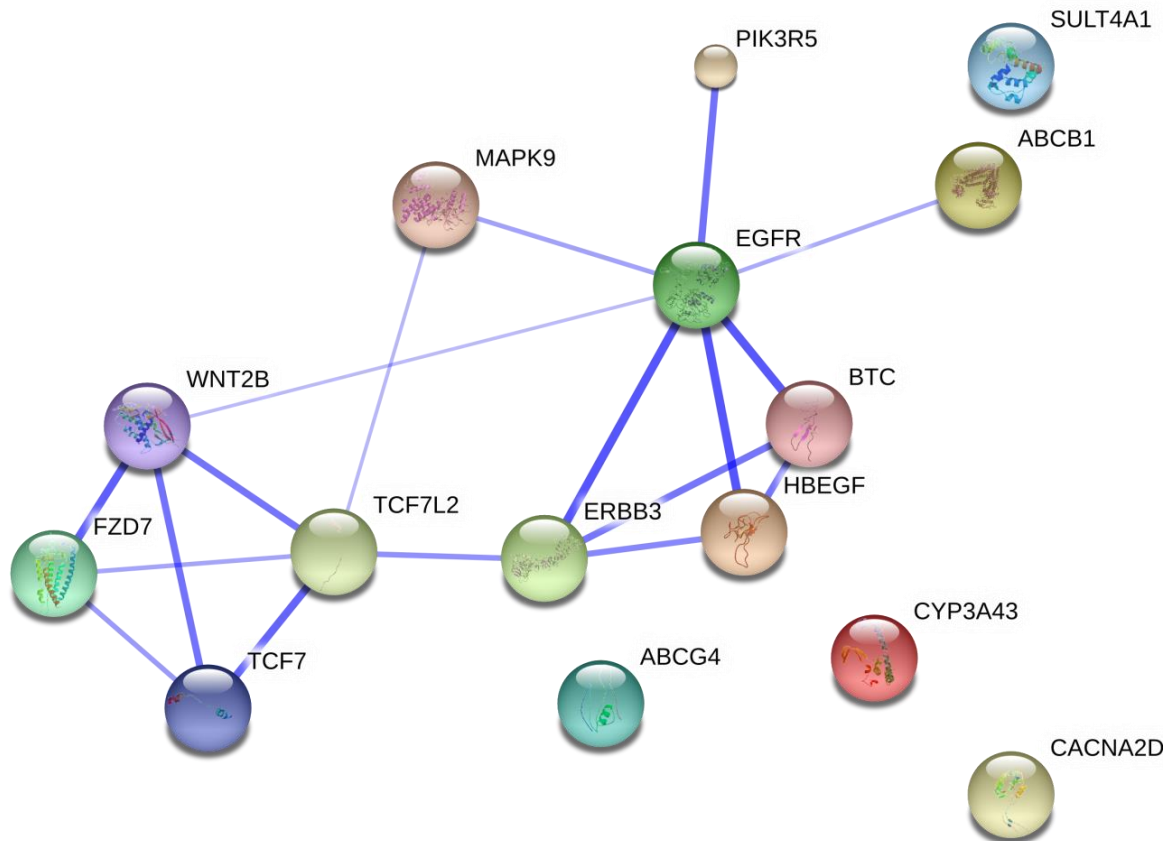


Figure 20: STRING based protein interaction network of the 15 top-hit genes from microarray experiments after three weeks of incubation with therapeutical concentrations of fluoxetine. Network lines represent interactions between the proteins and the thicker the lines the stronger are the associations between the different gene products. The *in-silico* predictions of protein interactions such as physical or functional connections are based on scores from the STRING interaction database ¹⁵³.

To assess the potential of the identified candidate genes and their association with individual LCL proliferation after *in-vitro* treatment with fluoxetine, gene expression was analyzed in an edge-group approach (in similarity to the work of Morag and colleagues ¹¹⁷). Both the basal gene expression and fluoxetine-induced changes in gene expression were compared between the two phenotypic edges of EdU phenotyping (five cell lines each) which is similar to those cell lines with the most distinct fluoxetine-induced anti-proliferative and pro-proliferative effects. Among the 15 identified genes from the microarray experiments, the basal gene expression of four genes was significantly different from non-proliferator cell lines compared to proliferator cell lines: *WNT2B* ($p=0.046$), *TCF7L2* ($p=0.018$), *SULT4A1* ($p=0.035$) and *ABCB1* ($p=0.046$) (Figure 21). After consideration of the clinical response status from the donors of these cell lines, no significant differences were detectable between LCL gene expression and donor's clinical response and non-response or between donor's clinical remission and non-remission after five and eight weeks of antidepressant treatment during the MARS study (Figure 22).

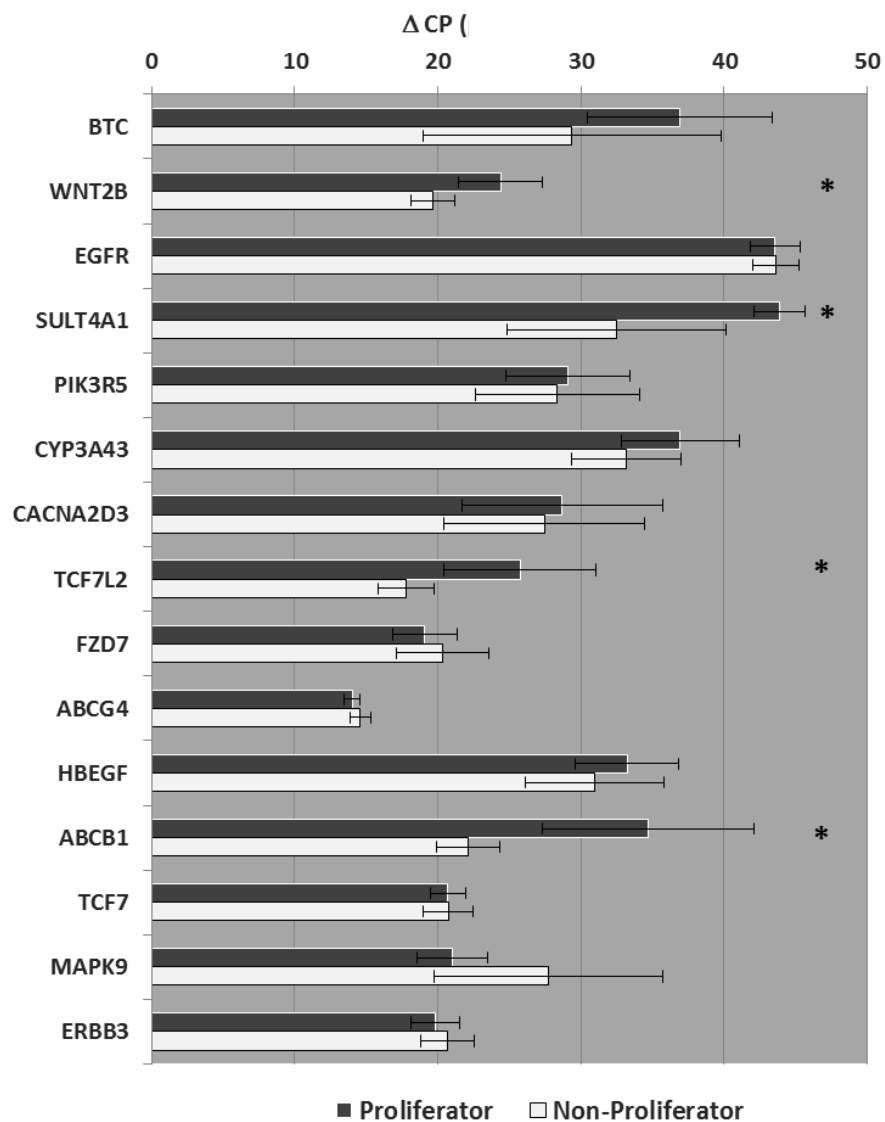


Figure 21: Basal gene expression of the candidate genes in an edge-group analysis from EdU phenotyping experiments (proliferators vs. non-proliferators). Basal gene expression is indicated as ΔCT values using GAPDH as reference gene. Significance was tested by unpaired Student's t test.

Additionally, fold change analyses were performed to characterize the effect of fluoxetine on the gene expression of the candidate genes. Results of the fold change analyses significantly correlated with *in-vitro* proliferation of genes *WNT2B* ($p=0.032$), *TCF7L2* ($p=0.008$) and *FZD7* ($p=0.016$) (Table 11). The remaining genes showed no statistically significant effects of fluoxetine on gene expression levels between non-proliferator and proliferator cell lines.

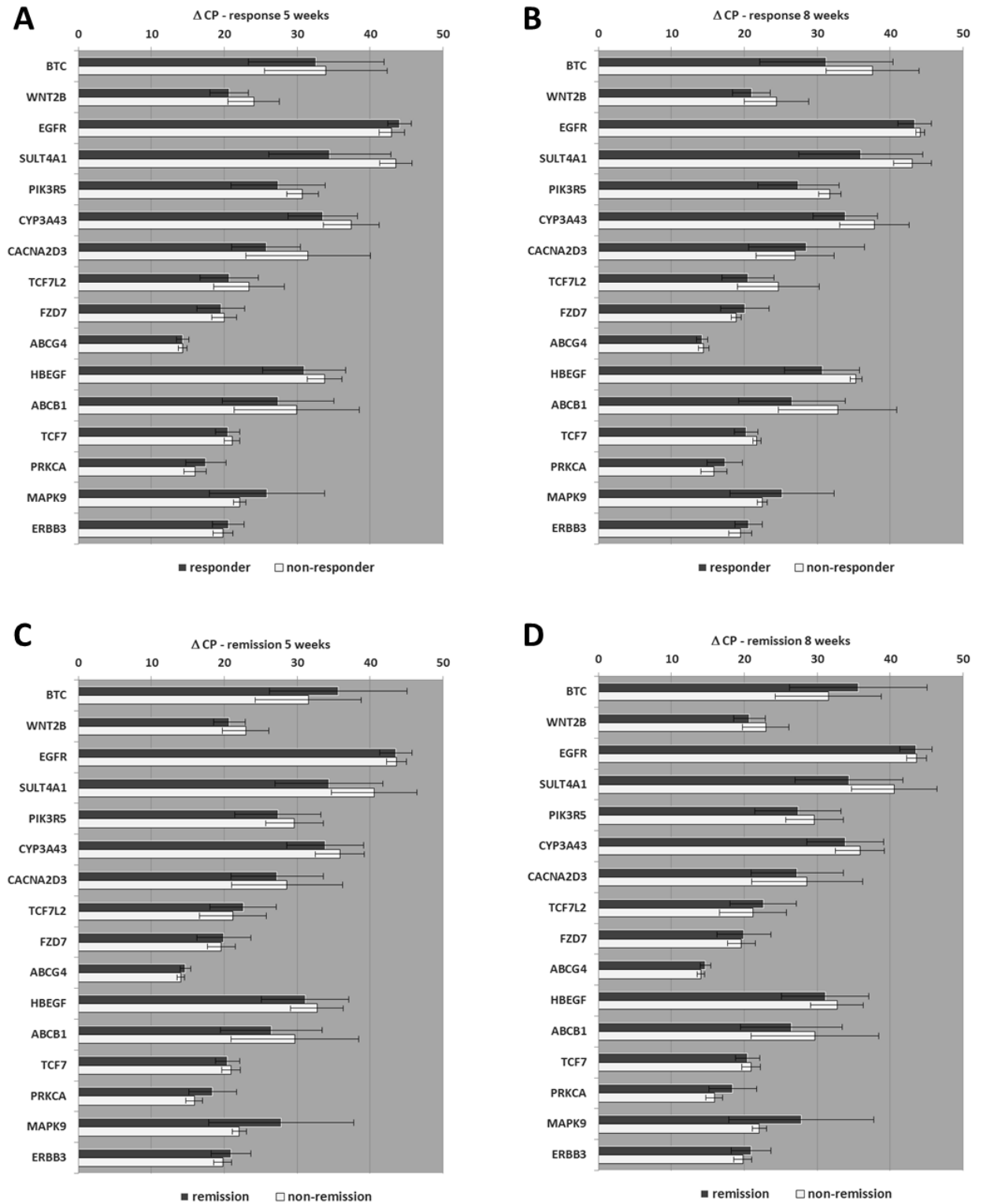


Figure 22: Basal gene expression of the candidate genes in cell lines derived from donors with non-response or response after five (A) and eight weeks (B) and cell lines derived from donors with remission or non-remission after five (C) and eight weeks (D). Clinical improvement was rated after five and eight weeks by HDRS. No significant correlations between basal gene expressions of the candidate genes with clinical parameters of LCL donors were detectable.

Table 11: Fold change values of the candidate genes identified through microarray experiments after three weeks of *in-vitro* treatment with therapeutic concentrations of fluoxetine obtained in ten different LCLs in an edge-group approach after EdU phenotyping. Statistical analysis was carried out by Wilcoxon-Mann-Whitney rank-sum test and significant p-values are bold and underlined.

	cell line	<i>BTC</i>	<i>WNT2B</i>	<i>EGFR</i>	<i>SULT4A1</i>	<i>PIK3R5</i>	<i>CYP3A43</i>	<i>TCF7L2</i>	<i>FZD7</i>	<i>ABCG4</i>	<i>HBEGF</i>	<i>ABCB1</i>	<i>TCF7</i>	<i>PRKCA</i>	<i>MAPK9</i>	<i>ERBB3</i>
Proliferators	744	51.2	10.4	1.2	n.e.	2.0	n.e.	>1,000	-60.4	1.2	2.7	>1,000	0.1	-0.1	1.3	0.1
	720	n.e.	0.01	n.e.	175.0	-40.2	-16.4	481.6	-2.8	1.3	-5.4	-1.9	1.5	-0.4	-2.7	-1.9
	725	>1,000	695.2	n.e.	>1,000	-1.2	>1,000	>1,000	<-1,000	5.8	<-1,000	>1,000	-0.8	37.9	0.4	1.1
	275U	n.e.	29.5	n.e.	n.e.	-110.9	-8.6	6.9	-119.8	-1.9	<-1,000	>1,000	2.5	0.0	-5.8	-2.1
	VO24	n.e.	>1,000	n.e.	n.e.	1.3	n.e.	>1,000	-306.5	6.1	n.e.	>1,000	>1,000	-1.4	3.3	2.1
	mean	>1,000	>1,000	1.2	>1,000	-29.8	349.7	>1,000	<-1,000	2.5	<-1,000	>1,000	>1,000	7.2	-0.7	-0.1
Non-Proliferators	2EN5	-2.1	1.4	-18.4	n.e.	-2.1	1.1	1.7	2.0	-1.6	-2.4	1.1	-4.6	-3.0	1.7	-5.1
	740	n.e.	-0.7	n.e.	n.e.	-1.1	1.7	0.3	-6.5	-1.1	2.7	-5.6	0.1	-2.1	-7.4	-0.9
	2EMM	n.e.	-63.7	n.e.	n.e.	27.4	6.0	6.8	44.8	-0.7	27.6	0.3	-0.2	506.4	>1,000	11.5
	732	n.e.	-1.6	n.e.	-0.3	-0.1	-28.9	1.8	1.9	-0.2	0.5	0.1	-2.1	2.6	390.7	-0.1
	739	<-1,000	2.6	n.e.	-3.6	1.7	2.9	2.7	2.5	4.1	2.1	1.4	3.1	2.2	95.0	0.7
	mean	<-1,000	-12.4	-18.4	-1.9	5.2	-3.4	2.6	8.9	0.1	6.1	-0.5	-0.7	101.2	>1,000	1.2
p-value	0.095	<u>0.032</u>	1.000	0.333	0.421	1.000	<u>0.008</u>	<u>0.016</u>	0.310	0.571	0.095	0.222	1.000	0.222	1.000	

n.e. - not expressed ($C_p > 55$)

Further validation of the candidate genes was performed: Changes in candidate gene expression were assessed after 21 days incubation with fluoxetine in all LCLs from EdU phenotyping experiments (n=50) limited to the five remaining genes showing significant differences in the EdU phenotyping edge-group approach. The associations between LCL gene expression and both the LCL donor's remission and response status were investigated (Table 12). Basal gene expression of *SULT4A1* correlated with donor's clinical response after five weeks (p=0.029). However, basal gene expression of *SULT4A1* was low and only detectable in 10 out of 50 cell lines (n=4 non-responder derived cell lines vs. n=6 responder derived cells). Furthermore, the gene expression fold changes of *WNT2B* after treatment with fluoxetine correlated with clinical remission status after five weeks (p=0.025). The remaining genes *TCF7L2*, *FZD7* and *ABCB1* showed no significant correlations with clinical parameters of LCL donors.

Table 12: Statistical overview of LCL donor's clinical outcome and LCL gene expression of the candidate genes in all tested MARS LCLs (n=50). Significant p-values are bold and underlined. Significance was calculated Student's t test (basal gene expression) and Wilcoxon rank sum test (gene expression fold changes).

		<i>WNT2B</i>	<i>SULT4A1</i>	<i>TCF7L2</i>	<i>FZD7</i>	<i>ABCB1</i>
basal gene expression	Response	n.s.	<u>0.029</u>	n.s.	n.s.	n.s.
	Remission	n.s.	n.s.	n.s.	n.s.	n.s.
fold changes after <i>in-vitro</i> treatment with fluoxetine	Response	n.s.	n.s.	n.s.	n.s.	n.s.
	Remission	<u>0.025</u>	n.s.	n.s.	n.s.	n.s.

n.s. - not significant

1.2. Results from the STAR*D Cohort

STAR*D was an open label, randomized, multicenter, controlled clinical study aiming on the definition of effective subsequent treatment strategies after a first unsuccessful antidepressant therapy. All patients were treated with a citalopram monotherapy at the initial phase of this study. A total of 50 cell lines were obtained and were chosen to cover n=25 first-line therapy responders to citalopram and n=25 treatment resistant patients. Similar to previous experiments using LCLs from the MARS cohort, proliferation phenotyping was carried out after three weeks of *in-vitro* treatment with therapeutical concentrations of fluoxetine and citalopram. Additionally, the potential candidate gene expression biomarkers identified by microarray experiments of the MARS LCLs were further characterized and validated within this STAR*D cohort.

1.2.1. Proliferation Phenotyping

Individual variability of cell proliferative effects by SSRIs between n=50 STAR*D LCLs from various donors treated with citalopram monotherapy over the course of the STAR*D trial was assessed by EdU proliferation assays. After incubation of LCLs with therapeutic concentrations of citalopram or fluoxetine for three weeks, EdU-based proliferation phenotyping experiments revealed strong inter-individual differences between single cell lines (Figure 23). Both anti- and pro-proliferative effects were reported with relative proliferation rates ranging from 0% to 428%.

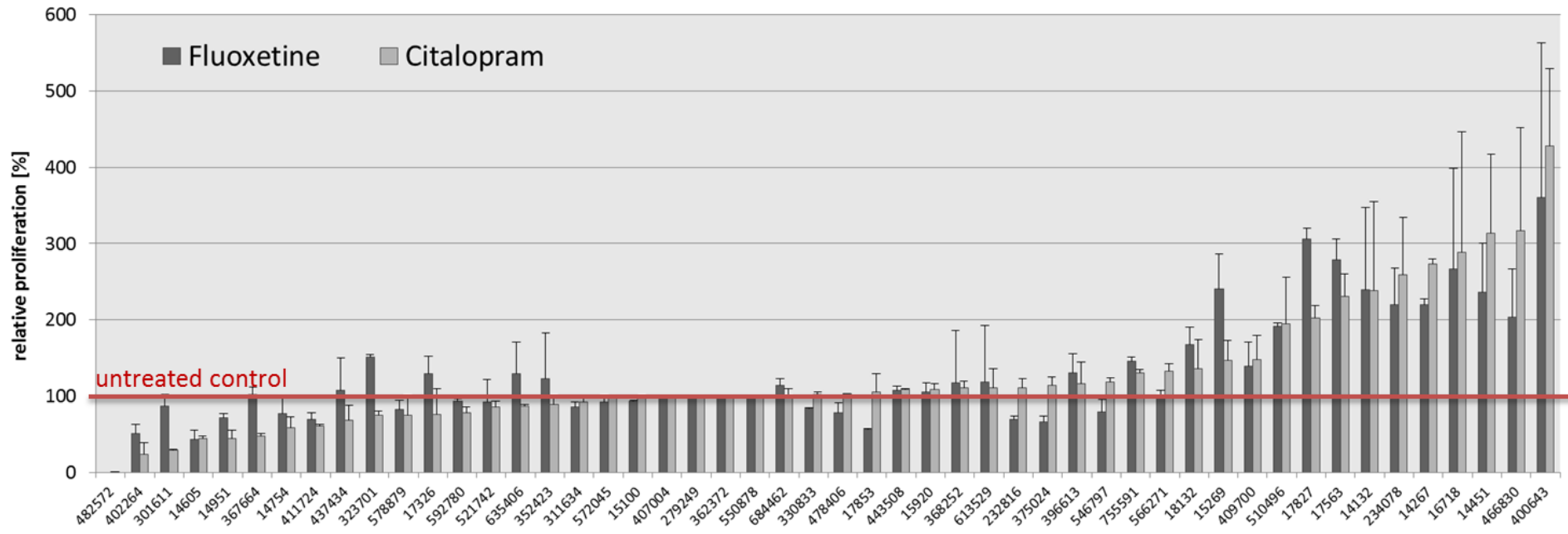


Figure 23: EdU phenotyping of STAR*D cell lines. A total of n=50 cell lines (n=25 treatment resistant and n=25 responder derived cell lines) were treated for 21 days with therapeutical concentrations of fluoxetine (0.5 µg/ml) or citalopram (0.3 µg/ml). Proliferation rates were measured by EdU proliferation assay and are indicated as values relative to untreated control samples of the same cell lines (relative proliferation values of >100% mean increased proliferation after fluoxetine treatment). Strong interindividual differences are detectable between the different cell lines ranging from 0% to 428% of relative proliferation rates.

Averaged over all $n=50$ cell lines, significant overall proliferative effects were reported compared to MOCK treated controls (Figure 24). By definition control was set to 100% and fluoxetine and citalopram treated LCLs achieved mean relative proliferation rates of 130.34 ± 10.45 ($p=0.006$) and 127.59 ± 12.04 ($p=0.026$), respectively. Furthermore, a significant correlation between the fluoxetine and citalopram (both SSRIs) mediated proliferation rates was detected ($\rho=0.875$, $p<0.001$) (Figure 25). Basal proliferation, *i.e.* LCL proliferation without antidepressants, is not associated with LCL donor's clinical response status (non-responder 17.44 ± 1.83 vs. responder 15.92 ± 2.13 ; $p=0.591$).

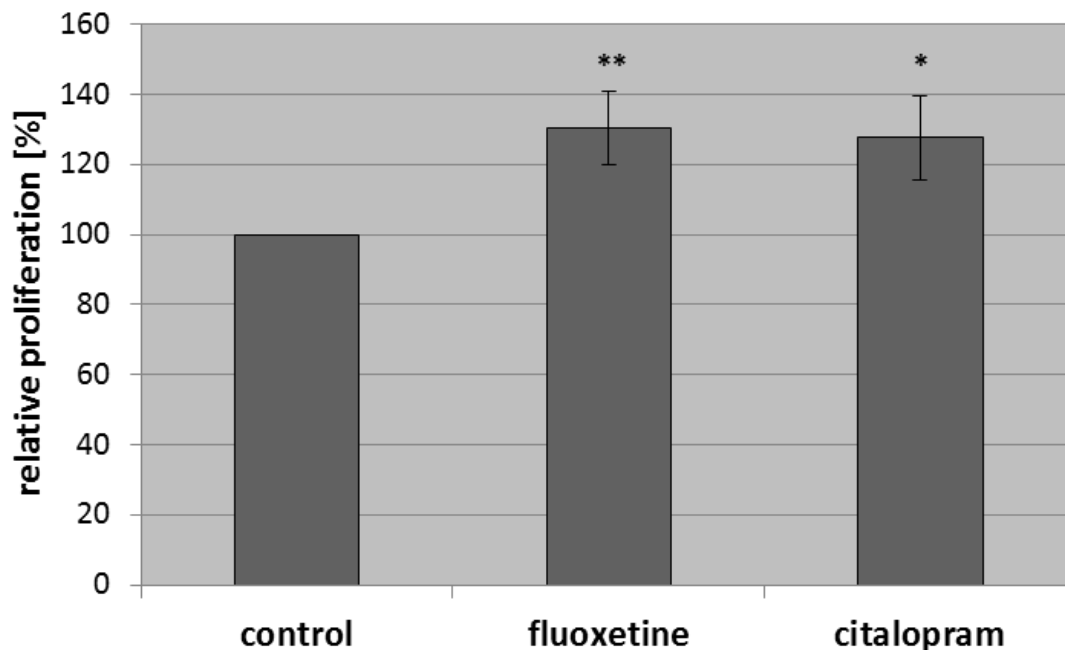


Figure 24: Overall proliferative effects of fluoxetine and citalopram after three weeks of *in-vitro* treatment in therapeutic concentrations ($n=50$). Significance was tested by paired Student's t test (p -values: * < 0.05 , ** < 0.01) and significantly increased relative proliferation rates were reported for both fluoxetine ($p=0.006$) and citalopram ($p=0.026$).

Further, the association between relative LCL proliferation rates and LCL donor's clinical response status was investigated (Figure 26). Responder derived cell lines showed significantly increased proliferation after *in-vitro* treatment with fluoxetine ($p=0.001$) and citalopram ($p=0.001$), whereas non-responder derived cell lines showed decreased proliferation with fluoxetine ($p=0.374$) and citalopram ($p=0.028$). The differences in proliferation rates between LCLs derived from first-line responder versus LCLs derived from treatment resistant patients were highly significant ($p_{\text{fluoxetine}} < 0.001$, $p_{\text{citalopram}} < 0.001$).

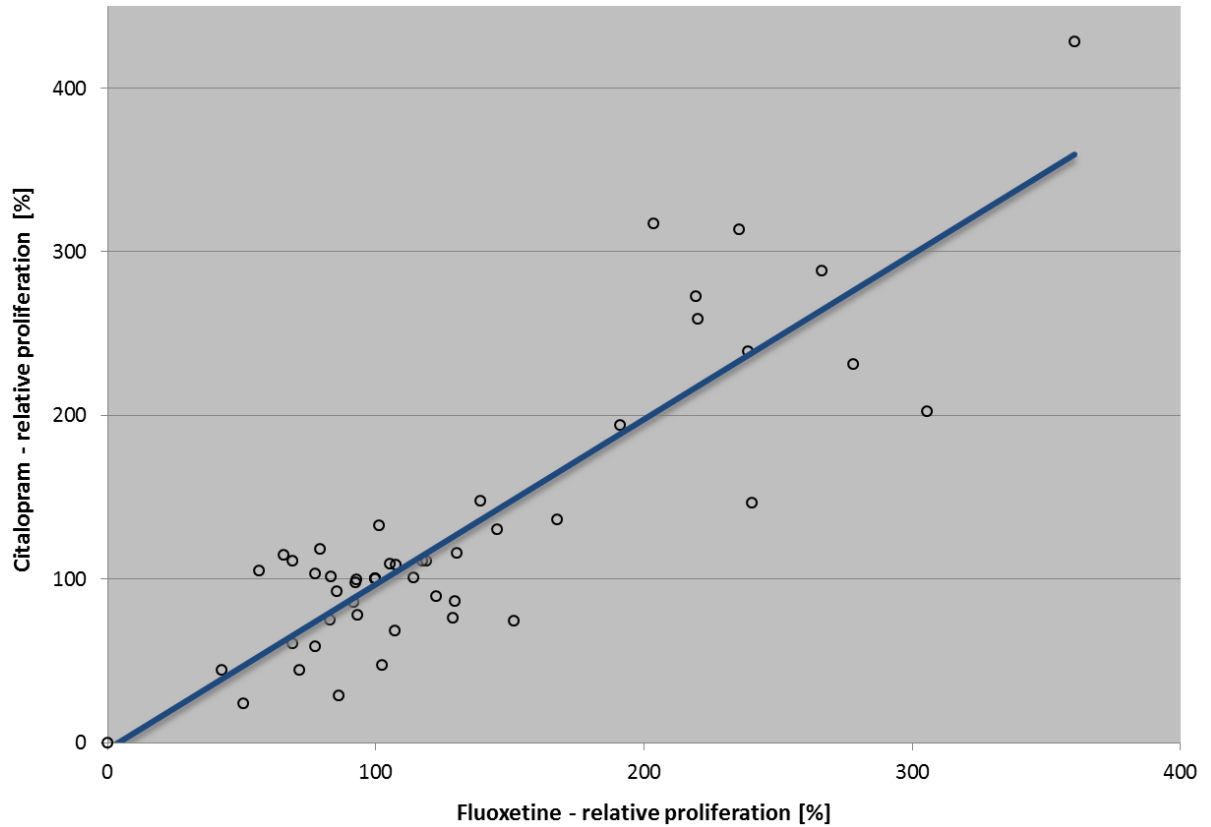


Figure 25: Correlation plot of fluoxetine and citalopram induced relative proliferation after *in-vitro* treatment with the SSRI antidepressants in therapeutic concentrations for three weeks. A highly significant correlation was observable ($\rho=0.875$, $p<0.001$) between fluoxetine induced LCL proliferation and citalopram induced LCL proliferation.

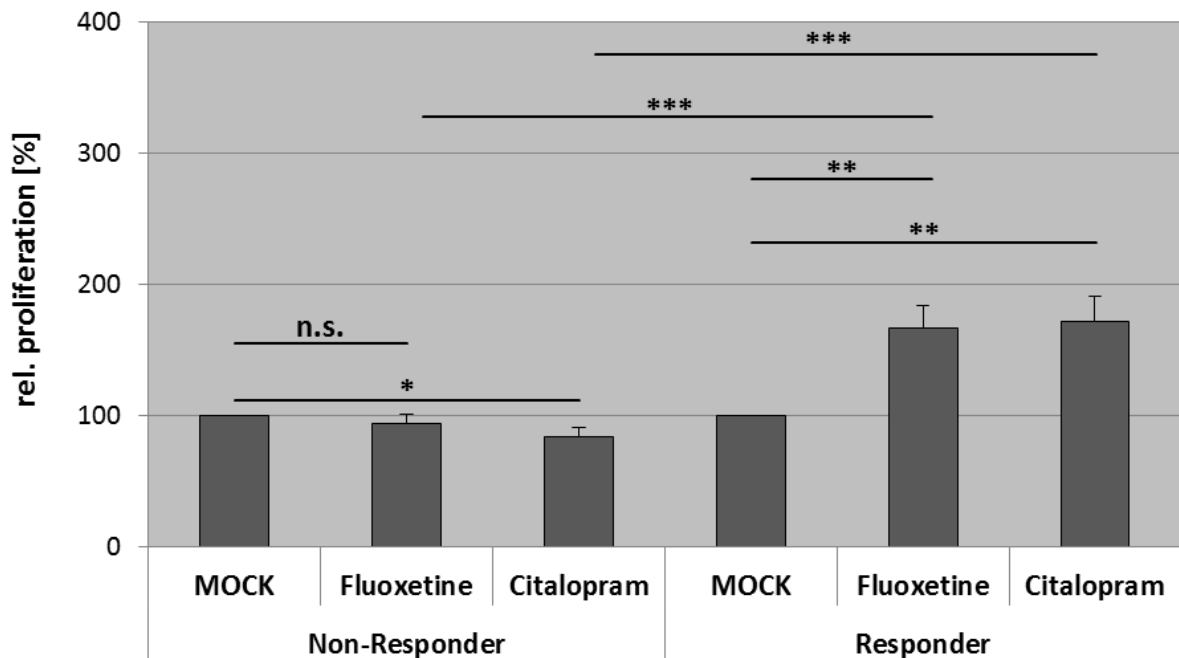


Figure 26: Mean relative proliferation rates of non-responder and responder derived cell lines treated with fluoxetine or citalopram for 21 days. Proliferation rates were significantly increased in responder derived cell lines and decreased in non-responder derived cell lines treated with citalopram. Significant differences between responder and non-responder derived cell lines were observable (deviations are indicated as standard error; p-values: * < 0.05, ** < 0.01, *** < 0.001).

The correlation between QIDS reduction (as degree of LCL donor's clinical response) and the experimentally determined relative proliferation rates was analyzed by Pearson's correlation analysis: A positive significant correlation between percentage QIDS reduction and proliferation was detected for both citalopram ($\rho=0.331$, $p=0.019$) and fluoxetine ($\rho=0.387$, $p=0.006$) treated cell lines (Figure 27).

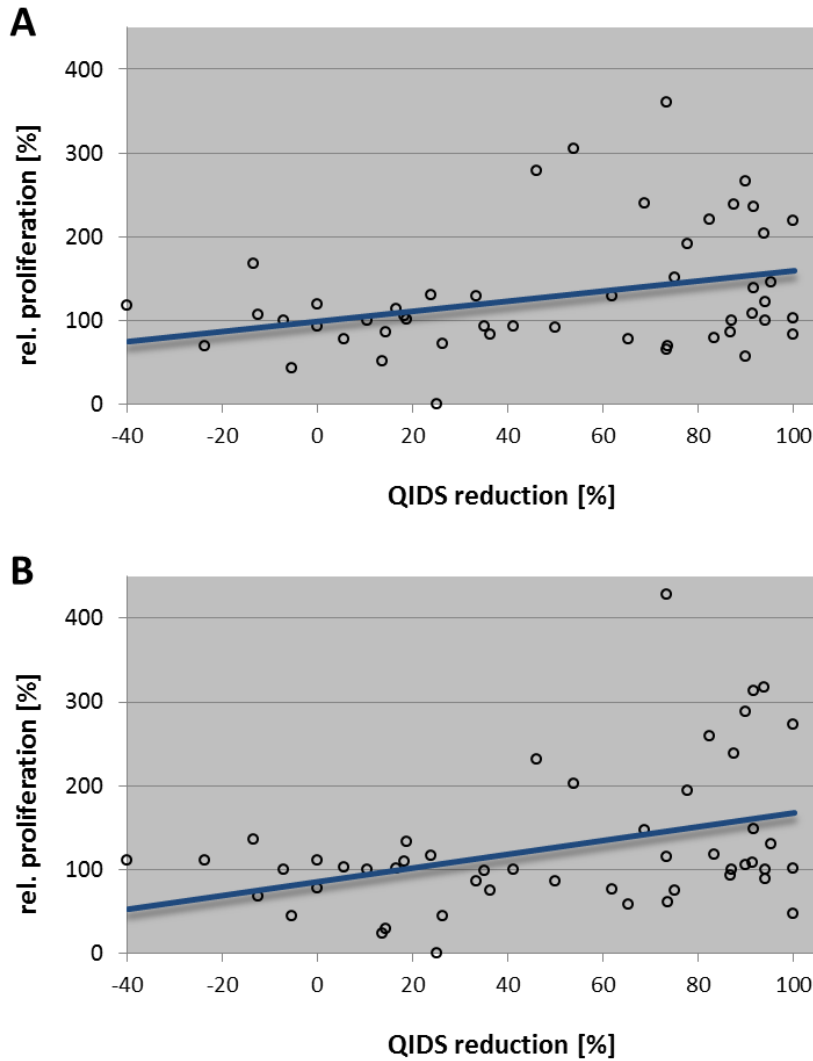


Figure 27: Correlation plots of QIDS reduction and fluoxetine (A) or citalopram (B) induced relative proliferation.

The impact of covariates such as gender, age, citalopram dosage, menopausal status or anxiety status on relative proliferation rates was investigated. No significant associations were found for both gender ($\rho_{\text{Fluoxetine}}=0.142$, $\rho_{\text{Citalopram}}=0.052$) and age ($\rho_{\text{Fluoxetine}}=-0.802$ with $p_{\text{Fluoxetine}}=0.581$; $\rho_{\text{Citalopram}}=0.054$ with $p_{\text{Citalopram}}=0.710$) (Figure 28, A-D). The same applies for the menopausal status of participating female subjects ($\rho_{\text{Fluoxetine}}=0.731$, $\rho_{\text{Citalopram}}=0.416$) (Figure 28, E) as well as the LCL donor's occurrence of anxious or non-anxious types of depression during the STAR*D study ($\rho_{\text{Fluoxetine}}=0.771$, $\rho_{\text{Citalopram}}=0.330$) (Figure 28, F). Further, the amount of citalopram, *i.e.* the

citalopram dosage the donors were treated with over the course of the STAR*D study showed no influence on relative proliferation rates (fluoxetine: $p_{10\text{mg}}=0.186$, $p_{20\text{mg}}=0.180$; citalopram: $p_{10\text{mg}}=0.061$, $p_{20\text{mg}}=0.165$) (Figure 28, G).

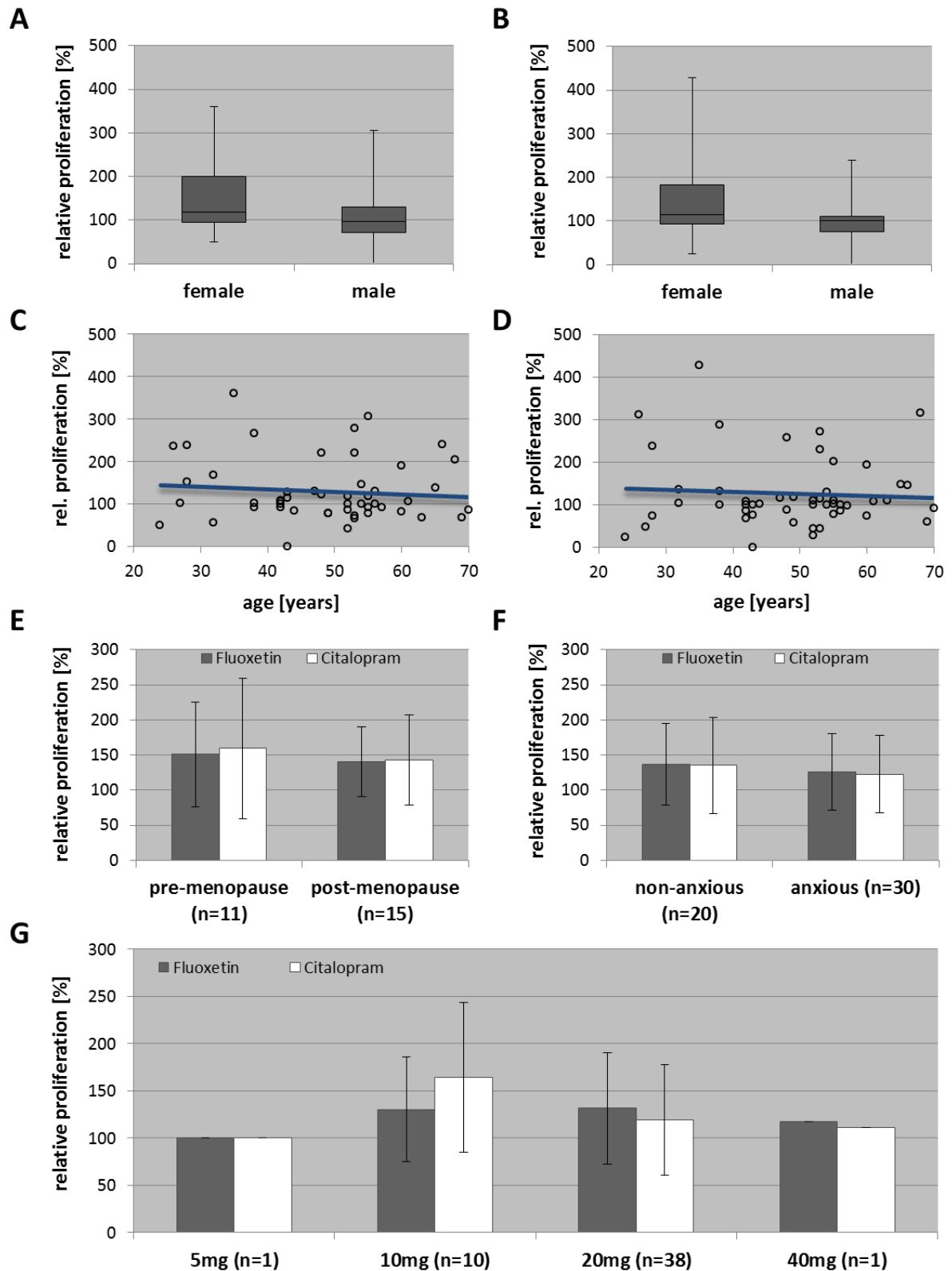


Figure 28: Covariates analysis. No significant associations were found for gender (A - fluoxetine, B - citalopram), age (C - fluoxetine, D - citalopram), menopausal status (E), anxiety status (F) or dosage (G) by particular statistical methods (Student's t test and Pearson's correlation analysis).

1.2.2. Gene Expression Analyses of Candidate Genes

Within the same cohort of n=50 STAR*D LCLs the gene expression of the five candidate genes (*ABCB1*, *FZD7*, *TCF7L2*, *SULT4A1* and *WNT2B*) was measured - including basal gene expression and gene expression after three weeks of *in-vitro* treatment with therapeutic concentrations of fluoxetine and citalopram. Subsequently, the relationship between LCL donor's clinical response status and the LCL gene expression status was investigated. The basal gene expression levels of both *WNT2B* and *ABCB1* are significantly elevated in non-responder derived cell lines relative to responder derived cell lines. Significant associations between LCL donor's clinical response and LCL basal gene expression of *WNT2B* ($p=0.0001$) and *ABCB1* ($p=0.009$) but not for *FZD7* ($p=0.643$), *TCF7L2* ($p=0.355$) or *SULT4A1* ($p=0.943$) could be found (Figure 29, A). Basal gene expression of *SULT4A1* was low and only detectable in 11 out of 50 cell lines (n=5 non-responder derived cell lines vs. n=6 responder derived cells).

The relationship between gene expression fold changes (after three weeks of *in-vitro* treatment with fluoxetine and citalopram) and LCL donor's clinical response status was explored as well (Figure 29, B and C). The fold changes of *WNT2B* ($p_{\text{Fluoxetine}}=0.046$, $p_{\text{Citalopram}}=0.003$), *FZD7* ($p_{\text{Fluoxetine}}=0.003$, $p_{\text{Citalopram}}=0.002$) and *ABCB1* ($p_{\text{Fluoxetine}}=0.009$, $p_{\text{Citalopram}}=0.010$) showed significant associations with LCL donor's clinical response status. No significant associations of gene expression fold changes of *TCF7L2* ($p_{\text{Fluoxetine}}=0.140$, $p_{\text{Citalopram}}=0.369$) and *SULT4A1* ($p_{\text{Fluoxetine}}=0.548$, $p_{\text{Citalopram}}=0.413$) with the LCL donor's clinical response status were found. A correlation matrix for the fluoxetine and citalopram induced fold changes in gene expression is shown in Table 13. Gene expression changes by fluoxetine or citalopram significantly correlate within genes *WNT2B* ($\rho=0.752$), *TCF7L2* ($\rho=0.477$), *FZD7* ($\rho=0.501$) and *ABCB1* ($\rho=0.413$) but not for *SULT4A1* ($\rho=0.367$).

Table 13: Correlation matrix of fold changes by fluoxetine and citalopram. Indicated are the correlation coefficients calculated by Spearman's correlation and their appropriate significance (p-values: * < 0.05, ** < 0.01, * < 0.001; n.s. not significant).**

		Fold changes by Citalopram				
		<i>WNT2B</i>	<i>SULT4A1</i>	<i>TCF7L2</i>	<i>FZD7</i>	<i>ABCB1</i>
Fold changes by Fluoxetine	<i>WNT2B</i>	0.752 ^{***}	-	-	-	-
	<i>SULT4A1</i>	-	0.367 ^{n.s.}	-	-	-
	<i>TCF7L2</i>	-	-	0.477 ^{***}	-	-
	<i>FZD7</i>	-	-	-	0.501 ^{***}	-
	<i>ABCB1</i>	-	-	-	-	0.413 ^{**}

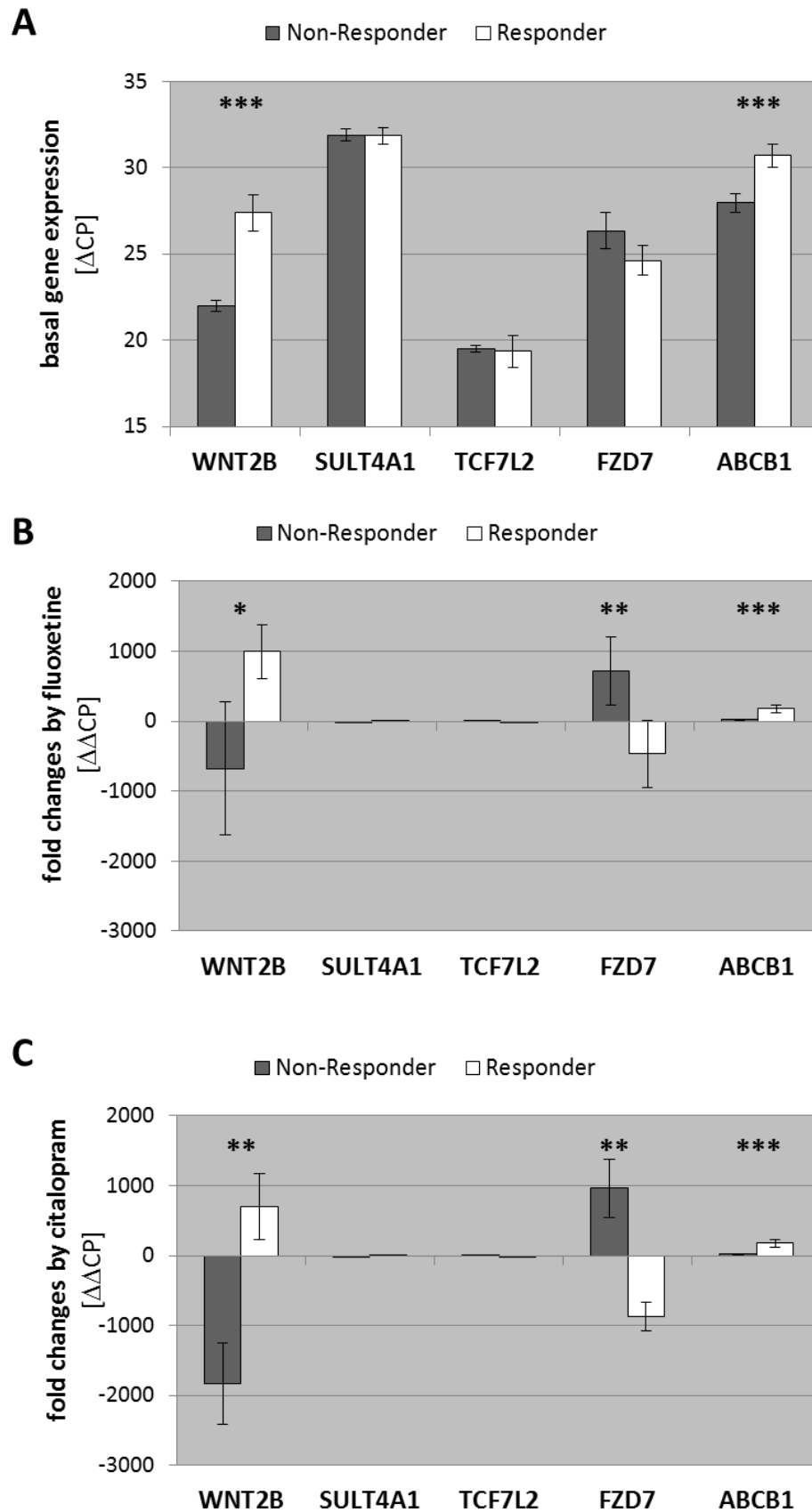


Figure 29: Results of gene expression experiments of the candidate genes. Basal gene expression indicated as difference of maximal cycle number of RT-PCR experiments and Δ CP values of untreated samples (A). Gene expression fold changes after 21-day *in-vitro* treatment of LCLs with fluoxetine (B) or citalopram (C) (deviations are indicated as standard error; p-values: * < 0.05, ** < 0.01, *** < 0.001).

2. Neuroimaging of Interferon-induced Depressive-like Behavior

The RESI study is a prospective, open-label clinical study whose participants received a nine-day standard therapy with recombinant interferon beta. Participants of the RESI study were screened for depressive symptoms by psychometric testing. MRI methods were applied in order to find some evidence for the depression inducing side-effects of interferon beta and to characterize the particular individual variability. A modified CONSORT (Consolidated Standards of Reporting Trials) flow diagram is shown in Figure 30. A total of 18 healthy volunteers received interferon beta therapy. One participant discontinued intervention due to intolerable side effects (high fever, heavy pain and chills). The remaining study cohort consisted of n=7 men and n=10 women with an average age of 26.5 ± 4.9 years.

modified CONSORT 2010 Flow Diagram

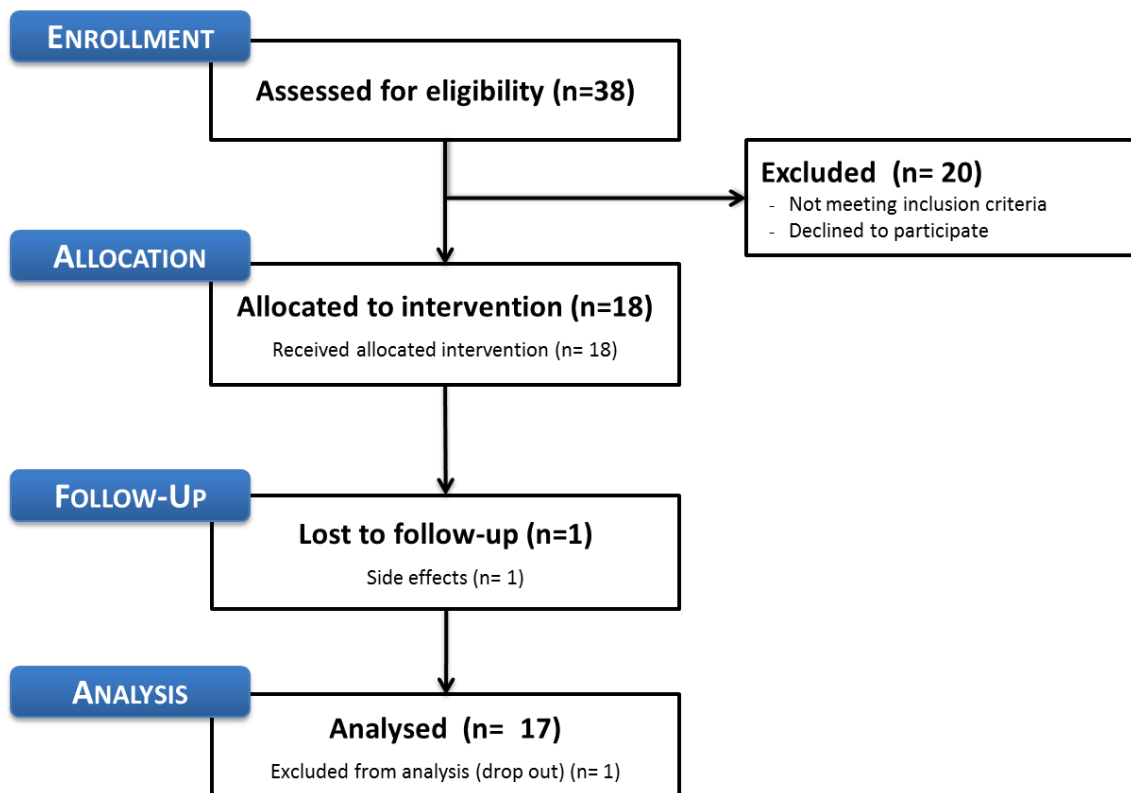


Figure 30: Overview of the course of the study by CONSORT flow diagram. From 38 volunteers, 18 were allocated to intervention with interferon beta. A total of 20 volunteers were excluded because they either did not meet inclusion criteria (e.g. normal inflammation parameters, adequate liver, kidney and bone marrow function) or declined to further participate in the study. One participant receded from the study due to severe side effects like high fever, heavy pain and chills.

2.1. Psychometric Testing

To ascertain the impact of interferon beta mediated changes of psychiatric parameters, anxiety and depression symptoms were examined by the widely-used questionnaires STAI and HDRS, respectively. The STAI measures the two main forms of anxiety, namely current and general anxiety. In both parts of this questionnaire no statistical significant differences were observable ($p_{\text{current}}=0.793$ and $p_{\text{general}}=0.351$) before (baseline) and after (steady-state) the nine-day treatment of 17 volunteers with interferon beta (Figure 31, A). However, individual variability was detectable with increases, decreases or constant levels in STAI scoring being observable depending on the individual participant (Figure 31, B).

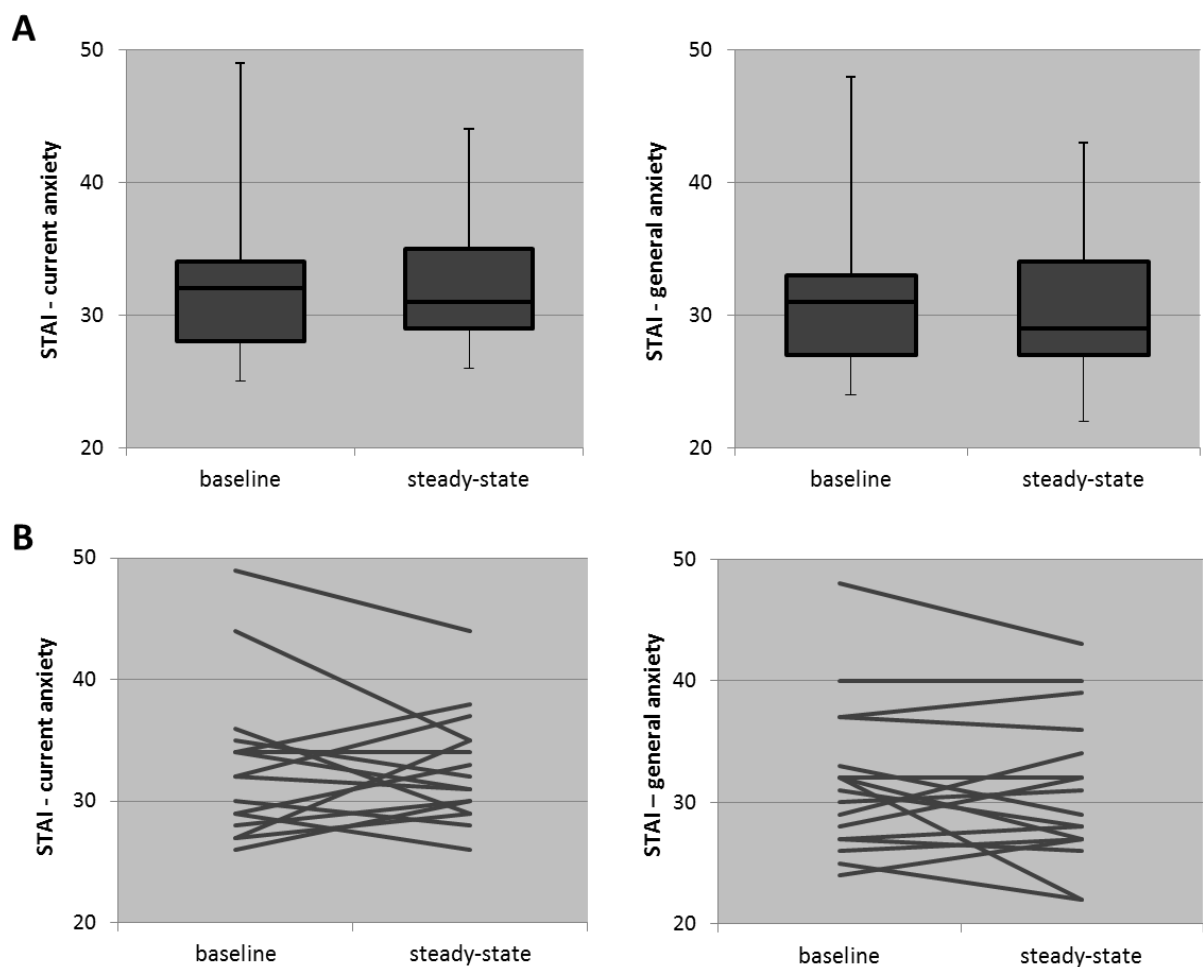


Figure 31: Box plots of the current (left) and general (right) STAI anxiety scores before (baseline) and after (stead-state) the nine-day standard therapy with interferon beta (A). The line graphs illustrates the individual variability of the current (left) and general (right) STAI anxiety scoring of each single participant over the course of the nine-day standard treatment with interferon beta (B).

In contrast, depression scores using HDRS almost exclusively showed increases over the time (Figure 32, A) and consequently, highly significant changes were observed from baseline to steady-state with a resulting p-value of 0.003 (Figure 32, B).

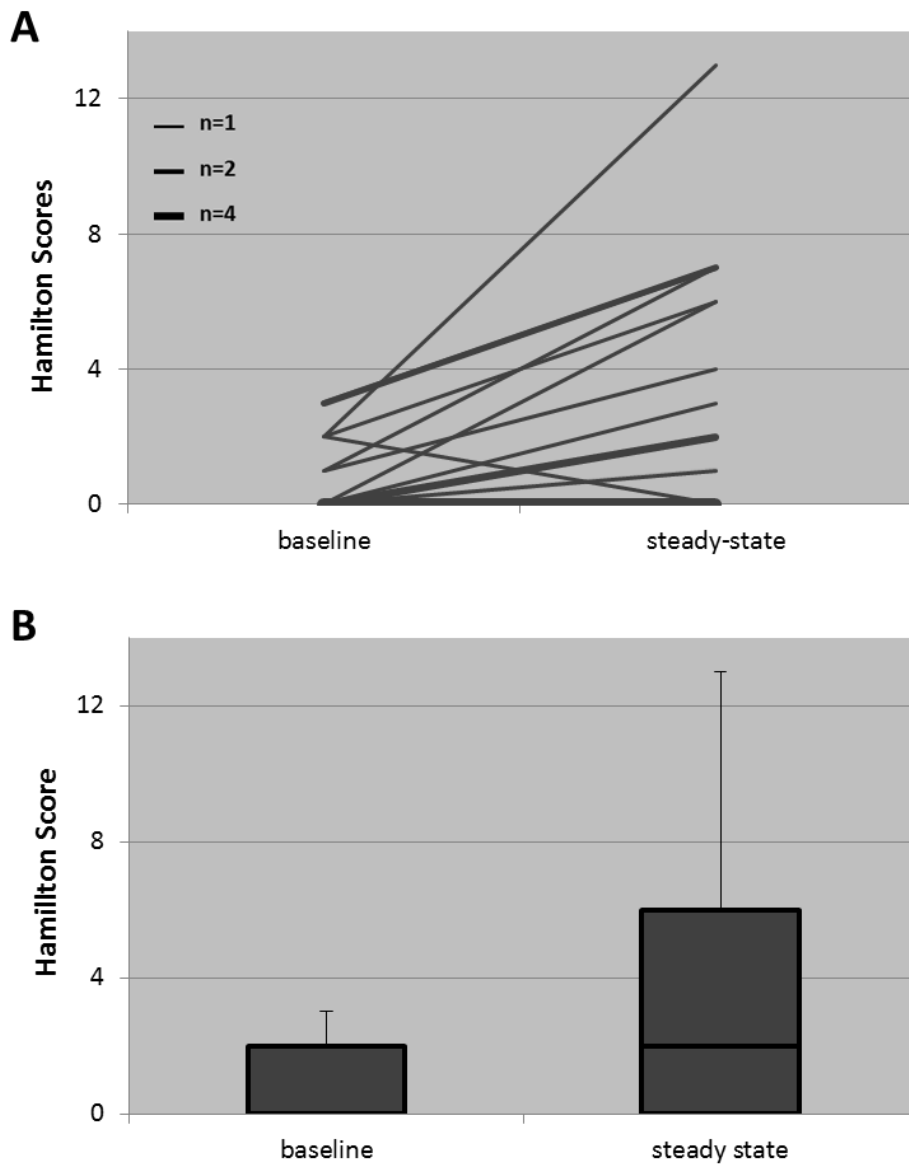


Figure 32: Progress of HDRS scores before (baseline) and after (steady-state) treatment with interferon beta. A strong increase of Hamilton-Scores was reported for individual participants (A) and the total cohort (B). Thicker lines represent more individuals with identical, overlapping HDRS values.

When analyzing the single items of the HDRS, it becomes obvious from which parameters these effects were brought from (Figure 33): Strongest impairments were reported in the single items concerning “psychomotor retardation” (e.g. slowness of thought or difficulty in concentration), “work & activities” (characterized by feelings of incapacity, fatigue or weakness), “insomnia” (early, middle or late over the night span), “gastrointestinal symptoms” (e.g. loss of appetite or loss of weight) and “somatic symptoms” (e.g. indigestion, diarrhea, stomach cramps, heaviness in limbs, loss of energy). Weaker effects but still of note were found for the items “anxiety” (e.g. subjective tension or irritability, worrying about minor matters), “genital symptoms” (e.g. menstrual disturbance, loss of libido) and “hypochondriasis” (characterized by increased self-absorption). Unexpected but of interest is that a decrease in parameters “agitation” (e.g. fidgetiness) and

“feelings of guilt” (*e.g.* self-reproaches) was reported. However, only 2 out of 17 participants complained about depressed mood and fortunately, no signs of suicidal behavior or suicidal ideation - neither before nor after study participation - were detectable. Taken together depressive symptoms in the strict sense were barely detected, but other depression-related symptoms were frequently recorded by usage of HDRS.

2.2. Functional Magnetic Resonance Imaging

All participants (n=17) were instructed to complete two tasks (see chapter 2.2.2) during the fMRI session before and after interferon beta administration to measure the specific brain activation patterns of depression-related area in the money-rewarding foraging paradigm and the passive exposure faces paradigm.

2.2.1. Foraging

A paradigm was employed in which participants could collect money at different amounts (0.01€ vs. 0.20€) to probe the impact of interferon beta on the sensitivity to reward cues. Table 14 gives an overview on the statistical analyses of this paradigm on set level, cluster level and peak level (for explanation see chapter 2.2.4).

In fMRI the activity of the ventral striatum decreases after the treatment with interferon beta in (interaction cue high vs. low x treatment: $x, y, z -14, 0, 2, t = 4.13, p = 0.06$, FDR cluster-level corrected). Figure 34 shows the brain mapping of this paradigm before (“control”) and after interferon treatment (“treatment”) as well as the interaction mode. The interaction mode statistically compares the effects of two conditions (here: before and after interferon administration) and constitutes the main result of such fMRI measurements (Figure 34).

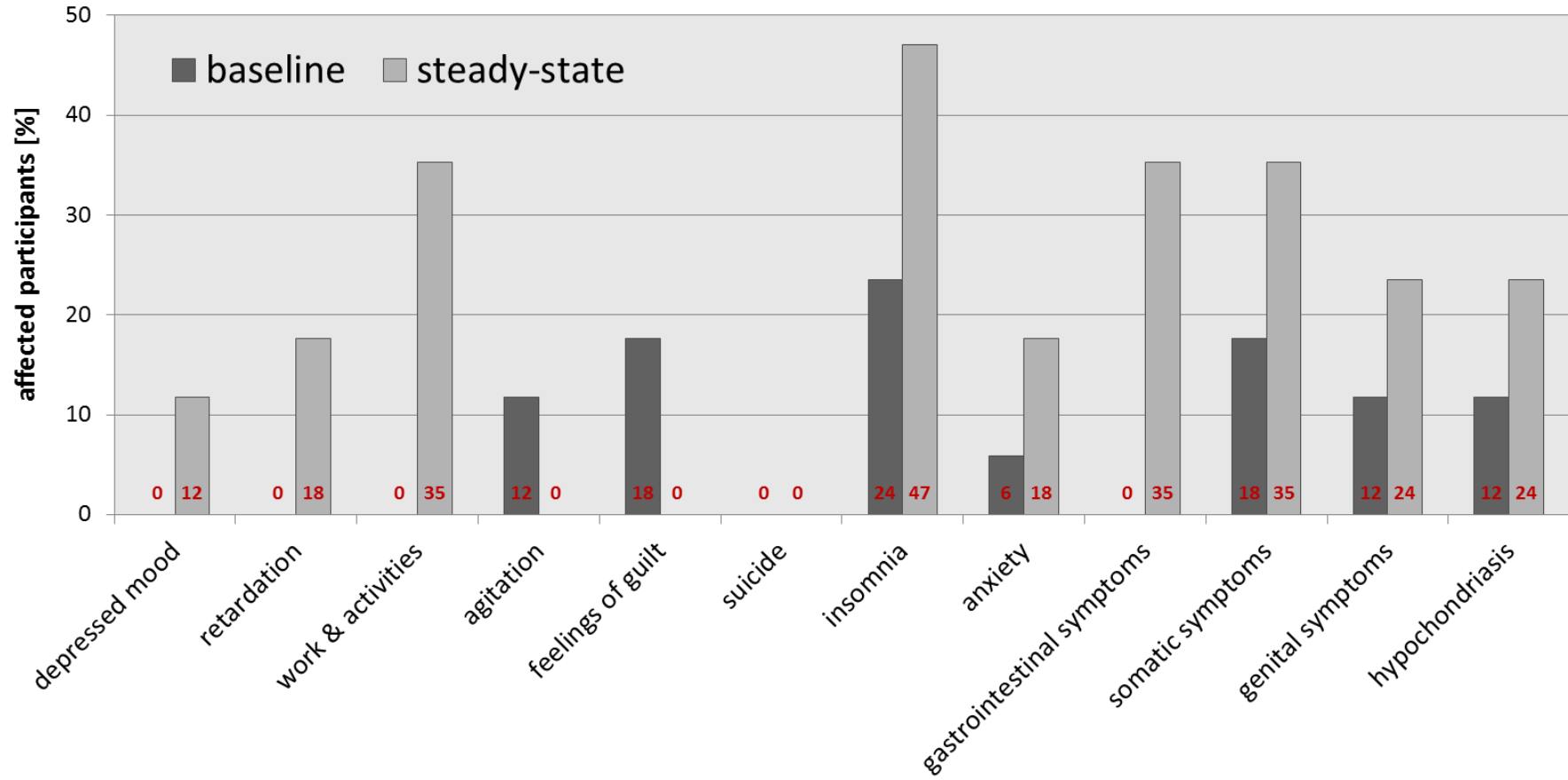


Figure 33: Single-item-analysis of results obtained from HDRS scoring before (baseline) and after (steady-state) a nine-day standard therapy with interferon beta.

Table 14: Statistical report of the foraging paradigm measurements before and after interferon beta administration including results on set, cluster and peak level with an uncorrected p value cut-off of 0.001.

set level		cluster level		peak level		coordinates (mm)			brain areas
size	p	size	p	T	p	x	y	z	
60	0.419	39	0.042	6.50	3.66E-06	-46.5	8	-16	Temporal pole superior left
		99	0.003	6.03	8.67E-06	7.5	30.5	27.5	Cingulum anterior right
		306	0.000	5.91	1.10E-05	28.5	32	41	Frontal middle right
				5.23	4.09E-05	24	44	38	Frontal superior right
				4.43	2.11E-04	27	27.5	33.5	Frontal middle right
		54	0.020	5.53	2.29E-05	-43.5	-37	15.5	Temporal pole superior left
				4.35	2.50E-04	-51	-32.5	12.5	Frontal inferior triangularis left
		27	0.084	5.33	3.40E-05	-27	3.5	-23.5	Amygdala left
		13	0.218	5.29	3.64E-05	-30	11	12.5	Insula left
		27	0.084	5.08	5.62E-05	-58.5	6.5	11	Rolandic operculum left
		195	0.000	4.89	8.21E-05	-25.5	45.5	29	Frontal middle left
				4.76	1.06E-04	-27	36.5	36.5	Frontal superior left
		10	0.278	4.80	9.91E-05	1.5	17	57.5	Supplementary motor area right
		1	0.759	4.77	1.04E-04	-67.5	-16	30.5	Postcentral left
		20	0.131	4.71	1.17E-04	31.5	24.5	0.5	Insula right
		7	0.365	4.54	1.67E-04	9	-20.5	8	Thalamus right
		32	0.062	4.50	1.81E-04	12	26	39.5	Cingulum middle right
		6	0.403	4.48	1.88E-04	6	6.5	62	Supplementary motor area right
		3	0.564	4.48	1.90E-04	9	-37	41	Cingulum middle right
		4	0.500	4.43	2.09E-04	1.5	11	60.5	Supplementary motor area right
		10	0.278	4.32	2.64E-04	7.5	-11.5	2	Thalamus right
		3	0.564	4.30	2.77E-04	-37.5	-7	-16	Hippocampus left
		3	0.564	4.27	2.90E-04	-9	30.5	30.5	Frontal superior medial left
		11	0.256	4.22	3.27E-04	-37.5	-32.5	41	Postcentral left
		1	0.759	4.21	3.30E-04	-13.5	6.5	53	Frontal superior left
		1	0.759	4.18	3.50E-04	7.5	-20.5	26	not allocated
		10	0.278	4.18	3.54E-04	18	-16	51.5	not allocated
		4	0.500	4.17	3.58E-04	-40.5	12.5	-23.5	Temporal pole superior left
		7	0.365	4.14	3.86E-04	-7.5	24.5	38	Cingulum middle right
		3	0.564	4.14	3.86E-04	-27	27.5	-4	Insula left
		5	0.447	4.11	4.06E-04	19.5	20	51.5	Frontal superior right
		3	0.564	4.11	4.11E-04	37.5	44	14	Frontal middle right
		1	0.759	4.06	4.57E-04	-25.5	26	0.5	not allocated
		2	0.646	4.05	4.60E-04	-31.5	9.5	6.5	Putamen left
		1	0.759	4.05	4.65E-04	6	-17.5	26	not allocated
		3	0.564	4.01	5.04E-04	-18	3.5	62	Frontal superior left
		1	0.759	4.00	5.15E-04	16.5	23	42.5	Frontal superior right
		1	0.759	3.98	5.42E-04	-55.5	11	17	Frontal inferior operculum left
		2	0.646	3.97	5.45E-04	-64.5	-17.5	26	Postcentral left
		1	0.759	3.97	5.45E-04	-31.5	8	0.5	Putamen left
		1	0.759	3.97	5.51E-04	-4.5	-25	24.5	not allocated
		1	0.759	3.95	5.76E-04	-16.5	3.5	59	Frontal superior left
		1	0.759	3.94	5.89E-04	33	44	11	Frontal middle right
		1	0.759	3.92	6.06E-04	30	-2.5	-23.5	Amygdala right
		2	0.646	3.92	6.12E-04	40.5	44	15.5	Frontal middle right
		1	0.759	3.90	6.37E-04	4.5	-8.5	-1	Thalamus right
		1	0.759	3.90	6.39E-04	4.5	-17.5	30.5	Cingulum middle right
		1	0.759	3.88	6.68E-04	-9	32	8	not allocated
		1	0.759	3.86	6.90E-04	9	-31	42.5	Cingulum middle right
		2	0.646	3.84	7.22E-04	13.5	-65.5	26	Precuneus right
		1	0.759	3.84	7.24E-04	-13.5	32	35	Frontal superior medial left
		1	0.759	3.82	7.51E-04	-67.5	-29.5	32	Supra marginal left
		1	0.759	3.79	8.04E-04	12	21.5	38	Cingulum middle right
		1	0.759	3.76	8.53E-04	30	27.5	-10	Frontal inferior orbital right
		1	0.759	3.75	8.66E-04	-19.5	-68.5	51.5	Parietal superior left
		3	0.564	3.75	8.80E-04	-40.5	8	-26.5	Temporal pole superior left
		1	0.759	3.73	9.06E-04	-43.5	41	20	Frontal middle left
		1	0.759	3.73	9.07E-04	-10.5	-46	57.5	Precuneus left
		1	0.759	3.72	9.23E-04	18	23	48.5	Frontal superior right
		1	0.759	3.71	9.41E-04	-58.5	-31	12.5	Temporal superior left
		1	0.759	3.71	9.48E-04	10.5	-62.5	24.5	Precuneus right
		1	0.759	3.70	9.71E-04	-4.5	32	20	Cingulum anterior left
		1	0.759	3.70	9.74E-04	-66	-31	30.5	Supra marginal left
		1	0.759	3.69	9.85E-04	-67.5	-26.5	29	Supra marginal left

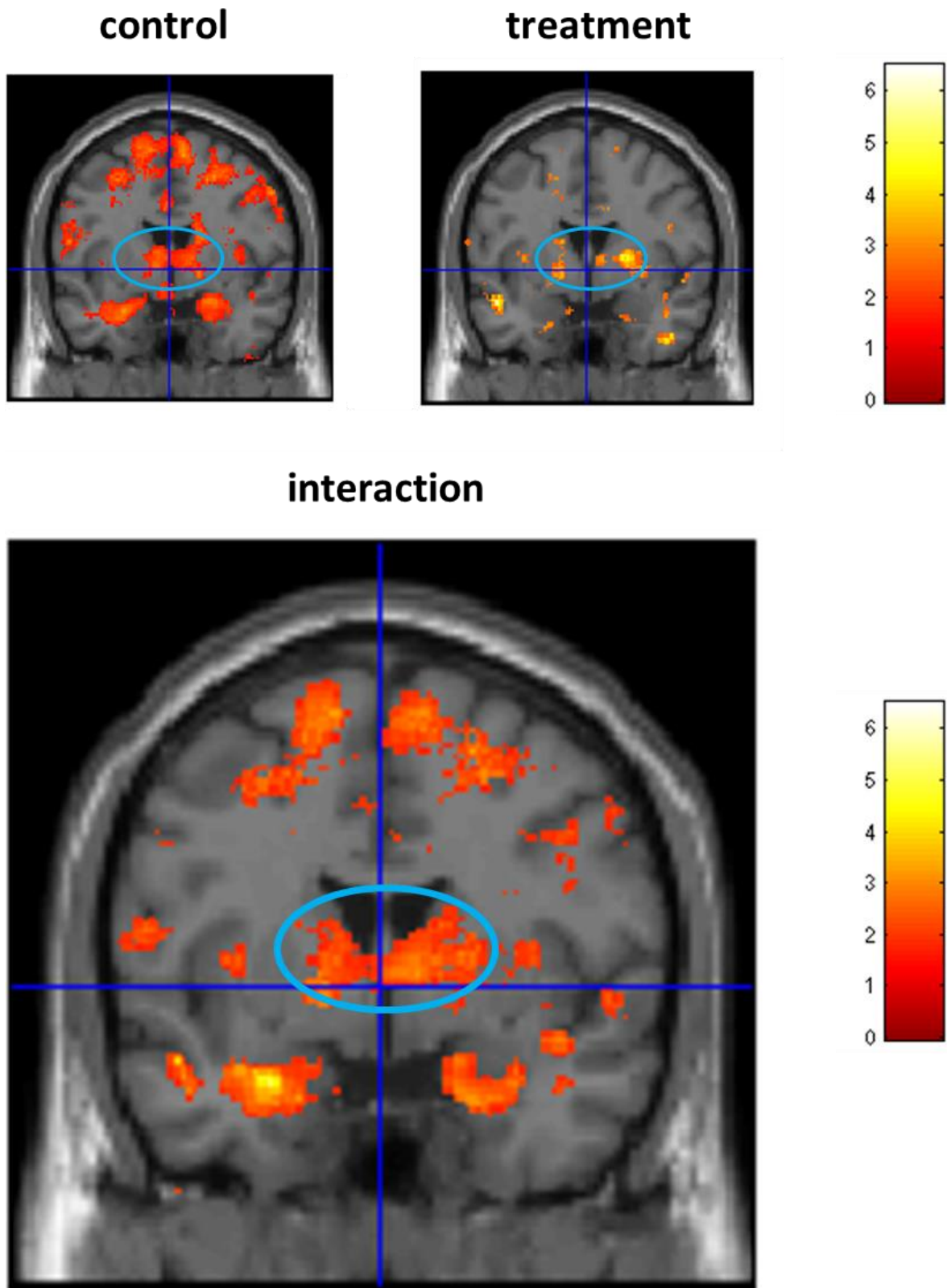


Figure 34: Results of the foraging paradigm indicate a lowered activity of the ventral striatum (blue circle) after interferon beta administration. The brain mapping shows activation patterns of this money-rewarding paradigm before (“control”) and after interferon treatment (“treatment”) as well as the interaction mode - a statistical comparison of the effects at the both mentioned time points. The slices are shown at $y=+5\text{mm}$ and the key indicates the level of activation (T-values).

2.2.2. Faces

Blocks of emotional faces were displayed in a passive exposure paradigm to target the amygdala and to evaluate the reactivity to emotional stimuli before and after interferon administration. Table 15 gives an overview on the statistical analyses of this paradigm on set level, cluster level and peak level with no relevant activation differences in the amygdala. In general the amygdala was active at both time points (“control” and “treatment”, see upper part of Figure 35) which indicates the faces paradigm was successful in eliciting its activation but no significant changes in amygdala activation before and after interferon treatment were detectable as can be seen in the interaction mode of the particular brain mapping (Figure 35).

Table 15: Statistical report of the faces paradigm measurements before and after interferon beta administration including results on set, cluster and peak level with an uncorrected p value cut-off of 0.001.

set level		cluster level		peak level		coordinates (mm)			brain areas
size	p	size	p	T	p	x	y	z	
32	0.200	91	0.003	5.36	3.219E-05	24	-30	32	not allocated
		47	0.023	5.32	3.443E-05	38	6	20	Insula right
				4.45	2.013E-04	32	14	26	not allocated
				4.20	3.414E-04	36	6	28	Frontal inferior operculum right
		20	0.117	4.90	8.043E-05	40	-52	-6	Temporal inferior right
		19	0.126	4.68	1.264E-04	32	-24	-6	Hippocampus right
				4.18	3.554E-04	38	-28	-10	Hippocampus right
		8	0.312	4.62	1.410E-04	-26	-40	22	not allocated
		10	0.259	4.50	1.808E-04	4	4	-28	not allocated
		4	0.480	4.48	1.896E-04	26	-48	34	not allocated
		7	0.345	4.47	1.946E-04	42	-44	20	not allocated
		8	0.312	4.46	1.956E-04	34	-62	-4	not allocated
		6	0.383	4.43	2.085E-04	20	26	32	Frontal superior right
		4	0.480	4.32	2.641E-04	16	-10	20	Caudate right
		1	0.748	4.29	2.806E-04	-20	-12	48	not allocated
		1	0.748	4.22	3.256E-04	38	0	28	not allocated
		2	0.630	4.20	3.388E-04	18	30	26	not allocated
		1	0.748	4.10	4.217E-04	44	-34	2	Temporal middle right
		1	0.748	4.09	4.252E-04	40	-28	-6	Hippocampus right
		7	0.345	4.03	4.814E-04	-30	-60	10	not allocated
		1	0.748	4.02	4.899E-04	18	22	32	not allocated
		3	0.546	3.98	5.347E-04	-4	-26	68	Cingulum anterior left
		2	0.630	3.96	5.635E-04	-40	-54	-4	Temporal middle left
		1	0.748	3.95	5.767E-04	-14	8	36	not allocated
		1	0.748	3.92	6.141E-04	34	20	20	not allocated
		1	0.748	3.90	6.396E-04	44	0	22	not allocated
		2	0.630	3.88	6.587E-04	-18	-14	46	not allocated
		1	0.748	3.87	6.747E-04	0	28	-20	Frontal medial orbital right
		1	0.748	3.85	7.077E-04	-46	-22	-16	Temporal middle left
		2	0.630	3.84	7.164E-04	16	48	30	Frontal superior right
		1	0.748	3.81	7.676E-04	34	-50	-6	Fusiform right
		1	0.748	3.77	7.878E-04	-18	28	28	not allocated
		1	0.748	3.77	8.440E-04	40	-42	4	not allocated
		1	0.748	3.73	8.459E-04	18	26	36	Frontal superior right
		1	0.748	3.73	9.019E-04	46	2	24	Precentral right

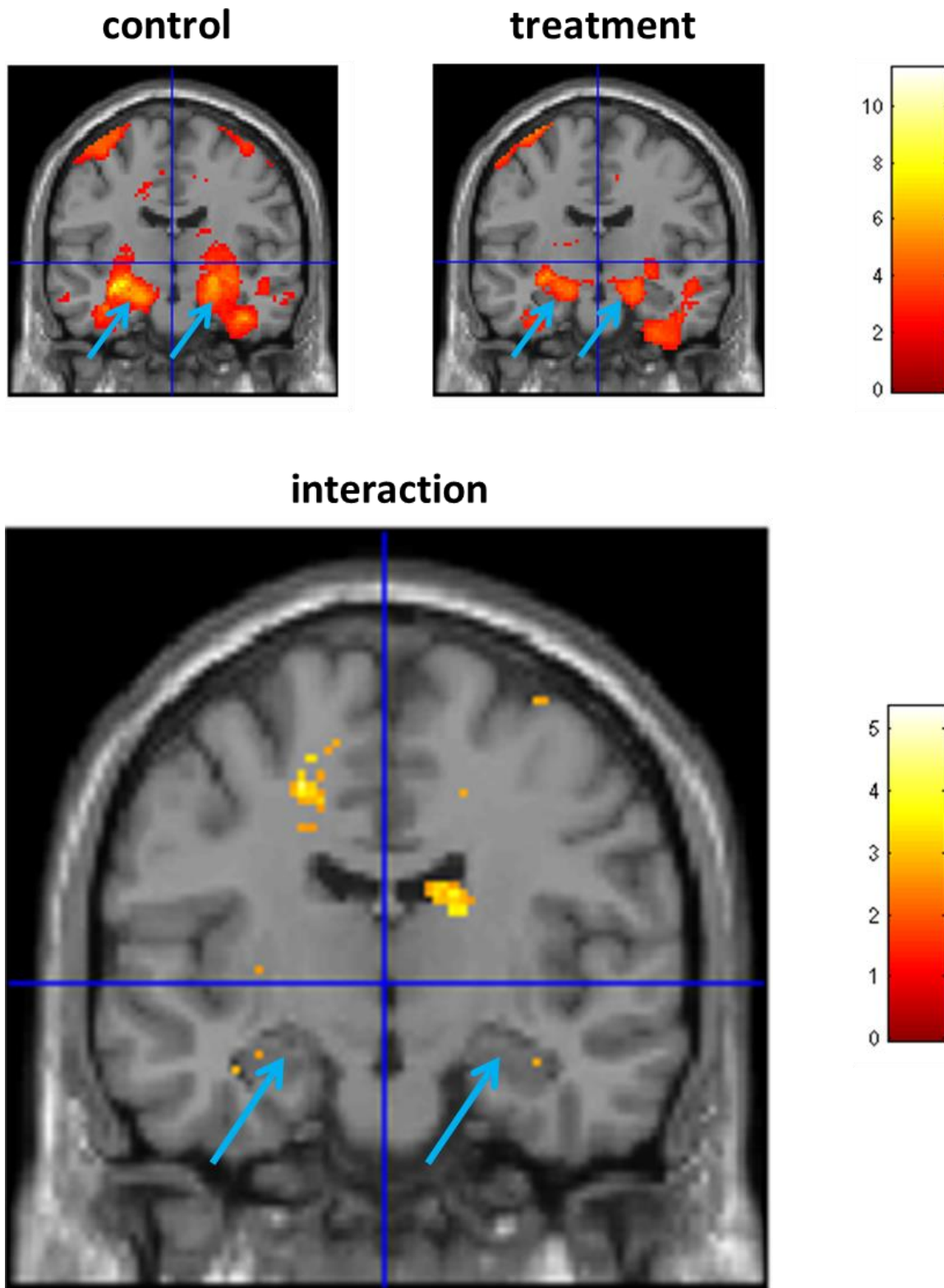


Figure 35: Results of the faces paradigm indicate no significant changes of the activity of the amygdala and the central nucleus region (blue arrows) after interferon beta administration. The slices are shown at $y=-8\text{mm}$ and the key indicates the level of activation (T-values).

Chapter V - Discussion

1. Previous Findings from MARS and STAR*D

The cell lines utilized over the course of this work were derived from large clinical trials focusing on depressive disorders, namely the MARS and STAR*D studies. The MARS trial attempted to identify a biomarker portfolio for the prediction of the individual treatment guidance using transcriptomics, proteomics and metabolomics techniques as well as neuroendocrine testing and neuroimaging. More than 1,000 depressive patients took part in this naturalistic study showing response and remission rates of up to 80.8% and 57.9%, respectively¹³⁷. Polymorphisms within the *FKBP5* (FK506 Binding Protein 5; a glucocorticoid receptor involved in the regulation of the HPA axis) gene and an increased expression of *FKBP5* significantly correlated with the relapse of depressive symptoms and with the remission¹⁸¹. Furthermore, polymorphisms of other genes such as *HTR2A* (5-hydroxytryptamine receptor 2A), *ER22/23EK* (glucocorticoid receptor), *ABCB1* or *GAD2* (glutamate decarboxylase 2) were identified as potential biomarkers for the treatment response and the susceptibility to develop depressions¹⁸²⁻¹⁸⁹. Genetic variations of *TPH2* (tryptophan dehydroxylase 2) or *NTRK2* (neurotrophic tyrosine kinase receptor type 2) were also linked to antidepressant's side effects or suicidal behavior^{190, 191}. An increased cortisol response was associated with the relapse of depressive symptoms after six months of remission renders it a potential biomarker to predict the clinical outcome^{139, 140}. In contrast a decreased reactivity to cortisol and adrenocorticotropin was associated with both suicidal ideation and suicide attempts¹⁹². Behavioral testing was shown to be able to predict response to antidepressant treatment and the risk to relapse^{193, 194}. Furthermore, obese patients demonstrated minor neuroendocrinological changes accompanied by worse response relative to normal-weighted patients¹⁹⁵.

The STAR*D trial was designed to ascertain which treatment strategy would be generalizable optimal by prospectively recording the therapy tolerability and outcome throughout up to four different defined treatment levels¹⁹⁶. A time period of over six years and more than 4,000 depressive patients were making this study to one of the largest of its kind with total costs of \$35 million¹⁹⁷. In level one - where all patients were treated with citalopram for up to 14 weeks - an overall response rate of 47% and remission rates of approximately 30% were reported. Non-remitters entered the subsequent levels until remission was achieved. Level two included seven

different treatment options in addition to citalopram (further antidepressants or psychotherapy) and level three consisted of a switch to another antidepressant (nortriptyline or mirtazapine with remission rates of 19.8% and 12.3%, respectively) or the addition of lithium as mood stabilizer. The fourth level included a combination therapy of mirtazapine and venlafaxine (average remission rate of 13%) or comedication with tranylcypromine^{198, 199}. The mean times to remission range from 5.4 to 7.4 weeks between the different treatment levels²⁰⁰ and the chances of remission were smaller with each failed treatment level pointing up to the importance of reliable predictive biomarkers²⁰¹.

2. Lymphoblastoid Cell Lines in Pharmacogenomical Research

Due to their wide availability from different individuals and their representation of individual donors properties, the applicability of LCLs in pharmacogenetics is emerging. They are suitable to cover various phenotypes like apoptosis, cell growth inhibition or gene expression^{202, 203}. In the past research with LCLs focused on pharmacogenetics of indications such as oncology^{204, 205}, cardiology²⁰⁶ or pulmonology²⁰⁷. However, interest in research of psychological disorders using LCLs is rapidly growing. LCLs are generated through immortalization of easily obtainable PBMCs performed by EBV transfections²⁰⁸, whereby these viruses specifically infect B-lymphocytes without integration of viral genes into the host genome but with maintenance as latent extrachromosomal episomes²⁰⁹. EBV transformation modifies gene expression profiles as well as the methylation pattern of promotor regions in approximately 50% of all genes, but individual differences between cell lines remain intact²¹⁰. Additionally, LCLs seem to cover naturally occurring variations of the whole genome and epigenome²¹¹. Because LCLs are long-living and can be stored as cryocultures and (re-)cultivated under laboratory conditions, they basically are an infinite source of individual patient's genetic material avoiding repeated resampling of blood samples which is an advantage for long-term studies aiming on personalized therapy²¹². Consequently, as cell-based models they might help to support the identification of predictive biomarkers for various diseases. LCLs allow to cost-effectively performing *ex-vivo* experiments under well-controlled conditions, *i.e.* without the impact of confounders such as concomitant medications, nutrition, smoking status, *etc.*²⁰⁴. However, being derived from one single cell type and being only a cell-based model, LCLs do neither represent the complexity of the whole human organism nor completely reflect cellular proliferation or gene expression changes of multicellular tissues such as the brain. For instance, LCLs do barely express CYP (cytochrome P450) enzymes - relevant for the metabolism of various antidepressants, neurotransmitters and other neuroactive agents - making them unsuitable models for pharmacokinetic studies²⁰⁵. One general concern is the transferability of results obtained from

LCLs into clinical practice which has so far for instance successfully been done in the indication of cancerous diseases ²¹³⁻²¹⁶ but not yet in psychiatry biomarker research. Although there is some evidence that LCLs do not faithfully represent pathological changes of psychiatric diseases ²¹⁷, logically LCLs from patients should be given preference to LCLs from healthy donors when looking for disease-specific biomarkers - as done over the course of this work. Despite LCLs express more than 4,000 brain specific transcripts ¹²⁰, it is unclear whether they are helpful to identify relevant gene expression changes of antidepressant response - especially due to the high heterogeneity of depressive disorders. Furthermore, the fact gene expression changes following drug exposure could be different in blood-derived cells in comparison to neural cells should find critical consideration as well as the circumstance that LCLs show different methylation signatures related to neurons which probably leads to epigenomic-mediated effects on transcription levels ²¹⁸. Only a few studies so far employed LCLs as models for the investigation of individual antidepressant response. Here, LCLs were used to study individual proliferation and gene expression changes following antidepressant drug treatment. We found significant and large antidepressant-induced gene expression changes of neural and non-neural genes including high inter-individual differences as well as group differences between non-responder and responder derived LCLs. Several other observations support the potential role of LCLs as model for individual variability of drug effects in the CNS. In experiments from Morag and colleagues using LCLs from healthy donors, antidepressant induced growth inhibition was used as surrogate phenotype leading to the identification of neuronal genes such as *CHL1* (close homologue of L1) through genome-wide gene expression profiling as top-hit gene with different basal expression levels between paroxetine sensitive and insensitive LCLs ^{117, 118}. *CHL1* encodes for a neural cell adhesion protein involved in neurite outgrowth regulation, neural connectivity and thalamocortical circuitry ²¹⁹⁻²²³. Further, in addition to an implication in depression ²²⁴, *CHL1* plays a role in other neurological diseases such as schizophrenia and autism ^{225, 226}. By usage of genome-wide gene expression profiling and genome-wide miRNA arrays after three weeks of *in-vitro* treatment with hyper-therapeutic concentrations of paroxetine, Oved *et al.* identified gene expression differences of *ITGB3* (integrin beta-3) and miRNAs targeting *ITGB3*, respectively ²²⁷. They proposed that *ITGB3* provides a missing link between *CHL1* and SERT: *ITGB3*, as a known co-activator for SERT, is necessary for the proper functioning of this transporter ²²⁸, whereby *CHL1* seems to reduce available *ITGB3* molecules by high-affinity binding and therefore regulates SERT activity ²²⁷. SERT in turn, is the target of SSRI antidepressant drugs and increases the availability of serotonin within the synaptic cleft especially in pathways of the prefrontal cortex and the hypothalamus inducing the initial phase of remission from depression. The potential of *CHL1* and *ITGB3* as tentative gene expression biomarker was confirmed in subsequent studies using LCLs derived from depressed patients ¹¹⁹ and SNPs in neuronal cell adhesion genes involved in synaptic

plasticity were recently shown to affect treatment response in depressive disorders ²²⁹. Moreover, within a STAR*D cohort, *CHL1* was nominated as a tentative SSRI sensitivity biomarkers implicated in adverse reactions of citalopram in combination therapy with buspirone ²³⁰. In the present work neither *CHL1* nor *ITGB3* were traceable as tentative gene expression biomarkers using genome-wide gene expression profiling before and after the *in-vitro* treatment of patient-derived LCLs with SSRIs. In another study with LCLs, growth inhibition profiles were used to assign shared pathways following *in-vitro* treatment with different drug classes including antidepressants that can be used to categorize distinct pathways ²³¹. In addition to these studies that focused on LCLs as tools for the identification of biomarkers for depressive disorders, a few studies explored the utility of LCLs in other psychological diseases such as bipolar disorders or autism ²³²⁻²³⁴. Consequently, all these findings point to the importance of LCLs in psychiatric pharmacogenomic research.

3. Peripheral Proliferation as Surrogate Marker for Antidepressant Response

In initial screening experiments using fluoxetine as indicator drug, several methods for the determination of individual proliferation as well as various drug concentrations and incubation times were compared in order to identify optimal experimental conditions. Fluoxetine was chosen as antidepressant drug because most of the MARS patients under antidepressant monotherapy received SSRI antidepressant drugs and the proliferative features of fluoxetine are well-studied ²³⁵⁻²⁴¹. Since antidepressants-mediated improvement of clinical symptoms usually appears with a delay of several weeks, LCLs were incubated with antidepressants for up to three weeks in different concentrations covering the therapeutic range of fluoxetine blood concentrations (0.1 µg/ml and 0.5 µg/ml). Additionally, supra-therapeutic fluoxetine concentrations (10.0 µg/ml) were included as it was unclear in advance which amounts of fluoxetine will cause detectable proliferation effects (fluoxetine shares high protein binding properties and higher concentrations might be required in cell culture experiments) ²⁴². However, no fluoxetine induced increases in cell proliferation were observable over the three week incubation period by cell counting and subsequent creation of growth curves. Chang *et al.* were able to detect significant effects after 15 days of incubation with fluoxetine - by application of the same experimental design (0.5 µg/ml fluoxetine dissolved in DMSO, change of culture medium every second day) and evaluation method as performed here (CPDL) - in adherently growing neural precursor cells derived from human embryonic stem cells ²⁴³. Gene expression analysis of *MKI67* is a widely applied method for the quantification of proliferation

on a molecular level. MKI67 is a nuclear protein required for cell proliferation which is exclusively expressed in active phases of the cell cycle like G1, S and G2²⁴⁴. Although interindividual differences were detectable as well as statistically significant increases in gene expression levels of *MKI67* after chronic *in vitro* treatment with fluoxetine, no biological relevant effects were detectable. Biologically relevant in this context means an increase of fold changes to values larger than two²⁴⁵. The EdU assay is the only method that directly measures proliferation allowing single cell evaluations. We reported significant biological and statistical effects after three weeks of chronic exposure with concentrations of fluoxetine equal to therapeutic blood concentrations in fluoxetine-treated patients suffering from depression which is in accordance with the already described neurotrophic hypothesis of antidepressants action. Interestingly, higher concentrations of fluoxetine (10 µg/ml) already showed toxic or anti-proliferative effects. Toxic effects might be based on a genotoxic and mutagenic potential²⁴⁶ and other studies reported fluoxetine-mediated cytotoxic effects²⁴⁷⁻²⁴⁹. However, molecular mechanisms of fluoxetine-induced toxicity are unclear but might be based on the interruption of chromosomal structures²⁵⁰, the inhibition of metabolizing enzymes²⁵¹ or the interference with the energy metabolism²⁵². Since LCLs do not or barely express major phase one CYP enzymes relevant for antidepressant metabolism such as CYP2D6, CYP2C9, CYP2C19 or CYP3A5, observed effects assuredly are ascribable to fluoxetine and citalopram but not to their metabolites like norfluoxetine and demethylcitalopram, respectively^{253, 254}.

Following the screening experiments and in search of tentative functional biomarkers for antidepressant response prediction, we tested fluoxetine effects on cell proliferation in LCLs from depressed patients participating in the MARS study. Individual effects on cell proliferation have been detected after 21 days of incubation with fluoxetine. Although the *in vitro* treatment of patient-derived LCLs with fluoxetine presents high inter-individual variability regarding the LCL proliferation behavior, this phenomenon has no association with the MARS patient's clinical outcome. Both pro- and anti-proliferative effects were reported and averaged over all cell lines, no significant overall effects after *in vitro* treatment with fluoxetine were observable. Further, no significant associations between the individual basal proliferation rates, *i.e.* under control conditions without fluoxetine, were detectable. The relative proliferation after fluoxetine incubation relative to untreated controls from the same donors showed no significant association with LCL donor's response or remission status as well. Additionally, the proliferation rates of 50 LCLs derived from depressed patients participating in the STAR*D trial were determined after three weeks of incubation with therapeutic concentrations of the antidepressant drugs fluoxetine and citalopram. Here, we could show strong inter-individual differences between single cell lines as well as significant overall proliferative effects. The fluoxetine and citalopram (both SSRIs) mediated proliferation were highly correlated. Additionally, a direct association between peripheral *in-vitro*

proliferation rates of patient derived LCLs and clinical outcome in depression was shown: A significant correlation between percentage QIDS reduction, *i.e.* the improvement of clinical symptoms and LCLs proliferation rates was detected. Responder derived cell lines showed significantly increased proliferation after *in vitro* treatment with antidepressants compared to non-responder derived cell lines.

In cohorts from both antidepressant studies, no influence of general covariates like age or gender on proliferation rates was observable. These results are coherent with recent findings of Morag *et al.* who studied the influence of age and gender in antipsychotic drug sensitivities in human LCLs ²⁵⁵. The same applies for study specific covariates such as co-medication and individual's underlying diseases (MARS) or citalopram dosage, menopausal or anxiety status (STAR*D). In contrast anxious depression was shown to be associated with decreased remission rates compared with outcomes from patients with non-anxious depression ^{256, 257}. In general LCLs derived from the STAR*D study showed stronger antidepressant-mediated increases (up to 428%) of relative cellular proliferation rates compared to cell lines obtained from the MARS study (up to 155%) which might have several reasons. Firstly, extreme groups of clinical improvement from the STAR*D trial were used for proliferation phenotyping (cell lines from treatment resistant donors vs. cell lines from strongest/fastest responders). Secondly, LCL donors of STAR*D were treated with citalopram monotherapy whereas those from MARS were - due to the naturalistic study character - frequently treated with numerous different antidepressants at the same time accompanied by phase prophylactics and other co-medicated drugs (*e.g.* neuroleptics, benzodiazepines or sleeping medication). Consequently, the classification of the cell lines into responders and non-responders might be error-prone which could lead to impaired results. For instance it is not possible to distinguish between single drug effects of patients polymedicated with various antidepressants: A patient - like donor of cell line "734" - treated with an SSRI and a NaSSA at the same time might be classified as responder whereby the main effect of recovery could be based on the treatment with the NaSSA and would not be reproducible in laboratory conditions using fluoxetine as indicator drug. A similar problem occurs in patients who were treated with a given antidepressant for a too short period of time to evaluate its effectiveness (*e.g.* less than three weeks). Although the patient would have been a responder to the given antidepressant, such switches probably were performed due to harming severe side effects which do not occur in cell cultures. Last but not least, further impairments of the results probably might be based on the fact that patients with different underlying diseases such as bipolar disorders, single episode major depressive disorders or recurrent major depressive disorders were recruited for the MARS study. Due to the heterogeneity of the MARS cohort the significance of our results might be reduced. In contrast, in STAR*D only patients with defined, nonpsychotic major depressive disorders were enrolled. A further limitation

is that the *in vitro* proliferation in LCLs was determined after incubation only with fluoxetine or citalopram which does not reflect the real treatment regimens. Taken together, the LCL cohort from the STAR*D study seems to be the more suitable one for our experimental approach because it is a defined cohort with uniform disease background which received antidepressant monotherapy so that the LCL donor's response status is unambiguous.

The individual proliferative effects observed here after long-term incubation with antidepressant drugs do not correlate with *in vivo* proliferative effects. No signs of cell proliferation stimulus on blood cells or bone marrow have ever been described for antidepressant drug therapy, but such *ex vivo* effects in the cell lines of depressed patients might contribute to the puzzle of explaining the high variability in antidepressant efficacy observed in clinical routine. However, one has to keep in mind that individual patient's clinical efficacy could be different from those observed in LCLs and that the applicability of peripheral proliferation after long-term incubation with antidepressants as response biomarker seems limited. Aggravating, it is assumed that cellular proliferation as well as neurogenesis could be influenced by factors such as age²⁵⁸, alcohol²⁵⁹ and exercise²⁶⁰. Our hypothesis is based on the assumption that antidepressants induce the proliferation of neuronal cells and therefore modulate the neural plasticity²⁶¹. Depressed patients show a volume reduction of depression-associated brain parts¹⁶ that might be reversed by antidepressant-induced proliferation²⁶². The induction of neural stem cell proliferation is directly linked to an enhanced neuroplasticity which in turn leads to a normalization of the depressed brain function²⁶³. This explanation helps understanding the delay in symptomatic improvement (from weeks up to several months) because cerebral remodeling processes are complex and time-consuming. Such direct proliferative effects of antidepressants and the role of neurotrophic proteins were analyzed by Chang and colleagues in human neuronal precursor cells²⁴³. Other research groups reported proliferative effects in rodents, *e.g.* in hippocampal granule cells of adult mice^{264, 265} and non-human primates²⁶⁶. Chen *et al.* studied the effect of chronic treatment with antidepressants on the number of hippocampal neurons in a genetic rat model of depression and concluded that antidepressants are able to induce neurogenesis and synaptogenesis²⁶⁷. The molecular mechanisms underlying these neuro-proliferative effects and the remission of depression remain poorly understood, although neurotrophic growth factors - like BDNF - may play an important role during remission processes²⁶⁸. Antidepressant effects are restricted to type 2 but not type 1 neuronal progenitor cells accelerating the maturation of neurons^{269, 270}. Fluoxetine probably conveys the integration of newborn neurons into the functional networks like the dentate gyrus network or the hippocampal pyramidal cells of the HPA axis which leads to an improved cellular survival¹³⁰. All those findings along with our results support the neurotrophic hypothesis of antidepressant's action which suggests an antidepressant-mediated reversal of impaired

hippocampal structure and activity. However, the relationship between SSRI-mediated *in vitro* proliferation and clinical efficacy remains in need of further investigation. Studying of molecular backgrounds and the identification of potential gene expression biomarkers associated with peripheral or CNS proliferation might be advantageous as well.

4. Microarray-based Identification of Tentative Gene Expression Biomarkers

Analysis of whole genome gene expression in LCLs becomes more and more important for the identification of tentative gene expression candidate biomarkers. In general microarray based gene expression has manifold advantages such as the simultaneous determination of expression levels of nearly all known human genes in one single experiment. Due to the hypothesis-free nature of genome-wide expression studies, results are unbiased and do not necessarily require pre-experimental knowledge about underlying mechanisms or involved pathways. However, care is called when it comes to the interpretation of such data because false-positive events occur frequently and so, data need independent confirmation.

Phenotyping the proliferative response of LCLs to fluoxetine (0.5 µg/ml; 21 d) followed by comparative microarray-based genome-wide gene expression profiling revealed 15 candidate genes out of 390 identified by pathway analyses. These genes can be assigned to either WNT signaling (*e.g. WNT2B, FZD7, TCF7L2*) or EGF signaling (*e.g. BTC, EGFR, HBEGF*) or to a group of pharmacokinetic genes (*e.g. CYP3A43, SULT4A1, ABCB1, ABCG4*) and will be further addressed in the following subsections (chapters 4.1 to 4.4). The gene *CACNA2D3* - which probably possesses a role in long-term antidepressants action¹⁷⁴ - cannot be classified into these groups. *CACNA2D3* is a member of the voltage-dependent calcium channel complex which is expressed in the cerebral cortex amongst other non-neuronal tissues. It was reported that the gene expression of *CACNA2D3* in mice is increased after 28 days of treatment with the antidepressant amitriptyline¹⁷⁴. A calcium or calmodulin-dependent role of *CACNA2D3* in regulation of transcription factors of cortical neuron formation was postulated but needs further investigation. However, Malmersjö *et al.* found calcium ion activity important for cellular proliferation in mouse neural progenitor cells²⁷¹. Another work reported calcium being involved in neurodevelopment, apoptosis or differentiation within a network of purinergic receptors²⁷².

4.1. Role of EGF Signaling in Depression

In the microarray experiments, by far the strongest gene expression differences compared between responder derived cell lines relative to non-responder derived cell lines were obtained for betacellulin (*BTC*). *BTC* belongs to the epidermal growth factor (EGF) protein family and has been reported to stimulate neurogenesis¹⁶⁵ as well as neural stem cell proliferation and differentiation into glial- and neuronal like cell types²⁷³. *BTC* is endogenously produced in the brain, especially by blood vessels and the choroid plexus and directly affects neuroblast differentiation and neuronal stem cell regeneration by activation of EGFR and ERBB4 (epidermal growth factor receptor 4). It is considered a potential therapeutic agent for treating neurodegenerative diseases¹⁶⁵. Further genes from the EGF pathway being involved in individual fluoxetine drug response were identified by our microarray approach such as *ERBB3*, *MAPK9*, *PIK3R5*, *HBEGF* and *EGFR*. *ERBB3* is a receptor for EGF and an important element of the nervous system development¹⁸⁰. Furthermore it is required for the development and differentiation of the neural crest and glial cells^{180, 274}. *HBEGF* and *EGFR* are crucial for proliferation of astrocytes and neurogenesis as well as neural progenitor proliferation and migration, respectively^{167, 177}. *HBEGF* is an 87-amino acid glycoprotein and a growth factor targeting the *EGFR* amongst others. It is widely distributed in neuroglia and cerebral neurons where it is required to stimulate neurogenesis²⁷⁵. A stimulation of *EGFR* on the other hand - through for example EGF, TGF alpha, *HBEGF*, *BTC* and many more²⁷⁶ - activates a signaling cascade ending in increased cell proliferation, adhesion and survival. A recent study presented a role of *EGFR* in neuronal protection from stress²⁷⁷ and mutations within the *EGFR* gene have been associated with a decreased frequency of depressions and a lower depression severity in oncologic patients²⁷⁸. *MAPK9* is an enzyme involved in a wide variety of cellular processes like proliferation and transcription regulation. This kinase inhibits the degradation of cell cycle protein p53 and therefore, regulates apoptosis - mainly in dopaminergic brain areas¹⁷⁸. Mitogen activated protein kinases are generally required for neuronal plasticity, survival and differentiation. Additionally, it was recently shown that *MAPK9* was downregulated in dermal cells derived from patients suffering from bipolar depressive disorders²⁷⁹ suggesting a role in psychiatric dysfunction. *PIK3R5* is a regulatory subunit for PI3Ks (phosphatidylinositide 3-kinases) that play important roles in cell growth and proliferation. Furthermore, *PIK3R5* is a circadian gene involved in sleep-wake cycles and therefore, in insomnia¹⁶⁹ - one of the main side symptoms of depressive disorders. An impaired gene expression of *PIK3R5* is a risk factor for suicidal behavior^{170, 171}.

4.2. Role of WNT Signaling in Depression

The transcription factor *TCF7L2* and the receptor *FZD7* belong to the canonical WNT signaling pathway which plays an important role for regulation of stem cell pluripotency and cell

differentiation by integrating signals from other pathways and their associated signal molecules such as fibroblast growth factor and bone morphogenic protein^{280, 281}. Both growth factors are involved in depression pathogenesis^{282, 283} and - together with other downstream growth factors like BDNF, VEGF (vascular endothelial growth factor) and other signaling pathways - in the maintenance of adult hippocampal neurogenesis^{284, 285}. Further, WNT signaling regulates neurogenesis, synaptic plasticity and dendritic arborization²⁸⁶. WNT2B is a highly conserved signal peptide and a ligand for members of the frizzled transmembrane receptor family. FZD7 - being a receptor for WNT proteins in the brain - belongs to this family of G protein-coupled receptors¹⁷³. WNT2B is involved in regulation of cell growth and differentiation¹⁶⁶. WNT glycoproteins usually are liberated from hippocampal astrocytes and show short-ranged action. They take effects through gene expression activation of NeuroD (neurogenic helix-loop-helix protein) and Dcx (neuronal migration protein doublecortin)^{287, 288}, a transcription factor involved in CNS development and a microtubule-associated protein almost exclusively expressed in actively dividing neuronal precursor cells, respectively^{289, 290}. An activated Wnt signaling pathway supports the differentiation of specific glial neuronal precursors²⁹¹, controls stem cell pluripotency and tissue regeneration²⁹² and regulates the expansion of CNS progenitor cells²⁹³. Furthermore, WNT proteins are involved in immunological processes of microglia²⁹⁴ - macrophage-like cells of the brain that are required for CNS homeostatic functions²⁹⁵. Neurotoxic agents reduce *WNT* expression in developmental hippocampal neurons²⁹⁶. Furthermore, Wnt signaling regulates adult hippocampal neurogenesis²⁹⁷ and the expansion of CNS progenitor cells²⁹⁸. Moreover, it is important for synaptic function as well as for the formation of hippocampal spines^{299, 300}. A malfunction of Wnt signaling in the hippocampus by targeted knockdown is associated with decreased neurogenesis, increased depression-like behavior and various neuropsychiatric disorders^{286, 301}. It has been shown that Wnt signaling is responsive to various antidepressant drugs³⁰² while mice with constitutively activated Wnt signaling become unresponsive to antidepressant treatments³⁰³. Furthermore, a role of Wnt signaling via the fast acting antidepressant ketamine has been proposed³⁰⁴.

4.3. Role of Drug Metabolizing Enzymes in Depression

Although the sequence of *SULT4A1* is highly conserved between mammals suggesting an important function^{305, 306}, little is known so far about the brain specific phase II metabolizing enzyme SULT4A1. It may be involved in the metabolism of antidepressant drugs and neuroactive substances. However, since expression of *SULT4A1* was low in LCLs and only detectable in 21 out of 100 cell lines, our results should be seen with caution and warrants further analysis of *SULT4A1*

expression in brain. *SULT4A1* seems to conjugate drugs and neurotransmitters specifically within the brain^{172, 307}. An association of polymorphisms within the *SULT4A1* gene and the susceptibility to neurological disorders like schizophrenia has been described³⁰⁸. Its higher expression in females³⁰⁹ may be associated with the higher prevalence of depression in women. Interestingly, the gene expression of *SULT4A1* is regulated by CREB (cAMP response element-binding protein)³¹⁰, a transcription factor that plays a major role in neurogenesis and synaptic plasticity³¹¹. Furthermore, CREB is involved in pathological and pharmacological actions of depressions, since decreased levels of CREB in the prefrontal cortex of depressed patients were shown³¹². Effects of SSRIs on CREB concentrations through the course of treatment were reported with lowered CREB levels in responders than in non-responders³¹³.

The monooxygenase CYP3A43 shares a testosterone hydroxylase activity and seems to be involved in lipid and steroid synthesis as well as in antipsychotic drug metabolism^{168, 314}. It is a homologue to other drug metabolizing CYP enzymes, but it shows no proven cerebral expression and probably does not significantly contribute to the metabolism of xenobiotics or drugs³¹⁵. However, since CYP3A43 is involved in hormone metabolism, one might speculate about a role of CYP3A43 within the context of the hormone-based hypothesis of the pathogenesis of depression (see chapter 2.1). Levels of steroidal hormones such as cortisol or estrogen have been associated with a higher risk of depressions and with more effective antidepressant therapies^{20, 21}.

4.4. Role of Drug Transporters in Depression

ABCG4 belongs to the ATP binding cassette (ABC) superfamily and is involved in the regulation of cholesterol and lipid homeostasis in neurons and astrocytes^{175, 176}. It plays a role in fear processing in mice³¹⁶ and was suggested to be implicated in the development of neurodegenerative disorders such as the Alzheimer's disease³¹⁷. A known direct relation between ABCG4 activity and depressive disorders is missing. However, abnormality in lipid homeostasis may lead to increased production of reactive oxygen species which in turn, is connected to pathophysiological processes in depressions^{318, 319}.

The plasma membrane transporter ABCB1 possesses a key role in cellular detoxification and transmembrane transport across the BBB back into the circulatory system. Furthermore, it contributes to the biliary and renal elimination of drugs^{320, 321} and represents a major component of the intestinal barrier³²². ABCB1 is an efflux pump with a broad allocrite spectrum including a variety of drugs (*e.g.* antidepressants, glucocorticoids), xenobiotics as well as neurotoxic agents¹⁷⁹ and thus, ABCB1 holds neuroprotective effects eventually resulting in an increased response to antidepressant mediated induction of neural proliferation and plasticity. Peripheral glucocorticoids are stress response factors in the HPA axis, normally have toxic effects on neurons and are

suspected to be causative for depressions³²³. Furthermore, a dysfunction of glucocorticoid receptors modifies the functional integration of neurons in the hippocampus and therefore, leads to an impaired synaptic connectivity and fear-motivated behavior in animal experiments³²⁴. Studies using *ABCB1* knock-out mice or ATPase assays in human *ABCB1* membranes have shown that most antidepressants such as amitriptyline, doxepin, paroxetine or citalopram are strong allocrites of this transporter^{185, 325-328} and overexpression of *ABCB1*, *i.e.* increased removal of antidepressants from the brain, might explain non-responsiveness to various antidepressant drugs³²⁹. Hence, numerous variations in the *ABCB1* gene were reported influencing the plasma levels of antidepressants as well as the treatment efficacy³³⁰⁻³³⁶. Fluoxetine, one of the antidepressants we employed for *in vitro* LCL phenotyping, is only a weak allocrite of *ABCB1*^{337, 338}. One may speculate that the absence of a correlation between fluoxetine induced *ABCB1* expression and clinical response of the MARS cohort could reflect the low *ABCB1* allocrite properties of this antidepressant drug. Carriers of defined haplotypes within the *ABCB1* gene show decreased risk of developing depressions³³⁹ and polymorphisms of the *ABCB1* gene are thought to predict adverse antidepressant drug effects³⁴⁰. Furthermore, other polymorphisms might predict the individual response and dose adjustment to the antidepressant escitalopram and are associated with depression severity^{335, 341}. All these findings point to a significant involvement of *ABCB1* in depression.

5. Validation of Tentative Gene Expression Biomarkers

Five genes (*WNT2B*, *TCF7L2*, *FZD7*, *SULT4A1* and *ABCB1*) were differently expressed in an edge-group approach, *i.e.* in cell lines with the highest increase vs. highest decrease in cell proliferation following 21 d fluoxetine incubation. Analyzing extreme phenotypes is an emerging method in pharmacogenomical research since it time- and cost-effectively allows the discrimination of genes involved in processes of interest. The observed effect size is increased compared with results from cell lines with average phenotypes and consequently - as done over the course of this work - the findings need to be verified in the total population³⁴². Initially, this approach was developed in the field of oncology leading to the identification of various biomarkers to predict effects of anticancer drugs like cisplatin³⁴³, cytosine arabinoside³⁴⁴ or etoposide³⁴⁵ but is now of growing interest in neuropsychiatric indications. For example, Morag *et al.* identified potential genetic biomarkers in edge-groups from paroxetine sensitivity phenotyping experiments¹¹⁷.

Further data analysis containing results from all available cell lines showed a correlation between LCL donor's clinical responses with the LCL basal gene expression of *SULT4A1*. Furthermore, the gene expression fold changes of *WNT2B* by fluoxetine incubation correlated with clinical remission.

None of the remaining genes *TCF7L2*, *FZD7* and *ABCB1* showed significant correlation with clinical parameters of LCL donors from the MARS study. In contrast, associations between LCL donor's clinical response and LCL basal gene expression of *WNT2B* and *ABCB1* but not for *FZD7*, *TCF7L2* or *SULT4A1* could be found in the cohort derived from patients participating in the STAR*D study. Furthermore, the fold changes by fluoxetine and citalopram of *WNT2B*, *FZD7* and *ABCB1* showed correlations with LCL donor's clinical response and remission status. In general remission - defined as the virtual absence of depressive symptoms - is assumed to be the more robust outcome parameter compared to response which is characterized by a 50% reduction of symptomatology³⁴⁶. This, together with the fact that patients showing remission demonstrated decreased relapse and suicide³⁴⁷, is why remission predicting biomarkers should be given the virtue. Since the results were more or less reproducible in the different cohorts (MARS and STAR*D), the genes can be assigned as putative gene expression biomarkers acting as potential temporal mediators (variables whose initial early change during treatment could be associated with future treatment outcome) or baseline gene expression predictors (variables associated with treatment efficacy before therapy start) that eventually advance the personalized treatment approach in depressions in the future.

6. Interferon beta, Sickness Behavior and Depression

In 17 healthy participants (7 males and 10 females with a mean age of 26.5±4.9 years), questionnaire based evaluations of interferon-induced mood changes (STAI and HDRS) were carried out. The STAI intends to measure general propensities to be anxious and current symptoms of anxiety through simple self-report algorithms. Since anxiety is one of the main symptoms of depressive disorders a correlation of STAI results with depressive states has been described frequently³⁴⁸. Furthermore, high test-retest reliability coefficients as well as the ability to detect individual changes were reported in the literature³⁴⁹. The HDRS was actually developed to provide indications of depressions and to evaluate recovery, but here it was used to assess interferon-induced changes in behavior and mood. It is one of the most used depression rating scales characterized by high internal consistency, inter-rater reliability and test-retest reliability³⁵⁰. The observations from behavioral testing showed significant increased depression scores (HDRS) but no significant changes in anxiety levels (STAI). Maybe a possible individual interferon-induced anxiety interferes with increased anxiety level of fearful participants during their first MRI scan session (questionnaires were conducted immediately before the MRI measurement) leading to impaired results. When analyzing the single items of the HDRS, depressive main symptoms (*e.g.* depressed mood or anhedonia) were barely detected, but other depression-related symptoms such as feelings

of fatigue or weakness, concentration problems, insomnia, *etc.* were frequently recorded. These results suggest an induction of sickness behavior by interferon beta but not of depression itself which is an interesting new aspect of the current pharmacological research. For that reason the following part summarizes the knowledge about the connection between immune system activation and the development of depressions considering molecular backgrounds, brain functioning in the key sites, treatment effects and the possible role in personalized medicine.

In the early 1990s a role for cytokines in depression was proposed as a part of the macrophage theory of depressions³⁵¹. A few years later it was described that pro-inflammatory cytokines are able to cause some clinical aspects of depressive disorders such as the disturbance of the serotonin metabolism, the hyperactivity of the HPA axis and most of the neuro-vegetative symptoms (*e.g.* appetite disturbance, fatigue, concentration problems, *etc.*)³⁵². Depressions have been associated with a pathologic activation of the immune system characterized by increased levels of T cells and acute phase proteins^{353, 354}. In general symptoms of sickness behavior and depression are tightly connected and a common pathophysiology is suggested³⁵⁵. For instance both phenomena are caused by or led to a decreased reactivity to reward, a withdrawal from social or physical environment as well as pain and malaise²⁵. The detailed mechanisms behind these behavioral changes remain unclear. The amygdala seems to be a neural key region that is involved in sickness induced social withdrawal in animals³⁵⁶. In accordance to this, social avoidance tendencies are associated with elevated amygdala activities to negative social cues in humans³⁵⁷⁻³⁵⁹. In animal models induced depression-like behavior was linked to an exaggerated inflammatory response in the brain with aged mice being more sensitive³⁶⁰. Consistent with this the onset of depression was shown to be preceded by elevated biomarkers of inflammation in a cohort of elderly participants³⁶¹. Furthermore, the symptoms of both sickness behavior and depression can be successfully treated by antidepressive drugs. Patients with exaggerated inflammatory blood markers are more likely to show treatment resistance to antidepressants³⁶². However, in this context depressive disorders seem to be caused by a dysfunction in neuronal circuits of cytokine-induced responses since an increased vulnerability to depressions was reported in persons with an overactive CRH system³⁶³. In such vulnerable individuals, (chronic) inflammatory processes like systemic infections or autoimmune diseases are able to influence the brain functions and therefore, to guide from sickness behavior to depression³⁶⁴. Several mechanisms to explain these effects of peripheral cytokines on the CNS are proposed, *e.g.* a role of post-infection activation of primary afferent neural tracts like the vagal nerve is discussed^{365, 366}. Furthermore, peripherally circulating cytokines are able to increase the production of centrally-acting pro-inflammatory cytokines by activation of macrophage-like cells from the circumventricular organ - a specialized organ of the brain ventricular system that is an integral part of the neuroendocrine function³⁶⁷ - in a toll-like receptor mediated

manner as part of the humoral pathway response. Additionally, blood cytokines are able to enter the brain directly either by volume diffusion³⁶⁸ or by active transport mediated by cytokine transporters of the BBB^{369, 370}. Cytokines are able to counteract and prevent antidepressant actions including effects on neurotransmitter function and synaptic plasticity⁶³. Cytokines can influence neurotransmitter synthesis, release and reuptake by various mechanisms. A cytokine-induced activation of the indoleamine-2,3-dioxygenase (IDO) that metabolizes tryptophan - the serotonin precursor - leads to a reduced availability of serotonin in the brain²⁵ and to the development of depression-like behavior in animal experiments^{371, 372}. The expression of neurotransmitter reuptake transporters is increased by inflammatory cytokines in a mitogen-activated protein kinase (MAPK) dependent manner³⁷³⁻³⁷⁵. Interferons are glycosylated hormone proteins with immunomodulatory effects that probably act via receptor-associated tyrosine kinases followed by an activation of the JAK/STAT cascade resulting in an activation of immune cells (*e.g.* monocytes, leucocytes) as well as an increased expression of human leukocyte antigen molecules and other mediators of immune reactions like cytokines. This might be a possible mechanism of action with respect to the mentioned immunologic effects. Pro-inflammatory cytokines such as interleukins or TNFs usually are responsible for acute-phase reactions (*e.g.* after an infection) and they are peripherally produced by accessory immune cells like dendritic cells or macrophages. Cytokine-induced sickness behavior is caused by pro-inflammatory events in the brain mediated mainly by the interleukins IL-1a, IL-1b, IL-6, IFN- β and TNF- α . A stimulation of the sympathetic nervous system by stress is also able to activate inflammatory signaling pathways³⁷⁶. Consequently, the option to treat depressions with anti-inflammatory drugs was hypothesized and some evidence for a positive therapeutic effect of TNF or COX inhibitors was identified recently, but further investigations concerning the pathophysiology of inflammation and depression-like behavior are necessary to advance this approach³⁷⁷⁻³⁸¹. The identification of subgroups of depressed patients being responsive to immunotherapies would be beneficial in the view of treatment personalization. Additionally, lower levels of TNF- α have been linked to response to the antidepressant amitriptyline³⁶². There is growing evidence that inflammatory processes might have a greater influence on the pathogenesis of depressions than the traditional psychosocial factors (*e.g.* negative life events, chronic stress or lack of social contacts). In animal experiments, an activation of the immune system led to a decrease of the preference for drinking and food intake³⁵⁶ and the effect size was reduced after the pre-treatment with antidepressants³⁸². A higher sensitivity towards interleukin-induced negative mood was reported in a genetic model of depression³⁸³ and cytokines were shown to be able to increase the serotonin turnover in the brain^{373, 384}. Furthermore, both physiological and psychological risk factors play an important role in the vulnerability to immunotherapy-induced depression. For example an enhanced response of the HPA axis^{385, 386} and

elevated depression scores before begin of the therapy have been associated with depression severity ¹⁰⁹. The HPA axis can be activated by neuropeptides like vasopressin or corticotropin-releasing factors which are known to account for depressive symptoms ^{387, 388}.

7. Functional Neuroimaging

Functional neuroimaging is an important instrument to assess neurobiological correlates of drug effects in the brain due to its non-invasivity and wide applicability in the clinical setting. Several MRI studies have been successful in identifying the changes in specific brain structures induced by medication ^{389, 390}. As the core symptoms of depressions are reflected by an impaired reward processing and emotion regulation ³⁰, we focused on these neural circuits using particular fMRI paradigms (foraging and faces, respectively). One important concern was to evaluate the applicability to depict cytokine-induced sickness behavior or depressions via fMRI. However, a few limitation of our fMRI study have to be mentioned. First, no control group was enrolled so far (but is planned for the future) in this study leading to the fact that effects of repeated measurements remain unconsidered. Since the study was not double-blinded and randomized, the implementation of a well-matched control group is absolutely essential. The sample size of this study is small and therefore the results possess only low statistical power. Additionally, since the relationship between clinical characteristics and brain activity is very complex and not well understood so far, the transferability of our result's use remains unknown. But the measurement of dysfunctions in above described neural circuits detected by fMRI will provide further information regarding this issue and may be helpful in individual guidance of diagnostics of depression and antidepressant treatment selection in the future.

7.1. Responses to Emotional Faces after Interferon Administration

The faces paradigm was assigned to evaluate reactivity to emotional stimuli like anger, sadness or disgust in a passive exposure paradigm whereby the region of interest was the amygdala. No significant differences in amygdala activation before and after interferon administration were detectable which might be based on different reasons (such as the unsuitability of the faces paradigm to depict processes of drug-induced depressions, *i.e.* other regions - that are not covered by the faces paradigm - might be more relevant to the pathogenesis of drug-induced depressions under consideration of emotional processes or the fact that the duration of drug intake was not sufficient to fully develop activation differences in the amygdala). However, the faces paradigm is a

robust standard method to measure amygdala activation¹⁵⁹, since the amygdala activation can be measured (also when the presentation of the faces is subliminal) and drug effects are depictable³⁹¹. Nevertheless, the latest literature regarding the phenomenon of facial emotion deficits in depressive disorders will be discussed in the following section since it is widely accepted that such processes play a key role in depression and there is huge evidence for abnormal emotion recognition in this disorder.

Impaired facial emotion recognition is symptomatic for many psychological diseases including schizophrenia, alcoholism, autism, anxiety, bipolar disorder and depression³⁹²⁻³⁹⁷. Since emotional perception is crucial to social interaction which is one important factor of individual well-being in depressions^{398, 399}, the role of emotion recognition in depression is of high relevance (reviewed by Bourke *et al.*⁴⁰⁰). Emotional processes are usually regulated by the interaction of top-down control processes in the prefrontal cortex and bottom-up processes triggered by emotional stimuli¹³³. However, here we did not find any significant changes in amygdala activation after the short-term treatment with interferon beta indicating no specific role of the amygdala in the rapid action of interferon-induced sickness behavior or depression. In contrast, Whalen *et al.* reported a modulated reactivity in the limbic system after interferon beta treatment in depressive patients⁴⁰¹. Many studies have demonstrated a relationship between local inflammation, regional brain activation and emotional processing⁴⁰². Additionally, using fMRI techniques it was convincingly shown in numerous studies that the reactivity of the limbic and paralimbic systems to emotional stimuli (*e.g.* sad faces) is impaired in depressive patients. Recent meta-analyses identified moderate emotion recognition deficits in depressed patients^{403, 404}. Another meta-analysis reported uniquely preserved recognition of sadness while the recognition of the other basic emotions (anger, disgust, fear, happiness, surprise) is impaired⁴⁰⁵. Frodl *et al.* reported an increased activity in the limbic system to emotional stimuli in depressed patients compared to healthy controls⁴⁰⁶. Such abnormalities are associated with constructs in the negative valence system like acute and chronic anxiety or fear. Pharmacological treatments have been shown to normalize pathologically elevated activity in these circuits⁴⁰⁷⁻⁴¹². Antidepressant drugs were shown to alter the recognition of emotion^{413, 414} and to reduce the neural responses to negative facial expressions⁴¹⁵. Several genetic variants within neural genes were associated with impaired emotion processing and with poor response to antidepressants. For example a variant of neuropeptide Y (rs16147) - a neurotransmitter of the autonomic nervous system involved in stress and anxiety processing - has been linked to an exaggerated amygdala reactivity to emotional faces and to a decreased treatment outcome in patients with anxious depression⁴¹⁶. Another study reported a connection between reduced response of the striatum and the thalamus to happy faces, a decreased response to antidepressant drugs and a genetic variant of the cannabinoid receptor type 1 (rs1049353) - a

receptor of the endogenous cannabinoid system that is required for the development of the brain and for the response to stress and anxiety⁴¹⁷. Furthermore, an aberrant activity of the amygdala to sad facial emotions is specific to depressive states and therefore appointed as a potential biomarker for negative affective bias during depressive episodes⁴¹⁰. Consequently, the limbic reactivity to emotional faces measured by MRI techniques could be helpful in the future for early medication screening or to predict the individual treatment outcome in depression^{410, 418}.

7.2. Responses to Monetary Reward after Interferon Administration

The foraging paradigm was employed to probe the impact of interferon therapy on the sensitivity to reward cues. We measured a decreased activity of the dopaminergic ventral striatum following the treatment with interferon beta in this money-rewarding paradigm. Changes in dopamine function are correlated with behavioral changes such as depression or sickness symptoms. The dopamine-modulated cortical cortex including the ventral striatum possesses a key role in reward processing regulated by the orbitofrontal cortex^{419, 420}. Other brain structures like anterior cingulate cortices or the ventromedial prefrontal cortex were described being involved in reward expectancy or processing⁴²¹⁻⁴²³. Dysfunctional reward circuitries have frequently been associated with depression. For example, depressed patients showed increased activities of the anterior cingulate cortex to previously rewarding stimuli (but less activity of the ventral striatum), to expectancy of monetary reward or to reward learning⁴²⁴⁻⁴²⁶. Other studies reported reduced ventral striatal activities during reward learning and to rewarding stimuli in depressed patients relative to healthy controls^{425, 427-430}. Dopamine and various pharmacological treatments (*e.g.* levodopa, duloxetine or dextroamphetamine) were shown to alter these processes by modulation of the activity of the ventral striatum⁴³¹⁻⁴³³. Furthermore, a normalization of functional abnormalities within the reward system was observed after psychotherapy⁴³⁴. Interferons are known to target CNS structures like the basal ganglia of the ventral striatum amongst others which has been shown by positron emission tomography imaging or fMRI^{364, 435}. For example a decreased activation in the ventral striatal region was shown in a reward paradigm of patients suffering from hepatitis C being treated with interferon⁴³⁶. Another study demonstrated that inflammation alters reward-related neural correlates of anhedonia - a key symptom of depression - to monetary reward cues by a reduction of the ventral striatum activity⁴³⁷. Abnormalities in reward neural circuits are responsible for the depressive symptoms of apathy and anhedonia that in turn might be connected to constructs in the positive valence system^{427, 438}.

8. Outlook / Future Perspectives

Since depressions already belong to the most prevalent mental illnesses affecting over 350 million people worldwide and the prediction that depressive disorders will account for the largest part of the economic burden within the next twenty years ⁹, the improvement of the individual antidepressant therapy of this serious mental illness will become inevitable. The total number of affected people will raise even more dramatically in the future because the world population is rapidly growing, diagnostical tools will find their way in the improving medical systems of today's third world countries (where depression might be underdiagnosed nowadays ⁴³⁹) and environmental conditions as contributory causes (*e.g.* chronic stress and fear, progressing urbanization accompanied by increasing social isolation *etc.*) will worsen. Additionally, more significance will be given to heritability factors of depressions. The introduction of gene therapeutical approaches into clinical practice might be a solution. Another interesting approach to reduce depression rates could be vaccination ⁴⁴⁰, normalizing the imbalance between pro- and anti-inflammatory cytokines frequently reported in depressive disorders (compare with chapter 2.1, immunological hypothesis). However, gene therapy and vaccination are experimental approaches that might become relevant in the distant future. Since genetic biomarkers are more objective parameters compared to behavioral scales they will be more efficacious in personalized therapies in the field of depressive disorders ⁴⁴¹. For that reason treatment individualization using genetic biomarkers remains in the focus of research in the short to medium term. This turned out being a challenging aim due to high complexity and individuality of depressions and consequently, identifying single universal parameters to predict individual treatment responses seems impossible. Hence, biomarker signatures of validated parameters on DNA, RNA and protein level will be necessary and be the future of personalized medicine in depressive disorders. The development of fast and easy to use methods (like the cobas[®] EGFR mutation test kit used for therapy individualization of patients suffering from non-small cell lung cancer ³) covering such biomarker signatures would be the best solution to further advance the field. The candidate genes reported here could be a part of such biomarker signatures. They should be further examined for their molecular validity, pharmacogenetical variability and their role in remission from depression. The molecular validity of these genes could be verified by detection of their gene products on protein level for instance using immunological methods like ELISAs (enzyme linked immunosorbent assay) or Western Blots. The pharmacogenetical validity may be proven by knockdown or miRNA silencing experiments of the mentioned genes in LCLs, animal models for depression or human neuronal cell lines (*e.g.* neuroblastoma cell line SH-SY5Y or cortical neuron cell line HCN-2) with subsequent determination of effects on the SSRI-mediated proliferation induction. Another interesting

approach is the generation of neuronal cells from LCLs derived from depressive patients by reprogramming technology using retroviral or virus free (transcription factors and small molecules) methods^{442, 443}. Additionally, the role of the candidate genes in remission from depression could be evaluated using longitudinal blood samples from major depression patients participating in prospective, controlled clinical trials. After confirmation of their predictive potential the gene expression levels of *ABCB1*, *FZD7*, *SULT4A1* and *WNT2B* might support the guidance of individual AD therapy choices in the future and therefore, such genetic biomarkers will further lead to the eradication of trial and error prescription.

Away from this, another interesting and promising approach to pave the way for the entry of the individualized medicine into the important indication of depressive disorders is the usage of neuroimaging techniques. Here, we found evidence for individual variability in drug-induced depression as well as an impaired reward system functionality being highly involved in interferon-beta induced sickness behavior. Transferring this knowledge to depression itself one might speculate about a more important role of a well-working reward system in depressions than previously thought. However, the short-term aim is to verify and validate the obtained results that so far lack evidence of no or insignificant impact of repeated measurements on individual brain activities targeted by our fMRI paradigms. Since the test-retest-reliability of fMRI paradigms is frequently underrated^{444, 445}, identical measurements in unmedicated, matched healthy volunteers should and will be added as a control cohort. Here, we only described two different paradigms targeting anxiety and reward behavior, but the actual MRI measurement battery consisted of more sequences such as other functional MRI paradigms targeting further depression-associated conditions (*e.g.* anhedonia, negative cognition) as well as perfusion and diffusion measurements. Since perfusion imaging is a hypotheses free approach to measure brain activity, it could shed light on further, unknown brain regions involved in interferon beta action and the development of depression-like behavior or depressions itself. Diffusion imaging is an innovative MRI-based technique that measures the degree and directionality of the diffusion of water molecules in the brain and that can be used to detect changes of the axonal organization (*e.g.* axon density, axon diameter, myelination) and neuroplasticity⁴⁴⁶. These approaches will surely deliver further interesting results improving our understanding of individual effects of interferon beta. One - so far unfinished - aspect of this study was to correlate MRI data with transcriptomic data. The connection of these "big data" may be beneficial to accelerate psychiatric biomarker and treatment development and to improve our understanding of the molecular neurochemical and neurogenetical mechanisms behind drug-induced depressions and depressions in general^{122, 447}. This approach might help to identify genetic vulnerability markers of psychiatric diseases as well as

the effects of gene expression differences to structure and function of the brain. Furthermore, the prediction of affective interferon side effects could be helpful for the therapy guidance of MS patients and to reduce their suffering⁸⁸. It was frequently shown that individual variability in brain functions can be depicted by MRI measurements⁴⁴⁸. In the future functional connectivity profiles may act as intrinsic fingerprints⁴⁴⁹ which probably allow the accurate distinction of depressed from healthy subjects or from subjects with other neurological diseases (*e.g.* epilepsy or schizophrenia) within large cohorts. Another application could be the prediction of non-response or response to a given antidepressant drug. However, the identification of such fingerprints being clearly associated with depression will be one challenge of the future. In contrast, inflammatory biomarkers that reflect activation of relatively unique and specific pathophysiologic pathways might be helpful in the individual therapy because here we have shown that interferons are able to decrease the reactivity of the reward system which is probably based on inflammatory processes.

Chapter VI - Summary

The understanding of the individual variability of depressive disorders is in urgent need of improvement which could be accelerated by identification of biomarkers for the diagnosis and treatment individualization of depressions. Here, we focused on the identification of potential biomarkers by application of cell based and neuroimaging based approaches to further advance the field of personalized medicine of depressive disorders.

The therapy effectiveness of antidepressant treatments requires improvement due to low response rates, a delay in clinical improvement and the lack of predictive biomarkers. Since depressions seem to be associated with decreased hippocampal volumes and antidepressant treatments are able to stimulate neurogenesis, individual susceptibility to antidepressant induced proliferation may act as a surrogate marker for the prediction of expected individual responses to antidepressant drugs. Here, we measured proliferative effects by SSRI antidepressant drugs in human LCLs derived from depressed patients participating in large depression trials (MARS and STAR*D) with monitored response progresses. LCLs are emerging models in neuropsychiatric biomarker research as they are widely available from different populations, represent individual donor's properties and show similar gene expression profiles with neuronal cells. Increased proliferation rates were detectable after three weeks of *in-vitro* treatment at the earliest with therapeutical concentrations of fluoxetine or citalopram which is in accordance with the observed delay in clinical improvement from several weeks up to a few months. A high variability in individual peripheral proliferation was reported in cohorts from both studies, but significant overall proliferative effects by antidepressants were restricted to the STAR*D cohort. Responder-derived LCLs showed significantly increased proliferation rates relative to non-responder derived cell lines and QIDS reduction was highly correlated with relative individual proliferation rates supporting the neurotrophic hypothesis of individual antidepressant efficacy. Because the underlying molecular backgrounds of individual antidepressant response remain poorly understood, we conducted transcriptome analyses in order to identify potential gene expression biomarkers associated with fluoxetine-induced peripheral or CNS proliferation. Comparative data analysis between non-responder and responder derived LCLs revealed 15 candidate biomarker genes being involved in either EGF signaling or WNT signaling or metabolism and transmembrane transport. Significant correlations between clinical parameters of LCL donors and gene expression levels have been

detected for *ABCB1*, *FZD7*, *SULT4A1* and *WNT2B*. The ABC transporter *ABCB1* - better known as Pgp or MRP1 - holds a key role in neuroprotection by exporting neurotoxic agents back into the circulatory system, whereas the brain specific phase II metabolizing enzyme *SULT4A1* is probably involved in the metabolism of neuroactive substances and antidepressant drugs. Both *FZD7* and *WNT2B* are important parts of the canonical WNT pathway that is crucial for the regulation of stem cell differentiation, neurogenesis and synaptic plasticity. With this we identified potential baseline gene expression predictors and temporal mediators that might support the guidance of individual therapy regimes in depressed patients and help to advance the personalized treatment approach in depressions in the future.

Another approach that might support the advancement of this field is the usage of neuroimaging techniques such as fMRI which has the potential to support the differential diagnosis of depression or to predict non-response or response to antidepressants. Here, we performed a clinical study to explore the individual variability of drug-induced depressions. Participants of this study were screened for depressive symptoms by psychometric testing and for changes in activation patterns of depression-related brain regions using fMRI techniques in order to find evidence for the depression inducing side-effects of interferon beta.

Psychometric testing included anxiety and depression questionnaires and showed individual responses to the interferon administration. Highly significant changes were reported only for the HDRS and the particular single item analysis led us to the conclusion that interferon treatment initiates inflammatory processes resulting in sickness-behavior but not in depression in the strict sense. Indeed, pathologic immune system activations and depressive-like behavior were frequently shown to be tightly connected and it is proposed that inflammatory processes might have a greater influence on the pathogenesis of depressions than the traditional psychosocial factors. Sickness-behavior and depressions share common pathophysiologic mechanism and are responsive to antidepressive therapies. During the fMRI sessions, conducted before and after interferon beta administration, the participants were instructed to complete two tasks that target specific depression-related brain functions (emotion processing and reward system). Although the role of emotion recognition in depression is usually of high relevance, we did not find any significant changes in amygdala activation after the short-term treatment with interferon using a passive exposure paradigm to emotional faces. In contrast, we measured a significantly decreased activity of the ventral striatum following the treatment with interferon beta in a money-rewarding paradigm. After exposure to interferon beta in healthy volunteers, we detected changes in the reward system functionality consistent with the existence of an anhedonia-like syndrome, while reactivity to salient negative stimuli was absent. This pattern was in accordance with the lack of

change in anxiety scores in behavioral testing (usually present in depression), outlining a specific syndrome accompanying the depression-inducing action or sickness behavior of interferon. After long-term therapy, this sickness behavior might turn into serious depression through cytokine actions in the brain because chronic inflammation seems to be a strong risk factor for the occurrence of depressive episodes. Based on our data one might speculate that interferon beta mainly affects dopaminergic circuits of reward and not serotonergic circuits of emotion recognition. We therefore propose that the depression-inducing effects of interferon beta after long-term therapy are at least partly based on an impaired reward system functionality.

Abbreviations

ABC	ATP binding cassette
ABCB1	ABC transporter subfamily B member 1
ABCG4	ABC transporter subfamily G member 4
ACE	angiotensin-converting enzyme
ADP	adenosine diphosphate
ATP	adenosine triphosphate
BBB	blood-brain barrier
BCL-1	B-cell lymphoma 1
BDI	Beck Depression Inventory
BDNF	brain-derived neurotrophic factor
BfArM	Bundesinstitut für Arzneimittel und Medizinprodukte
BOLD	blood-oxygen-level dependent
bp	base pair
BSA	bovine serum albumin
BTC	betacellulin
CACNA2D3	calcium channel, voltage-dependent, alpha 2/delta subunit 3
cAMP	cyclic adenosine monophosphate
CBF	cerebral blood flow
CD	cluster of differentiation
cDNA	complementary DNA
CHL1	close homolog to L1CAM
CRH	corticotropin-releasing hormone
CNS	central nervous system
CO ₂	carbon dioxide
CONSORT	Consolidated Standards of Reporting Trials
CP	crossing point
CREB	cAMP response element binding protein
cRNA	complementary RNA
CT	threshold point

Abbreviations

CY3	cyanin-3-cytidine triphosphate
CYP	cytochrome P450
CYP3A43	cytochrome P450 3A43
DCX	neuronal migration protein doublecortin
ddH ₂ O	double-distilled water
DMSO	dimethyl sulfoxide
DNA	deoxyribonucleic acid
dNTP	deoxyribonucleoside triphosphate
DSM	Diagnostic and Statistical Manual of Mental Disorders
EBV	Epstein-Barr-Virus
EDTA	ethylenediaminetetraacetic acid
EdU	5-ethynyl-2'-deoxyuridine
<i>e.g.</i>	<i>exempli gratia</i> ("for example")
EGF	epidermal growth factor
EGFR	epidermal growth factor receptor
ELISA	enzyme linked immunosorbent assay
ERBB3	epidermal growth factor receptor 3
ERBB4	epidermal growth factor receptor 4
<i>et al.</i>	<i>et alii</i> ("and others")
<i>etc.</i>	<i>et cetera</i> ("and so forth")
EudraCT	European Union Drug Regulating Authorities Clinical Trials
FACS	fluorescence-activated cell sorting
FC	fold change
FCS	fetal calf serum
FDR	false discovery rate
FKBP5	Tacrolimus (FK506) binding protein
fMRI	functional MRI
FoV	field of view
fwd	forward
FZD7	frizzled homolog 7
g	gravitational force
GAD2	glutamate decarboxylase 2
GAPDH	glyceraldehyde 3-phosphate dehydrogenase
GenMAPP	Gene Map Annotator and Pathway Profiler
GEO	gene expression omnibus

GO	gene ontology
GRIK4	glutamate receptor, ionotropic, kainate 4
HBEGF	heparin-binding EGF-like growth factor
HPA	hypothalamic-pituitary-adrenal
HDRS	Hamilton Depression Rating Scale
IDO	indoleamine-2,3-dioxygenase
<i>i.e.</i>	<i>id est</i> (“that is to say”)
ITGB3	integrin beta-3
KI67	marker of proliferation KI-67
L1CAM	neural cell adhesion molecule L1
LCLs	lymphoblastoid cell lines
MAO	monoamine oxidase
MAOI	monoamine oxidase inhibitors
MAPK	mitogen-activated protein kinase
MARS	Munich Antidepressant Response Signature
MINI	mini-international neuropsychiatric interview
miRNA	micro RNA
MRI	magnetic resonance imaging
mRNA	messenger RNA
MS	multiple sclerosis
n	number/quantity
NaCl	sodium chloride
NaSSA	noradrenergic and specific serotonergic antidepressants
NeuroD	neurogenic helix-loop-helix protein
NR	non-responder
NRI	norepinephrine reuptake inhibitors
nt	nucleotide
NTP	nucleoside triphosphate
NTRK2	neurotrophic tyrosine kinase receptor type 2
P2RX7	purinergic receptor P2X
PAT	parallel acquisition technique
PBMC	peripheral blood mononuclear cell
PBS	phosphate buffered saline
PCR	polymerase chain reaction
phMRI	pharmacological MRI

Abbreviations

PI3K	phosphatidylinositide 3-kinases
PIK3R5	phosphoinositide-3-kinase, regulatory subunit 5
QIDS	Quick Inventory of Depressive Symptomatology
r	Spearman's correlation coefficient
R	responder
RalA	Ras-related protein Ral-A
rev	reverse
RIN	RNA integrity number
RNA	ribonucleic acid
RNase	ribonuclease
rpm	revolutions per minute
RPMI	Roswell Park Memorial Institute
rs	reference SNP number
RT-PCR	real-time PCR
SERT	serotonin transporter
sMRI	structural MRI
SNRI	serotonin-norepinephrine reuptake inhibitors
SNP	single nucleotide polymorphism
SSRI	selective serotonin reuptake inhibitor
STAR*D	Sequenced Treatment Alternatives to Relieve Depression
STRING	Search Tool for the Retrieval of Interacting Genes/Proteins
SULT4A1	sulfotransferase family 4A, member 1
TAE	tris base/acetic acid/EDTA
TCA	tricyclic antidepressants
TCA	tricarboxylic acid
TCF7	transcription factor 7
TCF7L2	transcription factor 7-like 2
TeCA	tetracyclic antidepressant
Tm	melting temperature
TNF	tumor necrosis factor
TPH2	tryptophan dehydroxylase 2
TRIS	tris(hydroxymethyl)aminomethane
VEGF	vascular endothelial growth factor
VNTR	variable number tandem repeat
vs.	versus

WNT2B	wingless-type MMTV integration site family, member 2B
w/v	weight per volume
Δ	difference
ρ	Pearson's correlation coefficient

List of Figures

Figure 1: Cell identity before (day 0) and after (day 50) EBV transfection measured by cell specific antibody based flow cytometry.	15
Figure 2: Basic principle of the EdU proliferation assay.	17
Figure 3: Validation of custom-made primers was performed via melting curve analyse (A) and agarose gel electrophoresis (B).	20
Figure 4: Gel-like images (A) and electropherogram (B) of a successful Bioanalyzer run.	22
Figure 5: Overview of the study procedure.	25
Figure 6: Principle of the “reward” paradigm.	28
Figure 7: Principle of the faces paradigm.	28
Figure 8: Orientation of the measurement window.	30
Figure 9: Overview of the three phased project (screening, exploration and validation).	33
Figure 10: Result of the screening experiments using n=10 LCLs derived from the MARS study (values are indicated as means of these n=10 samples)	34
Figure 11: Heat-Map of EdU screening experiments.	35
Figure 12: EdU phenotyping of MARS cell lines.	36
Figure 13: Comparison of relative proliferation (after <i>in-vitro</i> treatment with fluoxetine relative to untreated samples from the same donor) between non-responder (n=25) and responder (n=25) derived LCLs (A) and between absolute, basal proliferation (untreated samples from the same donor) of non-responder (n=25) and responder (n=25) derived cell lines (B).	37
Figure 14: Correlation plot between response factor and relative proliferation	38
Figure 15: Analyses of the covariates gender (A) and age (B) and their impact on relative proliferation rates (after 21 days of continuous treatment of n=50 LCLs with therapeutical concentrations of fluoxetine compared to untreated controls from the same cell lines)	39
Figure 16: Box plot of relative proliferation and donor’s underlying diseases indicated as International Statistical Classification (ICD) codes.	39
Figure 17: Quantities of differentially regulated genes (FC > 2, FC > 5 and FC > 10) in ten LCLs after three-week incubation with fluoxetine compared to untreated controls of the same samples and measuring gene expression profiles by Agilent microarray system with approximately 27,000 biological features.	40

Figure 18: Dendrogram of the hierarchical clustering analysis of the ten LCLs after three weeks of incubation with fluoxetine compared to untreated samples of the same cell lines.....	42
Figure 19: Pathway analysis combined with Venn analysis revealed 14 pathways (yellow frame) differentially regulated between responder and non-responder indicator cell lines (24DC and 275U vs. 278H)..	44
Figure 20: STRING based protein interaction network of the 15 top-hit genes from microarray experiments after three weeks of incubation with therapeutical concentrations of fluoxetine.	47
Figure 21: Basal gene expression of the candidate genes in an edge-group analysis from EdU phenotyping experiments (proliferators vs. non-proliferators).....	48
Figure 22: Basal gene expression of the candidate genes in cell lines derived from donors with non-response or response after five (A) and eight weeks (B) and cell lines derived from donors with remission or non-remission after five (C) and eight weeks (D).	49
Figure 23: EdU phenotyping of STAR*D cell lines.....	53
Figure 24: Overall proliferative effects of fluoxetine and citalopram after three weeks of <i>in-vitro</i> treatment in therapeutic concentrations (n=50).	54
Figure 25: Correlation plot of fluoxetine and citalopram induced relative proliferation after <i>in-vitro</i> treatment with the SSRI antidepressants in therapeutic concentrations for three weeks.....	55
Figure 26: Mean relative proliferation rates of non-responder and responder derived cell lines treated with fluoxetine or citalopram for 21 days.....	55
Figure 27: Correlation plots of QIDS reduction and fluoxetine (A) or citalopram (B) induced relative proliferation.	56
Figure 28: Covariates analysis.....	57
Figure 29: Results of gene expression experiments of the candidate genes. Basal gene expression indicated as difference of maximal cycle number of RT-PCR experiments and Δ CP values of untreated samples (A). Gene expression fold changes after 21-day <i>in-vitro</i> treatment of LCLs with fluoxetine (B) or citalopram (C).....	59
Figure 30: Overview of the course of the study by CONSORT flow diagram.....	60
Figure 31: Box plots of the current (left) and general (right) STAI anxiety scores before (baseline) and after (steady-state) the nine-day standard therapy with interferon beta.	61
Figure 32: Progress of HDRS scores before (baseline) and after (steady-state) treatment with interferon beta	62
Figure 33: Single-item-analysis of results obtained from HDRS scoring before (baseline) and after (steady-state) a nine-day standard therapy with interferon beta.	64
Figure 34: Results of the foraging paradigm indicate a lowered activity of the ventral striatum (blue circle) after interferon beta administration..	66
Figure 35: Results of the faces paradigm indicate no significant changes of the activity of the amygdala and the central nucleus region (blue arrows) after interferon beta administration..	68

List of Tables

Table 1: Overview on antidepressant drug classes.....	5
Table 2: Characteristics of the MARS and STAR*D LCL study cohort.	13
Table 3: Detector parameters of the FACS Calibur flow cytometer of the EdU proliferation assays.	18
Table 4: Design parameters and specifications for custom made primers.	20
Table 5: Primers used for RT-PCR experiments.	21
Table 6: RT-PCR cycle conditions.	21
Table 7: Overview on fMRI measurement parameters	29
Table 8: Overview of different filtering methods for the identification of potential gene expression biomarkers out of the whole-genome gene expression data and their particular impact of remaining number of genes (n).	41
Table 9: Overview of the 30 most significant GO terms from the genes identified by Venn analysis.....	45
Table 10: Comparison of mean gene expression levels between responder and non-responder cell lines (n=10) and their annotated gene functions.	46
Table 11: Fold change values of the candidate genes identified through microarray experiments after three weeks of <i>in-vitro</i> treatment with therapeutic concentrations of fluoxetine obtained in ten different LCLs in an edge-group approach after EdU phenotyping.	50
Table 12: Statistical overview of LCL donor's clinical outcome and LCL gene expression of the candidate genes in all tested MARS LCLs (n=50).....	51
Table 13: Correlation matrix of fold changes by fluoxetine and citalopram	58
Table 14: Statistical report of the foraging paradigm measurements before/after interferon beta administration including results on set, cluster and peak level with an uncorrected p value cut-off of 0.001.	65
Table 15: Statistical report of the faces paradigm measurements before and after interferon beta administration including results on set, cluster and peak level with an uncorrected p value cut-off of 0.001.	67

References

1. Meyer UA. Pharmacogenetics—five decades of therapeutic lessons from genetic diversity. *Nature Reviews Genetics* 2004; **5**(9): 669-676.
2. Collins FS, McKusick VA. Implications of the Human Genome Project for medical science. *Jama* 2001; **285**(5): 540-544.
3. Roche Molecular Systems I. cobas® KRAS Mutation Test. 2011; **1.0**.
4. Willard HF. Organization, variation and expression of the human genome as a foundation of genomic and personalized medicine. *Elsevier Inc* 2009; **154**(6): 277-287.
5. Radden J. Is This Dame Melancholy?: Equating today's depression and past melancholia. *Philosophy, Psychiatry, & Psychology* 2003; **10**(1): 37-52.
6. *Diagnostic and statistical manual of mental disorders (DSM-5®)*. American Psychiatric Association, 2013.
7. Palazidou E. The neurobiology of depression. *British medical bulletin* 2012; **101**(1): 127-145.
8. *Mental Health Atlas* World Health Organization, 2005.
9. Bloom DE, Cafiero E, Jané-Llopis E, Abrahams-Gessel S, Bloom LR, Fathima S, *et al*. The global economic burden of noncommunicable diseases. *Program on the Global Demography of Aging* 2012.
10. Sullivan PF, Neale MC, Kendler KS. Genetic epidemiology of major depression: review and meta-analysis. *American Journal of Psychiatry* 2000.
11. Fernandez-Pujals AM, Adams MJ, Thomson P, McKechnie AG, Blackwood DH, Smith BH, *et al*. Epidemiology and Heritability of Major Depressive Disorder, Stratified by Age of Onset, Sex, and Illness Course in Generation Scotland: Scottish Family Health Study (GS: SFHS). *PloS one* 2015; **10**(11): e0142197.

References

12. Lohoff FW. Overview of the genetics of major depressive disorder. *Current psychiatry reports* 2010; **12**(6): 539-546.
13. Byrne E, Carrillo-Roa T, Henders A, Bowdler L, McRae A, Heath A, *et al.* Monozygotic twins affected with major depressive disorder have greater variance in methylation than their unaffected co-twin. *Translational psychiatry* 2013; **3**(6): e269.
14. Flint J, Kendler KS. The genetics of major depression. *Neuron* 2014; **81**(3): 484-503.
15. Ripke S, Wray NR, Lewis CM, Hamilton SP, Weissman MM, Breen G, *et al.* A mega-analysis of genome-wide association studies for major depressive disorder. *Molecular psychiatry* 2013; **18**(4): 497-511.
16. aan het Rot M, Mathew SJ, Charney DS. Neurobiological mechanisms in major depressive disorder. *Canadian Medical Association Journal* 2009; **180**(3): 305-313.
17. Konarski JZ, McIntyre RS, Kennedy SH, Rafi-Tari S, Soczynska JK, Ketter TA. Volumetric neuroimaging investigations in mood disorders: bipolar disorder versus major depressive disorder. *Bipolar disorders* 2008; **10**(1): 1-37.
18. Kessler RC, Berglund P, Demler O, Jin R, Merikangas KR, Walters EE. Lifetime prevalence and age-of-onset distributions of DSM-IV disorders in the National Comorbidity Survey Replication. *Archives of general psychiatry* 2005; **62**(6): 593-602.
19. Kuehner C. Gender differences in unipolar depression: an update of epidemiological findings and possible explanations. *Acta Psychiatrica Scandinavica* 2003; **108**(3): 163-174.
20. Cutter W, Norbury R, Murphy D. Oestrogen, brain function, and neuropsychiatric disorders. *Journal of Neurology, Neurosurgery & Psychiatry* 2003; **74**(7): 837-840.
21. Lasiuk G, Hegadoren K. The effects of estradiol on central serotonergic systems and its relationship to mood in women. *Biological research for nursing* 2007; **9**(2): 147-160.
22. Czirr E, Wyss-Coray T. The immunology of neurodegeneration. *The Journal of clinical investigation* 2012; **122**(4): 1156-1163.
23. Dowlati Y, Herrmann N, Swardfager W, Liu H, Sham L, Reim EK, *et al.* A meta-analysis of cytokines in major depression. *Biological psychiatry* 2010; **67**(5): 446-457.
24. Berk M, Williams LJ, Jacka FN, O'Neil A, Pasco JA, Moylan S, *et al.* So depression is an inflammatory disease, but where does the inflammation come from? *BMC medicine* 2013; **11**(1): 1.

25. Dantzer R, O'Connor JC, Freund GG, Johnson RW, Kelley KW. From inflammation to sickness and depression: when the immune system subjugates the brain. *Nat Rev Neurosci* 2008; **9**(1): 46-56.
26. Rudolf S, Bermejo I, Schweiger U, Hohagen F, Härter M. Zertifizierte medizinische Fortbildung: Diagnostik depressiver Störungen. *Dtsch Arztebl International* 2006; **103**(25): 1754.
27. Hamilton M. A rating scale for depression. *Journal of Neurology, Neurosurgery, and Psychiatry* 1960; **23**(1): 56-62.
28. Beck AT, Steer RA, Carbin MG. Psychometric properties of the Beck Depression Inventory: Twenty-five years of evaluation. *Clinical psychology review* 1988; **8**(1): 77-100.
29. Papakostas G, Shelton R, Kinrys G, Henry M, Bakow B, Lipkin S, *et al.* Assessment of a multi-assay, serum-based biological diagnostic test for major depressive disorder: a pilot and replication study. *Molecular psychiatry* 2013; **18**(3): 332-339.
30. Phillips ML, Swartz HA. A critical appraisal of neuroimaging studies of bipolar disorder: toward a new conceptualization of underlying neural circuitry and a road map for future research. *American Journal of Psychiatry* 2014.
31. Schröder J, Pantel J, Schönknecht P, Essig M. Die Magnetresonanztomographie in der klinischen Demenzdiagnostik. *Der Radiologe* 2003; **43**(7): 513-520.
32. Arnone D, Cavanagh J, Gerber D, Lawrie S, Ebmeier K, McIntosh A. Magnetic resonance imaging studies in bipolar disorder and schizophrenia: meta-analysis. *The British Journal of Psychiatry* 2009; **195**(3): 194-201.
33. Arnone D, McIntosh A, Chandra P, Ebmeier K. Meta-analysis of magnetic resonance imaging studies of the corpus callosum in bipolar disorder. *Acta Psychiatrica Scandinavica* 2008; **118**(5): 357-362.
34. Arnone D, McIntosh A, Tan G, Ebmeier K. Meta-analysis of magnetic resonance imaging studies of the corpus callosum in schizophrenia. *Schizophrenia research* 2008; **101**(1): 124-132.
35. Peterson BS, Warner V, Bansal R, Zhu H, Hao X, Liu J, *et al.* Cortical thinning in persons at increased familial risk for major depression. *Proceedings of the National Academy of Sciences* 2009; **106**(15): 6273-6278.
36. Duhamel B, Ferré J-C, Jannin P, Gauvrit J-Y, Vérin M, Millet B, *et al.* Chronic and treatment-resistant depression: a study using arterial spin labeling perfusion MRI at 3Tesla. *Psychiatry Research: Neuroimaging* 2010; **182**(2): 111-116.

References

37. Sämann PG, Höhn D, Czisch M. Magnetresonanztomographie (MRT) in der Depressionsforschung. *GIT-Labor – Portal für Anwender in Wissenschaft und Industrie* 2012.
38. Lopez-Munoz F, Alamo C. Monoaminergic Neurotransmission: The History of the Discovery of Antidepressants from 1950s Until Today. *Current pharmaceutical design* 2009; **15**(14): 1563-1586.
39. Peretti S, Judge R, Hindmarch I. Safety and tolerability considerations: tricyclic antidepressants vs. selective serotonin reuptake inhibitors. *Acta Psychiatrica Scandinavica* 2000; **101**(S403): 17-25.
40. Drevets WC, Bogers W, Raichle ME. Functional anatomical correlates of antidepressant drug treatment assessed using PET measures of regional glucose metabolism. *European Neuropsychopharmacology* 2002; **12**(6): 527-544.
41. Chen C-H, Suckling J, Ooi C, Fu CH, Williams SC, Walsh ND, *et al.* Functional coupling of the amygdala in depressed patients treated with antidepressant medication. *Neuropsychopharmacology* 2008; **33**(8): 1909-1918.
42. Malberg JE, Eisch AJ, Nestler EJ, Duman RS. Chronic antidepressant treatment increases neurogenesis in adult rat hippocampus. *The Journal of Neuroscience* 2000; **20**(24): 9104-9110.
43. Chen G, Rajkowska G, Du F, Seraji-Bozorgzad N, Manji HK. Enhancement of hippocampal neurogenesis by lithium. *Journal of neurochemistry* 2000; **75**(4): 1729-1734.
44. Hao Y, Creson T, Zhang L, Li P, Du F, Yuan P, *et al.* Mood stabilizer valproate promotes ERK pathway-dependent cortical neuronal growth and neurogenesis. *The Journal of neuroscience* 2004; **24**(29): 6590-6599.
45. Dierckx B, Heijnen WT, van den Broek WW, Birkenhäger TK. Efficacy of electroconvulsive therapy in bipolar versus unipolar major depression: a meta-analysis. *Bipolar disorders* 2012; **14**(2): 146-150.
46. Jelovac A, Kolshus E, McLoughlin DM. Relapse following successful electroconvulsive therapy for major depression: a meta-analysis. *Neuropsychopharmacology* 2013; **38**(12): 2467-2474.
47. Revesz D, Tjernstrom M, Ben-Menachem E, Thorlin T. Effects of vagus nerve stimulation on rat hippocampal progenitor proliferation. *Experimental neurology* 2008; **214**(2): 259-265.
48. Boldrini M, Hen R, Underwood MD, Rosoklija GB, Dwork AJ, Mann JJ, *et al.* Hippocampal Angiogenesis and Progenitor Cell Proliferation Are Increased with Antidepressant Use in Major Depression. *Biological Psychiatry* 2012; **72**(7): 562-571.

49. Boldrini M, Underwood MD, Hen R, Rosoklija GB, Dwork AJ, Mann JJ, *et al.* Antidepressants increase neural progenitor cells in the human hippocampus. *Neuropsychopharmacology* 2009; **34**(11): 2376-2389.
50. Sämann PG, Höhn D, Chechko N, Kloiber S, Lucae S, Ising M, *et al.* Prediction of antidepressant treatment response from gray matter volume across diagnostic categories. *European Neuropsychopharmacology* 2013; **23**(11): 1503-1515.
51. Russo-Neustadt AA, Alejandre H, Garcia C, Ivy AS, Chen MJ. Hippocampal brain-derived neurotrophic factor expression following treatment with reboxetine, citalopram, and physical exercise. *Neuropsychopharmacology* 2004; **29**(12).
52. Rogoz Z, Skuza G, Legutko B. Repeated co-treatment with imipramine and amantadine induces hippocampal brain-derived neurotrophic factor gene expression in rats. *Journal of Physiology and Pharmacology* 2007; **58**(2): 219.
53. S3-Leitlinie/Nationale Versorgungsleitlinie Unipolare Depression. *DGPPN, BÄK, KBV* 2009; **1**.
54. Crisafulli C, Fabbri C, Porcelli S, Drago A, Spina E, De Ronchi D, *et al.* Pharmacogenetics of antidepressants. *Frontiers in Pharmacology* 2011; **2**.
55. Boksa P. A way forward for research on biomarkers for psychiatric disorders. *J Psychiatry Neurosci* 2013; **38**(2): 75-77.
56. Martins-de-Souza D. Biomarkers for psychiatric disorders: where are we standing. *Dis Markers* 2013; **35**(1): 1-2.
57. Quitkin FM, Petkova E, McGrath PJ, Taylor B, Beasley C, Stewart J, *et al.* When should a trial of fluoxetine for major depression be declared failed? *American Journal of Psychiatry* 2003; **160**(4): 734-740.
58. Narasimhan S, Lohoff FW. Pharmacogenetics of antidepressant drugs: current clinical practice and future directions. *Pharmacogenomics* 2012; **13**(4): 441-464.
59. Thomas KL, Ellingrod VL. Pharmacogenetics of selective serotonin reuptake inhibitors and associated adverse drug reactions. *Pharmacotherapy: The Journal of Human Pharmacology and Drug Therapy* 2009; **29**(7): 822-831.
60. Leonard BE. Depression and physical illness. *Human Psychopharmacology: Clinical and Experimental* 2007; **22**(4): 253-254.
61. Couzin-Frankel J. Inflammation bares a dark side. *Science* 2010; **330**(6011): 1621-1621.

References

62. Frasure-Smith N, Lespérance F. Depression and coronary artery disease. *Herz* 2006; **31**: 64-68.
63. Miller AH, Maletic V, Raison CL. Inflammation and its discontents: the role of cytokines in the pathophysiology of major depression. *Biological psychiatry* 2009; **65**(9): 732-741.
64. Howren MB, Lamkin DM, Suls J. Associations of depression with C-reactive protein, IL-1, and IL-6: a meta-analysis. *Psychosomatic medicine* 2009; **71**(2): 171-186.
65. Hiles SA, Baker AL, de Malmanche T, Attia J. A meta-analysis of differences in IL-6 and IL-10 between people with and without depression: exploring the causes of heterogeneity. *Brain, behavior, and immunity* 2012; **26**(7): 1180-1188.
66. Kalkut EJ, Grote CL. Neuropsychological Aspects of Depression: Their Relevance in Depression in Neurologic Disorders. *Depression in Neurologic Disorders: Diagnosis and Management* 2012; **6**(4): 64-76.
67. Siegert R, Abernethy D. Depression in multiple sclerosis: a review. *Journal of Neurology, Neurosurgery & Psychiatry* 2005; **76**(4): 469-475.
68. Kessler RC, Gruber M, Hettema JM, Hwang I, Sampson N, Yonkers KA. Co-morbid major depression and generalized anxiety disorders in the National Comorbidity Survey follow-up. *Psychological medicine* 2008; **38**(03): 365-374.
69. Patten S, Beck C, Williams J, Barbu C, Metz L. Major depression in multiple sclerosis A population-based perspective. *Neurology* 2003; **61**(11): 1524-1527.
70. Egede LE. Major depression in individuals with chronic medical disorders: prevalence, correlates and association with health resource utilization, lost productivity and functional disability. *General hospital psychiatry* 2007; **29**(5): 409-416.
71. Schiffer RB, Babigian HM. Behavioral disorders in multiple sclerosis, temporal lobe epilepsy, and amyotrophic lateral sclerosis: an epidemiologic study. *Archives of Neurology* 1984; **41**(10): 1067-1069.
72. Di Legge S, Piattella M, Pozzilli C, Pantano P, Caramia F, Pestalozza I, *et al.* Longitudinal evaluation of depression and anxiety in patients with clinically isolated syndrome at high risk of developing early multiple sclerosis. *Multiple sclerosis* 2003; **9**(3): 302-306.
73. Glanz BI, Holland CM, Gauthier SA, Amunwa EL, Liptak Z, Houtchens MK, *et al.* Cognitive dysfunction in patients with clinically isolated syndromes or newly diagnosed multiple sclerosis. *Multiple Sclerosis* 2007; **13**(8): 1004-1010.

74. Chwastiak L, Ehde DM, Gibbons LE, Sullivan M, Bowen JD, Kraft GH. Depressive symptoms and severity of illness in multiple sclerosis: epidemiologic study of a large community sample. *American Journal of Psychiatry* 2014; **159**(11): 1862-1868.
75. Mohr D, Hart S, Julian L, Tasch E. Screening for depression among patients with multiple sclerosis: two questions may be enough. *Multiple Sclerosis* 2007; **13**(2): 215-219.
76. Charvet LE, Kluzer B, Krupp LB. Invisible symptoms of MS: Fatigue, Depression, and Cognition. *Multiple Sclerosis and CNS Inflammatory Disorders* 2014; **171**(3): 114-121.
77. Mikova O, Yakimova R, Bosmans E, Kenis G, Maes M. Increased serum tumor necrosis factor alpha concentrations in major depression and multiple sclerosis. *European Neuropsychopharmacology* 2001; **11**(3): 203-208.
78. Kiy G, Lehmann P, Hahn HK, Eling P, Kastrup A, Hildebrandt H. Decreased hippocampal volume, indirectly measured, is associated with depressive symptoms and consolidation deficits in multiple sclerosis. *Multiple Sclerosis Journal* 2011; **17**(9): 1088-1097.
79. Feinstein A, Roy P, Lobaugh N, Feinstein K, O'Connor P, Black S. Structural brain abnormalities in multiple sclerosis patients with major depression. *Neurology* 2004; **62**(4): 586-590.
80. Patten S. Diagnosing Depression in MS in the Face of Overlapping Symptoms. *The international MS journal* 2010; **17**(1): 3-5.
81. Sollom A, Kneebone I. Treatment of depression in people who have multiple sclerosis. *Multiple Sclerosis* 2007; **13**(5): 632-635.
82. Rintell DJ. Depression and other psychosocial issues in multiple sclerosis. *Multiple sclerosis: Diagnosis and therapy* 2012; **3**(2): 263-282.
83. Feinstein A. An examination of suicidal intent in patients with multiple sclerosis. *Neurology* 2002; **59**(5): 674-678.
84. Sadovnick A, Eisen K, Ebers GC, Paty DW. Cause of death in patients attending multiple sclerosis clinics. *Neurology* 1991; **41**(8): 1193-1193.
85. Berer K, Krishnamoorthy G. Microbial view of central nervous system autoimmunity. *FEBS letters* 2014; **588**(22): 4207-4213.
86. Serafin DJ, Weisbrot DM, Ettinger AB. Depression and multiple sclerosis. *Depression in Neurologic Disorders: Diagnosis and Management* 2012; **16**(1): 157-176.

References

87. Siracusano A, Niolu C, Sacchetti L, Ribolsi M. Depression and anxiety. *Neuropsychiatric Dysfunction in Multiple Sclerosis* 2012; **16**(1): 85-97.
88. Tedeschi G, Gallo A. Multiple sclerosis patients and immunomodulation therapies: the potential role of new MRI techniques to assess responders versus non-responders. *Neurological Sciences* 2005; **26**(4): 209-212.
89. Murdoch D, Lyseng-Williamson KA. Spotlight on Subcutaneous Recombinant Interferon- β -1a (Rebif®) in Relapsing-Remitting Multiple Sclerosis. *BioDrugs* 2005; **19**(5): 323-325.
90. Murdoch D, Lyseng-Williamson KA. Subcutaneous Recombinant Interferon- β -1a (Rebif®). *Drugs* 2005; **65**(9): 1295-1312.
91. McColl BW, Rothwell NJ, Allan SM. Systemic inflammatory stimulus potentiates the acute phase and CXC chemokine responses to experimental stroke and exacerbates brain damage via interleukin-1-and neutrophil-dependent mechanisms. *The Journal of neuroscience* 2007; **27**(16): 4403-4412.
92. Raison CL, Capuron L, Miller AH. Cytokines sing the blues: inflammation and the pathogenesis of depression. *Trends in Immunology* 2006; **27**(1): 24-31.
93. Malaguarnera M, Laurino A, Di Fazio I, Pistone G, Castorina M, Guccione N, et al. Neuropsychiatric effects and type of IFN- α in chronic hepatitis C. *Journal of Interferon & Cytokine Research* 2001; **21**(5): 273-278.
94. Castéra L, Zigante F, Bastie A, Buffet C, Dhumeaux D, Hardy P. Incidence of interferon alfa-induced depression in patients with chronic hepatitis C. *Hepatology* 2002; **35**(4): 978-979.
95. Lotrich FE, Rabinovitz M, Gironda P, Pollock BG. Depression following pegylated interferon-alpha: characteristics and vulnerability. *Journal of psychosomatic research* 2007; **63**(2): 131-135.
96. Pozzilli C, Schweikert B, Ecarl U, Oentrich W, Bugge J-P. Quality of life and depression in multiple sclerosis patients: longitudinal results of the BetaPlus study. *Journal of neurology* 2012; **259**(11): 2319-2328.
97. Feinstein A, O'Connor P, Feinstein K. Multiple Sclerosis, interferon beta-1b and depression. *Journal of neurology* 2002; **249**(7): 815-820.
98. Arnett PA, Randolph JJ. Longitudinal course of depression symptoms in multiple sclerosis. *Journal of Neurology, Neurosurgery & Psychiatry* 2006; **77**(5): 606-610.

99. Jacobs LD, Beck RW, Simon JH, Kinkel RP, Brownschidle CM, Murray TJ, *et al.* Intramuscular interferon beta-1a therapy initiated during a first demyelinating event in multiple sclerosis. *New England Journal of Medicine* 2000; **343**(13): 898-904.
100. Musselman DL, Lawson DH, Gumnick JF, Manatunga AK, Penna S, Goodkin RS, *et al.* Paroxetine for the prevention of depression induced by high-dose interferon alfa. *New England Journal of Medicine* 2001; **344**(13): 961-966.
101. Lotrich FE, Ferrell RE, Rabinovitz M, Pollock BG. Risk for depression during interferon-alpha treatment is affected by the serotonin transporter polymorphism. *Biological psychiatry* 2009; **65**(4): 344-348.
102. Bull S, Huezio-Diaz P, Binder E, Cubells J, Ranjith G, Maddock C, *et al.* Functional polymorphisms in the interleukin-6 and serotonin transporter genes, and depression and fatigue induced by interferon- α and ribavirin treatment. *Molecular psychiatry* 2009; **14**(12): 1095-1104.
103. Thomas KH, Martin RM, Potokar J, Pirmohamed M, Gunnell D. Reporting of drug induced depression and fatal and non-fatal suicidal behaviour in the UK from 1998 to 2011. *BMC pharmacology and toxicology* 2014; **15**(1): 54.
104. Patten SB, Love E. Can drugs cause depression? a review of the evidence. *Journal of Psychiatry and Neuroscience* 1993; **18**(3): 92.
105. Tisdale JE, Miller DA. *Drug-induced diseases: prevention, detection, and management.* ASHP, 2010.
106. Capuron L, Ravaud A, Neveu P, Miller A, Maes M, Dantzer R. Association between decreased serum tryptophan concentrations and depressive symptoms in cancer patients undergoing cytokine therapy. *Molecular psychiatry* 2002; **7**(5): 468-473.
107. Wirleitner B, Neurauter G, Schrocksnadel K, Frick B, Fuchs D. Interferon- γ -induced conversion of tryptophan: immunologic and neuropsychiatric aspects. *Current medicinal chemistry* 2003; **10**(16): 1581-1591.
108. Capuron L, Raison CL, Musselman DL, Lawson DH, Nemeroff CB, Miller AH. Association of exaggerated HPA axis response to the initial injection of interferon-alpha with development of depression during interferon-alpha therapy. *American Journal of Psychiatry* 2003; **160**(7): 1342-1345.
109. Capuron L, Ravaud A. Prediction of the depressive effects of interferon alfa therapy by the patient's initial affective state. *New England Journal of Medicine* 1999; **340**(17): 1370-1370.
110. Azoulay L, Blais L, Koren G, LeLorier J, Berard A. Does Isotretinoin Increase the Risk of Depression? *J Clin Psychiatry* 2008; **69**(4): 526-532.

References

111. Wysowski DK, Pitts M, Beitz J. An analysis of reports of depression and suicide in patients treated with isotretinoin. *Journal of the American Academy of Dermatology* 2001; **45**(4): 515-519.
112. Lopez-Gomez M, Ramirez-Bermudez J, Campillo C, Sosa A, Espinola M, Ruiz I. Primidone is associated with interictal depression in patients with epilepsy. *Epilepsy & Behavior* 2005; **6**(3): 413-416.
113. Patten SB, Williams JV, Love EJ. Self-reported depressive symptoms following treatment with corticosteroids and sedative-hypnotics. *The International Journal of Psychiatry in Medicine* 1996; **26**(1): 15-24.
114. Oinonen KA, Mazmanian D. To what extent do oral contraceptives influence mood and affect? *Journal of affective disorders* 2002; **70**(3): 229-240.
115. Porcelli S, Drago A, Fabbri C, Gibiino S, Calati R, Serretti A. Pharmacogenetics of antidepressant response. *Journal of Psychiatry & Neuroscience* 2010; **36**(2): 87-113.
116. Labermaier C, Masana M, Müller MB. Biomarkers predicting antidepressant treatment response: how can we advance the field? *Disease markers* 2013; **35**(1): 23-31.
117. Morag A, Pasmanik-Chor M, Oron-Karni V, Rehavi M, Stingl JC, Gurwitz D. Genome-wide expression profiling of human lymphoblastoid cell lines identifies CHL1 as a putative SSRI antidepressant response biomarker. *Pharmacogenomics* 2011; **12**(2): 171-184.
118. Oved K, Morag A, Pasmanik-Chor M, Oron-Karni V, Shomron N, Rehavi M, *et al.* Genome-wide miRNA expression profiling of human lymphoblastoid cell lines identifies tentative SSRI antidepressant response biomarkers. *Pharmacogenomics* 2012; **13**(10): 1129-1139.
119. Probst-Schendzielorz K, Scholl C, Efimkina O, Ersfeld E, Viviani R, Serretti A, *et al.* CHL1, ITGB3 and SLC6A4 gene expression and antidepressant drug response: results from the Munich Antidepressant Response Signature (MARS) study. *Pharmacogenomics* 2015; **16**(7): 689-701.
120. Rollins B, Martin MV, Morgan L, Vawter MP. Analysis of whole genome biomarker expression in blood and brain. *American Journal of Medical Genetics Part B: Neuropsychiatric Genetics* 2010; **153**(4): 919-936.
121. Brammer M. The role of neuroimaging in diagnosis and personalized medicine-current position and likely future directions. *Dialogues in Clinical Neuroscience* 2009; **11**(4): 389-396.

122. Falcone M, Smith RM, Chenoweth MJ, Kumar Bhattacharjee A, Kelsoe JR, Tyndale RF, *et al.* Neuroimaging in Psychiatric Pharmacogenetics Research: The Promise and Pitfalls. *Neuropsychopharmacology* 2013; **38**(12): 2327-2337.
123. Michael AM, King MD, Ehrlich S, Pearlson G, White T, Holt DJ, *et al.* A data-driven investigation of gray matter–function correlations in schizophrenia during a working memory task. *Frontiers in human neuroscience* 2011; **5**(1): 71.
124. de Kwaasteniet B, Ruhe E, Caan M, Rive M, Olabarriaga S, Groefsema M, *et al.* Relation between structural and functional connectivity in major depressive disorder. *Biological psychiatry* 2013; **74**(1): 40-47.
125. Wang J, Aguirre GK, Kimberg DY, Roc AC, Li L, Detre JA. Arterial spin labeling perfusion fMRI with very low task frequency. *Magnetic Resonance in Medicine* 2003; **49**(5): 796-802.
126. Poldrack RA. Can cognitive processes be inferred from neuroimaging data? *Trends in Cognitive Sciences* 2006; **10**(2): 59-63.
127. Dunlop BW, Mayberg HS. Neuroimaging-based biomarkers for treatment selection in major depressive disorder. *Dialogues in clinical neuroscience* 2014; **16**(4): 479.
128. Santarelli L, Saxe M, Gross C, Surget A, Battaglia F, Dulawa S, *et al.* Requirement of Hippocampal Neurogenesis for the Behavioral Effects of Antidepressants. *Science* 2003; **301**(5634): 805-809.
129. Dunkin JJ, Leuchter AF, Cook IA, Kasl-Godley JE, Abrams M, Rosenberg-Thompson S. Executive dysfunction predicts nonresponse to fluoxetine in major depression. *Journal of affective disorders* 2000; **60**(1): 13-23.
130. Tanti A, Belzung C. Hippocampal neurogenesis: a biomarker for depression or antidepressant effects? Methodological considerations and perspectives for future research. *Cell Tissue Res* 2013; **354**(1): 203-219.
131. Klapper J. Interferon beta treatment of multiple sclerosis. *Neurology* 1994; **44**(1): 188-188-a.
132. Vattakatuchery JJ, Rickards H, Cavanna AE. Pathogenic Mechanisms of Depression in Multiple Sclerosis. *The Journal of Neuropsychiatry and Clinical Neurosciences* 2011; **23**(3): 261-276.
133. Viviani R. Emotion regulation, attention to emotion, and the ventral attentional network. *Frontiers in Human Neuroscience* 2013; **7**(1): 746.

References

134. Rohe T, Weber B, Fließbach K. Dissociation of BOLD responses to reward prediction errors and reward receipt by a model comparison. *European Journal of Neuroscience* 2012; **36**(3): 2376-2382.
135. Treadway MT, Zald DH. Reconsidering anhedonia in depression: lessons from translational neuroscience. *Neuroscience & Biobehavioral Reviews* 2011; **35**(3): 537-555.
136. Siegle GJ, Steinhauer SR, Thase ME, Stenger VA, Carter CS. Can't shake that feeling: event-related fMRI assessment of sustained amygdala activity in response to emotional information in depressed individuals. *Biological psychiatry* 2002; **51**(9): 693-707.
137. Hennings JM, Ohashi T, Binder EB, Horstmann S, Menke A, Kloiber S, *et al.* Clinical characteristics and treatment outcome in a representative sample of depressed inpatients – Findings from the Munich Antidepressant Response Signature (MARS) project. *Journal of Psychiatric Research* 2009; **43**(3): 215-229.
138. Ising M, Lucae S, Binder EB, *et al.* A genomewide association study points to multiple loci that predict antidepressant drug treatment outcome in depression. *Archives of General Psychiatry* 2009; **66**(9): 966-975.
139. Ising M, Horstmann S, Kloiber S, Lucae S, Binder EB, Kern N, *et al.* Combined dexamethasone/corticotropin releasing hormone test predicts treatment response in major depression—a potential biomarker? *Biological psychiatry* 2007; **62**(1): 47-54.
140. Zobel AW, Nickel T, Sonntag A, Uhr M, Holsboer F, Ising M. Cortisol response in the combined dexamethasone/CRH test as predictor of relapse in patients with remitted depression: a prospective study. *Journal of Psychiatric Research* 2001; **35**(2): 83-94.
141. Rush AJ, Fava M, Wisniewski SR, Lavori PW, Trivedi MH, Sackeim HA, *et al.* Sequenced treatment alternatives to relieve depression (STAR*D): rationale and design. *Controlled Clinical Trials* 2004; **25**(1): 119-142.
142. Rush AJ, Trivedi MH, Ibrahim HM, Carmody TJ, Arnow B, Klein DN, *et al.* The 16-Item quick inventory of depressive symptomatology (QIDS), clinician rating (QIDS-C), and self-report (QIDS-SR): a psychometric evaluation in patients with chronic major depression. *Biological Psychiatry* 2003; **54**(5): 573-583.
143. Anderson MA, Gusella JF. Use of cyclosporin A in establishing Epstein-Barr virus-transformed human lymphoblastoid cell lines. *In vitro* 1984; **20**(11): 856-858.
144. Tosato G, Cohen JI. Generation of Epstein-Barr Virus (EBV)–Immortalized B Cell Lines. *Current protocols in immunology* 2007; **7**(7): 22 21-22 24.

145. Lin T-M, Tsai J-L, Lin S-D, Lai C-S, Chang C-C. Accelerated growth and prolonged lifespan of adipose tissue-derived human mesenchymal stem cells in a medium using reduced calcium and antioxidants. *Stem cells and development* 2005; **14**(1): 92-102.
146. Salic A, Mitchison TJ. A chemical method for fast and sensitive detection of DNA synthesis in vivo. *Proceedings of the National Academy of Sciences* 2008; **105**(7): 2415-2420.
147. Kolb HC, Finn MG, Sharpless KB. Click Chemistry: Diverse Chemical Function from a Few Good Reactions. *Angewandte Chemie International Edition* 2001; **40**(11): 2004-2021.
148. Molecular Probes I. Handbook EdU (5-ethynyl-2'-deoxyuridine) Assay. *Invitrogen* 2010; **1**(1): 1-7.
149. Kibbe WA. OligoCalc: an online oligonucleotide properties calculator. *Nucleic acids research* 2007; **35**(2): 43-46.
150. Kent WJ. BLAT—the BLAST-like alignment tool. *Genome research* 2002; **12**(4): 656-664.
151. Livak KJ, Schmittgen TD. Analysis of Relative Gene Expression Data Using Real-Time Quantitative PCR and the 2- $\Delta\Delta$ CT Method. *Methods* 2001; **25**(4): 402-408.
152. Mueller O, Lightfoot S, Schroeder A. RNA integrity number (RIN)—standardization of RNA quality control. *Agilent application note, publication* 2004: 1-8.
153. Szklarczyk D, Franceschini A, Wyder S, Forslund K, Heller D, Huerta-Cepas J, *et al.* STRING v10: protein–protein interaction networks, integrated over the tree of life. *Nucleic Acids Research* 2015; **43**(1): 447-452.
154. Ogawa S, Lee T-M, Kay AR, Tank DW. Brain magnetic resonance imaging with contrast dependent on blood oxygenation. *Proceedings of the National Academy of Sciences* 1990; **87**(24): 9868-9872.
155. Turner R, Jezzard P, Wen H, Kwong K, Le Bihan D, Zeffiro T, *et al.* Functional mapping of the human visual cortex at 4 and 1.5 tesla using deoxygenation contrast EPI. *Magnetic resonance in medicine* 1993; **29**(2): 277-279.
156. Knutson B, Westdorp A, Kaiser E, Hommer D. fMRI visualization of brain activity during a monetary incentive delay task. *Neuroimage* 2000; **12**(1): 20-27.
157. Viviani R, Dommes L, Steffens M, Breitfeld J, Paul AM, Kaumanns K, *et al.* Dissociation of neural substrates of temporal difference and mean reward rates in a foraging task. *Human Brain Mapping* 2016; **22**: 3403

References

158. Repeiski J, Smith M, Sansom I, Repetski J. A differential neural response in the human amygdala to fearful and happy facial expressions. *Nature* 1996; **383**: 31.
159. Vuilleumier P, Pourtois G. Distributed and interactive brain mechanisms during emotion face perception: evidence from functional neuroimaging. *Neuropsychologia* 2007; **45**(1): 174-194.
160. Lundqvist D, Flykt A, Öhman A (1998). The Karolinska Directed Emotional Faces-KDEF. CD-ROM from Department of Clinical Neuroscience, Psychology section, Karolinska Institutet, Stockholm, Sweden. ISBN 91-630-7164-9.
161. Friston KJ, Holmes AP, Worsley KJ, Poline J, Frith CD, Frackowiak RS. Statistical parametric maps in functional imaging: a general linear approach. *Human brain mapping* 1994; **2**(4): 189-210.
162. Ulmer S, Jansen O. *fMRI*. Springer, 2010.
163. Edgar R, Domrachev M, Lash AE. Gene Expression Omnibus: NCBI gene expression and hybridization array data repository. *Nucleic acids research* 2002; **30**(1): 207-210.
164. Barrett T, Wilhite SE, Ledoux P, Evangelista C, Kim IF, Tomashevsky M, *et al*. NCBI GEO: archive for functional genomics data sets—update. *Nucleic acids research* 2013; **41**(D1): D991-D995.
165. Gómez-Gaviro MV, Scott CE, Sesay AK, Matheu A, Booth S, Galichet C, *et al*. Betacellulin promotes cell proliferation in the neural stem cell niche and stimulates neurogenesis. *Proceedings of the National Academy of Sciences* 2012; **109**(4): 1317-1322.
166. Kubo F, Takeichi M, Nakagawa S. Wnt2b inhibits differentiation of retinal progenitor cells in the absence of Notch activity by downregulating the expression of proneural genes. *Development* 2005; **132**(12): 2759-2770.
167. Aguirre A, Rubio ME, Gallo V. Notch and EGFR pathway interaction regulates neural stem cell number and self-renewal. *Nature* 2010; **467**(7313): 323-327.
168. Brandl E, Chowdhury N, Tiwari A, Lett TP, Meltzer H, Kennedy J, *et al*. Genetic variation in CYP3A43 is associated with response to antipsychotic medication. *J Neural Transm* 2015; **122**(1): 29-34.
169. Le-Niculescu H, Levey D, Ayalew M, Palmer L, Gavrin L, Jain N, *et al*. Discovery and validation of blood biomarkers for suicidality. *Molecular psychiatry* 2013; **18**(12): 1249-1264.

170. Sequeira A, Morgan L, Walsh DM, Cartagena PM, Choudary P, Li J, *et al.* Gene expression changes in the prefrontal cortex, anterior cingulate cortex and nucleus accumbens of mood disorders subjects that committed suicide. *PLoS One* 2012; **7**(4): e35367.
171. McCall WV, Batson N, Webster M, Case LD, Joshi I, Derreberry T, *et al.* Nightmares and dysfunctional beliefs about sleep mediate the effect of insomnia symptoms on suicidal ideation. *J Clin Sleep Med* 2013; **9**(2): 135-140.
172. Allali-Hassani A, Pan PW, Dombrowski L, Najmanovich R, Tempel W, Dong A, *et al.* Structural and Chemical Profiling of the Human Cytosolic Sulfotransferases. *PLoS Biol* 2007; **5**(5): e97.
173. Wu Melody V, Hen R. The Young and the Restless: Regulation of Adult Neurogenesis by Wnt Signaling. *Cell Stem Cell* 2013; **12**(2): 139-140.
174. Boehm C, Newrzella D, Herberger S, Schramm N, Eisenhardt G, Schenk V, *et al.* Effects of antidepressant treatment on gene expression profile in mouse brain: cell type-specific transcription profiling using laser microdissection and microarray analysis. *Journal of Neurochemistry* 2006; **97**: 44-49.
175. Hayashi H. Lipid Metabolism and Glial Lipoproteins in the Central Nervous System. *Biological and Pharmaceutical Bulletin* 2011; **34**(4): 453-461.
176. Tarr PT, Edwards PA. ABCG1 and ABCG4 are coexpressed in neurons and astrocytes of the CNS and regulate cholesterol homeostasis through SREBP-2. *Journal of Lipid Research* 2008; **49**(1): 169-182.
177. Puschmann TB, Zandén C, Lebkuechner I, Philippot C, de Pablo Y, Liu J, *et al.* HB-EGF affects astrocyte morphology, proliferation, differentiation, and the expression of intermediate filament proteins. *Journal of Neurochemistry* 2014; **128**(6): 878-889.
178. Ries V, Silva RM, Oo TF, Cheng H-C, Rzhetskaya M, Kholodilov N, *et al.* JNK2 and JNK3 combined are essential for apoptosis in dopamine neurons of the substantia nigra, but are not required for axon degeneration. *Journal of Neurochemistry* 2008; **107**(6): 1578-1588.
179. Schinkel AH. P-Glycoprotein, a gatekeeper in the blood–brain barrier. *Advanced Drug Delivery Reviews* 1999; **36**(2–3): 179-194.
180. Britsch S, Li L, Kirchhoff S, Theuring F, Brinkmann V, Birchmeier C, *et al.* The ErbB2 and ErbB3 receptors and their ligand, neuregulin-1, are essential for development of the sympathetic nervous system. *Genes Dev* 1998; **12**(12): 1825-1836.
181. Binder EB, Salyakina D, Lichtner P, Wochnik GM, Ising M, Pütz B, *et al.* Polymorphisms in FKBP5 are associated with increased recurrence of depressive episodes and rapid response to antidepressant treatment. *Nature genetics* 2004; **36**(12): 1319-1325.

References

182. van Rossum EF, Binder EB, Majer M, Koper JW, Ising M, Modell S, *et al.* Polymorphisms of the glucocorticoid receptor gene and major depression. *Biological psychiatry* 2006; **59**(8): 681-688.
183. Lucae S, Salyakina D, Barden N, Harvey M, Gagné B, Labbé M, *et al.* P2RX7, a gene coding for a purinergic ligand-gated ion channel, is associated with major depressive disorder. *Human molecular genetics* 2006; **15**(16): 2438-2445.
184. Baghai T, Binder E, Schule C, Salyakina D, Eser D, Lucae S, *et al.* Polymorphisms in the angiotensin-converting enzyme gene are associated with unipolar depression, ACE activity and hypercortisolism. *Molecular psychiatry* 2006; **11**(11): 1003-1015.
185. Uhr M, Tontsch A, Namendorf C, Ripke S, Lucae S, Ising M, *et al.* Polymorphisms in the drug transporter gene ABCB1 predict antidepressant treatment response in depression. *Neuron* 2008; **57**(2): 203-209.
186. Unschuld PG, Ising M, Specht M, Erhardt A, Ripke S, Heck A, *et al.* Polymorphisms in the GAD2 gene-region are associated with susceptibility for unipolar depression and with a risk factor for anxiety disorders. *American Journal of Medical Genetics Part B: Neuropsychiatric Genetics* 2009; **150**(8): 1100-1109.
187. Lucae S, Ising M, Horstmann S, Baune BT, Arolt V, Müller-Myhsok B, *et al.* HTR2A gene variation is involved in antidepressant treatment response. *European Neuropsychopharmacology* 2010; **20**(1): 65-68.
188. Horstmann S, Lucae S, Menke A, Hennings JM, Ising M, Roeske D, *et al.* Polymorphisms in GRIK4, HTR2A, and FKBP5 show interactive effects in predicting remission to antidepressant treatment. *Neuropsychopharmacology* 2010; **35**(3): 727-740.
189. Kohli MA, Lucae S, Saemann PG, Schmidt MV, Demirkan A, Hek K, *et al.* The neuronal transporter gene SLC6A15 confers risk to major depression. *Neuron* 2011; **70**(2): 252-265.
190. Kloiber S, Kohli M, Brueckl T, Ripke S, Ising M, Uhr M, *et al.* Variations in tryptophan hydroxylase 2 linked to decreased serotonergic activity are associated with elevated risk for metabolic syndrome in depression. *Molecular psychiatry* 2010; **15**(7): 736-747.
191. Kohli MA, Salyakina D, Pfennig A, Lucae S, Horstmann S, Menke A, *et al.* Association of Genetic Variants in the Neurotrophic Receptor–Encoding Gene NTRK2 and a Lifetime History of Suicide Attempts in Depressed Patients. *Archives of general psychiatry* 2010; **67**(4): 348-359.
192. Pfennig A, Kunzel HE, Kern N, Ising M, Majer M, Fuchs B, *et al.* Hypothalamus-pituitary-adrenal system regulation and suicidal behavior in depression. *Biological psychiatry* 2005; **57**(4): 336-342.

193. Majer M, Ising M, Künzel H, Binder E, Holsboer F, Modell S, *et al.* Impaired divided attention predicts delayed response and risk to relapse in subjects with depressive disorders. *Psychological medicine* 2004; **34**(08): 1453-1463.
194. Reppermund S, Zihl J, Lucae S, Horstmann S, Kloiber S, Holsboer F, *et al.* Persistent cognitive impairment in depression: the role of psychopathology and altered hypothalamic-pituitary-adrenocortical (HPA) system regulation. *Biological psychiatry* 2007; **62**(5): 400-406.
195. Kloiber S, Ising M, Reppermund S, Horstmann S, Dose T, Majer M, *et al.* Overweight and obesity affect treatment response in major depression. *Biological psychiatry* 2007; **62**(4): 321-326.
196. Howland R. Sequenced Treatment Alternatives to Relieve Depression (STAR* D). Part 1: study design. *Journal of psychosocial nursing and mental health services* 2008; **46**(9): 21-24.
197. Sinyor M. The sequenced treatment alternatives to relieve depression (STAR* D) trial: a review. *Canadian Journal of Psychiatry* 2010; **55**(3): 126.
198. Nierenberg AA, Fava M, Trivedi MH, Wisniewski SR, Thase ME, McGrath PJ, *et al.* A comparison of lithium and T 3 augmentation following two failed medication treatments for depression: a STAR* D report. *American journal of Psychiatry* 2006; **163**(9): 1519-1530.
199. Fava M, A John Rush M, Wisniewski SR, Nierenberg AA, Alpert JE, McGrath PJ, *et al.* A comparison of mirtazapine and nortriptyline following two consecutive failed medication treatments for depressed outpatients: a STAR* D report. *American Journal of Psychiatry* 2006.
200. Rush AJ. STAR* D: what have we learned? *Am J Psychiatry* 2007; **164**(2): 201.
201. Warden D, Rush AJ, Trivedi MH, Fava M, Wisniewski SR. The STAR* D Project results: a comprehensive review of findings. *Current psychiatry reports* 2007; **9**(6): 449-459.
202. Stark AL, Dolan ME. Lymphoblastoid cell lines in pharmacogenomics: how applicable are they to clinical outcomes? *Pharmacogenomics* 2013; **14**(5): 447-450.
203. Zhang W, Dolan ME. Use of cell lines in the investigation of pharmacogenetic loci. *Current pharmaceutical design* 2009; **15**(32): 3782.
204. Welsh M, Mangravite L, Medina MW, Tantisira K, Zhang W, Huang RS, *et al.* Pharmacogenomic Discovery Using Cell-Based Models. *Pharmacological Reviews* 2009; **61**(4): 413-429.

References

205. Wheeler HE, Dolan ME. Lymphoblastoid cell lines in pharmacogenomic discovery and clinical translation. *Pharmacogenomics* 2012; **13**(1): 55-70.
206. Mangravite LM, Medina MW, Cui J, Pressman S, Smith JD, Rieder MJ, *et al.* Combined influence of LDLR and HMGCR sequence variation on lipid-lowering response to simvastatin. *Arteriosclerosis, thrombosis, and vascular biology* 2010; **30**(7): 1485-1492.
207. Tantisira KG, Lasky-Su J, Harada M, Murphy A, Litonjua AA, Himes BE, *et al.* Genomewide Association between GLCCI1 and Response to Glucocorticoid Therapy in Asthma. *New England Journal of Medicine* 2011; **365**(13): 1173-1183.
208. Ling PD, Huls HM. Isolation and immortalization of lymphocytes. *Current Protocols in Molecular Biology* 2005: 28.22. 21-28.22. 25.
209. Shirley MD, Baugher JD, Stevens EL, Tang Z, Gerry N, Beiswanger CM, *et al.* Chromosomal variation in lymphoblastoid cell lines. *Human mutation* 2012; **33**(7): 1075-1086.
210. Çalışkan M, Cusanovich DA, Ober C, Gilad Y. The effects of EBV transformation on gene expression levels and methylation profiles. *Human molecular genetics* 2011; **20**(8): 1643-4652.
211. Sie L, Loong S, Tan E. Utility of lymphoblastoid cell lines. *Journal of neuroscience research* 2009; **87**(9): 1953-1959.
212. Sie L, Loong S, Tan EK. Utility of lymphoblastoid cell lines. *Journal of Neuroscience Research* 2009; **87**(9): 1953-1959.
213. Mitra A, Crews K, Pounds S, Cao X, Downing J, Raimondi S, *et al.* Impact of genetic variation in FKBP5 on clinical response in pediatric acute myeloid leukemia patients: a pilot study. *Leukemia: official journal of the Leukemia Society of America, Leukemia Research Fund, UK* 2011; **25**(8): 1354.
214. Ziliak D, O'donnell PH, Im HK, Gamazon ER, Chen P, Delaney S, *et al.* Germline polymorphisms discovered via a cell-based, genome-wide approach predict platinum response in head and neck cancers. *Translational Research* 2011; **157**(5): 265-272.
215. Huang RS, Johnatty SE, Gamazon ER, Im HK, Ziliak D, Duan S, *et al.* Platinum Sensitivity–Related Germline Polymorphism Discovered via a Cell-Based Approach and Analysis of Its Association with Outcome in Ovarian Cancer Patients. *Clinical Cancer Research* 2011; **17**(16): 5490-5500.
216. Brown CC, Havener TM, Medina MW, Auman JT, Mangravite LM, Krauss RM, *et al.* A genome-wide association analysis of temozolomide response using lymphoblastoid cell lines reveals a clinically relevant association with MGMT. *Pharmacogenetics and genomics* 2012; **22**(11): 796.

217. Matigian NA, McCurdy RD, Féron F, Perry C, Smith H, Filippich C, *et al.* Fibroblast and lymphoblast gene expression profiles in schizophrenia: are non-neural cells informative? *PLoS One* 2008; **3**(6): 2412.
218. Horike S-i, Cai S, Miyano M, Cheng J-F, Kohwi-Shigematsu T. Loss of silent-chromatin looping and impaired imprinting of DLX5 in Rett syndrome. *Nature genetics* 2005; **37**(1): 31-40.
219. Montag-Sallaz M, Schachner M, Montag D. Misguided axonal projections, neural cell adhesion molecule 180 mRNA upregulation, and altered behavior in mice deficient for the close homolog of L1. *Molecular and Cellular Biology* 2002; **22**(22): 7967-7981.
220. Morellini F, Lepsveridze E, Kähler B, Dityatev A, Schachner M. Reduced reactivity to novelty, impaired social behavior, and enhanced basal synaptic excitatory activity in perforant path projections to the dentate gyrus in young adult mice deficient in the neural cell adhesion molecule CHL1. *Molecular and Cellular Neuroscience* 2007; **34**(2): 121-136.
221. Demyanenko GP, Siesser PF, Wright AG, Brennaman LH, Bartsch U, Schachner M, *et al.* L1 and CHL1 cooperate in thalamocortical axon targeting. *Cerebral Cortex* 2011; **21**(2): 401-412.
222. Demyanenko GP, Halberstadt AI, Rao RS, Maness PF. CHL1 cooperates with PAK1–3 to regulate morphological differentiation of embryonic cortical neurons. *Neuroscience* 2010; **165**(1): 107-115.
223. Huang X, Zhu L-l, Zhao T, Wu L-y, Wu K-w, Schachner M, *et al.* CHL1 negatively regulates the proliferation and neuronal differentiation of neural progenitor cells through activation of the ERK1/2 MAPK pathway. *Molecular and Cellular Neuroscience* 2011; **46**(1): 296-307.
224. Laifenfeld D, Karry R, Klein E, Ben-Shachar D. Alterations in cell adhesion molecule L1 and functionally related genes in major depression: a postmortem study. *Biological psychiatry* 2005; **57**(7): 716-725.
225. Sakurai K, Migita O, Toru M, Arinami T. An association between a missense polymorphism in the close homologue of L1 (CHL1, CALL) gene and schizophrenia. *Molecular psychiatry* 2002; **7**(4): 412-415.
226. Chen Q-Y, Chen Q, Feng G-Y, Lindpaintner K, Chen Y, Sun X, *et al.* Case-control association study of the close homologue of L1 (CHL1) gene and schizophrenia in the Chinese population. *Schizophrenia research* 2005; **73**(2): 269-274.
227. Oved K, Morag A, Pasmanik-Chor M, Rehavi M, Shomron N, Gurwitz D. Genome-wide expression profiling of human lymphoblastoid cell lines implicates integrin beta-3 in the mode of action of antidepressants. *Translational Psychiatry* 2013; **3**(10): 171-184.

References

228. Carneiro AMD, Cook EH, Murphy DL, Blakely RD. Interactions between integrin $\alpha\text{IIb}\beta\text{3}$ and the serotonin transporter regulate serotonin transport and platelet aggregation in mice and humans. *The Journal of clinical investigation* 2008; **118**(4): 1544-1552.
229. Fabbri C, Crisafulli C, Gurwitz D, Stingl J, Calati R, Albani D, *et al.* Neuronal cell adhesion genes and antidepressant response in three independent samples. *The pharmacogenomics journal* 2015.
230. Clark S, Adkins D, Aberg K, Hettema J, McClay J, Souza R, *et al.* Pharmacogenomic study of side-effects for antidepressant treatment options in STAR* D. *Psychological medicine* 2012; **42**(06): 1151-1162.
231. Morag A, Kirchheiner J, Rehavi M, Gurwitz D. Human lymphoblastoid cell line panels: novel tools for assessing shared drug pathways. *Pharmacogenomics* 2010; **11**(3): 327-340.
232. Squassina A, Costa M, Congiu D, Manchia M, Angius A, Deiana V, *et al.* Insulin-like growth factor 1 (IGF-1) expression is up-regulated in lymphoblastoid cell lines of lithium responsive bipolar disorder patients. *Pharmacological Research* 2013; **73**(0): 1-7.
233. Chen H, Wang N, Burmeister M, McInnis MG. MicroRNA expression changes in lymphoblastoid cell lines in response to lithium treatment. *International Journal of Neuropsychopharmacology* 2009; **12**(7): 975-981.
234. Hu VW, Frank BC, Heine S, Lee NH, Quackenbush J. Gene expression profiling of lymphoblastoid cell lines from monozygotic twins discordant in severity of autism reveals differential regulation of neurologically relevant genes. *BMC genomics* 2006; **7**(1): 1.
235. Kodama M, Fujioka T, Duman RS. Chronic olanzapine or fluoxetine administration increases cell proliferation in hippocampus and prefrontal cortex of adult rat. *Biological Psychiatry* 2004; **56**(8): 570-580.
236. Malberg JE, Duman RS. Cell proliferation in adult hippocampus is decreased by inescapable stress: reversal by fluoxetine treatment. *Neuropsychopharmacology* 2003; **28**(9): 1562-1571.
237. Zusso M, Debetto P, Guidolin D, Barbierato M, Manev H, Giusti P. Fluoxetine-induced proliferation and differentiation of neural progenitor cells isolated from rat postnatal cerebellum. *Biochemical pharmacology* 2008; **76**(3): 391-403.
238. Czéh B, Müller-Keuker JI, Rygula R, Abumaria N, Hiemke C, Domenici E, *et al.* Chronic social stress inhibits cell proliferation in the adult medial prefrontal cortex: hemispheric asymmetry and reversal by fluoxetine treatment. *Neuropsychopharmacology* 2007; **32**(7): 1490-1503.

239. Lee H, Kim J, Yim S, Kim M, Kim S, Kim Y, *et al.* Fluoxetine enhances cell proliferation and prevents apoptosis in dentate gyrus of maternally separated rats. *Molecular psychiatry* 2001; **6**(6): 725-728.
240. Sairanen M, Lucas G, Ernfors P, Castrén M, Castrén E. Brain-derived neurotrophic factor and antidepressant drugs have different but coordinated effects on neuronal turnover, proliferation, and survival in the adult dentate gyrus. *The Journal of Neuroscience* 2005; **25**(5): 1089-1094.
241. Sachs BD, Caron MG. Chronic fluoxetine increases extra-hippocampal neurogenesis in adult mice. *International Journal of Neuropsychopharmacology* 2015; **18**(4): 1-12.
242. Zhang F, Xue J, Shao J, Jia L. Compilation of 222 drugs' plasma protein binding data and guidance for study designs. *Drug discovery today* 2012; **17**(9): 475-485.
243. Chang E-A, Beyhan Z, Yoo M-S, Siripattarapivat K, Ko T, Lookingland KJ, *et al.* Increased cellular turnover in response to fluoxetine in neuronal precursors derived from human embryonic stem cells *The International Journal of Developmental Biology* 2010; **54**: 707-715.
244. Scholzen T, Gerdes J. The Ki-67 protein: from the known and the unknown. *Journal of cellular physiology* 2000; **182**(3): 311-322.
245. Tusher VG, Tibshirani R, Chu G. Significance analysis of microarrays applied to the ionizing radiation response. *PNAS* 2001; **98**(9): 5116-5121.
246. Kusakawa S, Yamauchi J, Miyamoto Y, Sanbe A, Tanoue A. Estimation of embryotoxic effect of fluoxetine using embryonic stem cell differentiation system. *Life sciences* 2008; **83**(25): 871-877.
247. Thibaut R, Porte C. Effects of fibrates, anti-inflammatory drugs and antidepressants in the fish hepatoma cell line PLHC-1: cytotoxicity and interactions with cytochrome P450 1A. *Toxicology in Vitro* 2008; **22**(5): 1128-1135.
248. Laville N, Ait-Aissa S, Gomez E, Casellas C, Porcher J. Effects of human pharmaceuticals on cytotoxicity, EROD activity and ROS production in fish hepatocytes. *Toxicology* 2004; **196**(1): 41-55.
249. Caminada D, Escher C, Fent K. Cytotoxicity of pharmaceuticals found in aquatic systems: comparison of PLHC-1 and RTG-2 fish cell lines. *Aquatic Toxicology* 2006; **79**(2): 114-123.
250. Düsman E, Almeida I, Mariucci R, Mantovani M, Vicentini V. Cytotoxicity and mutagenicity of fluoxetine hydrochloride (Prozac), with or without vitamins A and C, in plant and animal model systems. *Genetics and Molecular Research* 2014; **13**(1): 578-589.

References

251. Smith EM, Iftikar FI, Higgins S, Irshad A, Jandoc R, Lee M, *et al.* In vitro inhibition of cytochrome P450-mediated reactions by gemfibrozil, erythromycin, ciprofloxacin and fluoxetine in fish liver microsomes. *Aquatic toxicology* 2012; **109**: 259-266.
252. Souza MEJ, Polizello ACM, Uyemura SA, Castro-Silva O, Curti C. Effect of fluoxetine on rat liver mitochondria. *Biochemical pharmacology* 1994; **48**(3): 535-541.
253. Whirl-Carrillo M, McDonagh E, Hebert J, Gong L, Sangkuhl K, Thorn C, *et al.* Pharmacogenomics knowledge for personalized medicine. *Clinical pharmacology and therapeutics* 2012; **92**(4): 414.
254. Sangkuhl K, Klein TE, Altman RB. PharmGKB summary: citalopram pharmacokinetics pathway. *Pharmacogenetics and genomics* 2011; **21**(11): 769.
255. Morag A, Oved K, Gurwitz D. Sex Differences in Human Lymphoblastoid Cells Sensitivities to Antipsychotic Drugs. *J Mol Neurosci* 2013; **49**(3): 554-558.
256. Fava M, A John Rush M, Alpert JE, Balasubramani G, Wisniewski SR, Carmin CN, *et al.* Difference in treatment outcome in outpatients with anxious versus nonanxious depression: a STAR* D report. *American Journal of Psychiatry* 2008; **165**(3): 342-351.
257. Ising M, Lucae S, Binder EB, Bettecken T, Uhr M, Ripke S, *et al.* A genomewide association study points to multiple loci that predict antidepressant drug treatment outcome in depression. *Archives of general psychiatry* 2009; **66**(9): 966-975.
258. Kuhn HG, Dickinson-Anson H, Gage FH. Neurogenesis in the dentate gyrus of the adult rat: age-related decrease of neuronal progenitor proliferation. *The Journal of neuroscience* 1996; **16**(6): 2027-2033.
259. Nixon K, Crews FT. Binge ethanol exposure decreases neurogenesis in adult rat hippocampus. *Journal of neurochemistry* 2002; **83**(5): 1087-1093.
260. Van Praag H, Christie BR, Sejnowski TJ, Gage FH. Running enhances neurogenesis, learning, and long-term potentiation in mice. *Proceedings of the National Academy of Sciences* 1999; **96**(23): 13427-13431.
261. Castrén E, Hen R. Neuronal plasticity and antidepressant actions. *Trends in Neurosciences* 2013; **36**(5): 259-267.
262. Malberg JE, Duman RS. Cell proliferation in adult hippocampus is decreased by inescapable stress: reversal by fluoxetine treatment. *Neuropsychopharmacology : official publication of the American College of Neuropsychopharmacology* 2003; **28**(9): 1562-1571.

263. Pilar-Cuellar F, Vidal R, Diaz A, Castro E, dos Anjos S, Pascual-Brazo J, *et al.* Neural Plasticity and Proliferation in the Generation of Antidepressant Effects: Hippocampal Implication. *Neural Plasticity* 2013; **2013**: 537265-537265.
264. Wang J-W, David DJ, Monckton JE, Battaglia F, Hen R. Chronic Fluoxetine Stimulates Maturation and Synaptic Plasticity of Adult-Born Hippocampal Granule Cells. *The Journal of Neuroscience* 2008; **28**(6): 1374-1384.
265. Khemissi W, Farooq RK, Le Guisquet A-M, Sakly M, Belzung C. Dysregulation of the hypothalamus-pituitary-adrenal axis predicts some aspects of the behavioral response to chronic fluoxetine: association with hippocampal cell proliferation. *Frontiers in Behavioral Neuroscience* 2014; **8**: 340.
266. Perera TD, Coplan JD, Lisanby SH, Lipira CM, Arif M, Carpio C, *et al.* Antidepressant-Induced Neurogenesis in the Hippocampus of Adult Nonhuman Primates. *The Journal of Neuroscience* 2007; **27**(18): 4894-4901.
267. Chen F, Madsen TM, Wegener G, Nyengaard JR. Imipramine treatment increases the number of hippocampal synapses and neurons in a genetic animal model of depression. *Hippocampus* 2010; **20**(12): 1376-1384.
268. Yu H, Chen Z-y. The role of BDNF in depression on the basis of its location in the neural circuitry. *Acta Pharmacologica Sinica* 2011; **32**(1): 3-11.
269. Encinas JM, Vaahtokari A, Enikolopov G. Fluoxetine targets early progenitor cells in the adult brain. *Proceedings of the National Academy of Sciences* 2006; **103**(21): 8233-8238.
270. David DJ, Wang J, Samuels BA, Rainer Q, David I, Gardier AM, *et al.* Implications of the functional integration of adult-born hippocampal neurons in anxiety-depression disorders. *The Neuroscientist* 2010; **16**(5): 578-591.
271. Malmersjö S, Rebellato P, Smedler E, Planert H, Kanatani S, Liste I, *et al.* Neural progenitors organize in small-world networks to promote cell proliferation. *Proceedings of the National Academy of Sciences* 2013; **110**(16): E1524-E1532.
272. Glaser T, Resende RR, Ulrich H. Implications of purinergic receptor-mediated intracellular calcium transients in neural differentiation. *Cell Communication and Signaling* 2013; **11**(1): 1.
273. McKiernan E, O'Driscoll L, Kasper M, Barron N, O'Sullivan F, Clynes M. Directed differentiation of mouse embryonic stem cells into pancreatic-like or neuronal-and glial-like phenotypes. *Tissue engineering* 2007; **13**(10): 2419-2430.
274. Davies AM. Neuronal survival: early dependence on Schwann cells. *Current biology* 1998; **8**(1): R15-R18.

References

275. Jin K, Mao XO, Sun Y, Xie L, Jin L, Nishi E, *et al.* Heparin-binding epidermal growth factor-like growth factor: hypoxia-inducible expression in vitro and stimulation of neurogenesis in vitro and in vivo. *The Journal of neuroscience* 2002; **22**(13): 5365-5373.
276. Linggi B, Carpenter G. ErbB receptors: new insights on mechanisms and biology. *Trends in cell biology* 2006; **16**(12): 649-656.
277. Lemarchand E, Maubert E, Haelewyn B, Ali C, Rubio M, Vivien D. Stressed neurons protect themselves by a tissue-type plasminogen activator-mediated EGFR-dependent mechanism. *Cell Death & Differentiation* 2016; **23**(1): 123-131.
278. Pirl WF, Traeger L, Greer JA, Bemis H, Gallagher E, Lennes I, *et al.* Tumor Epidermal Growth Factor Receptor Genotype and Depression in Stage IV Non-Small Cell Lung Cancer. *The Oncologist* 2011; **16**(9): 1299-1306.
279. Logotheti M, Papadodima O, Chatziioannou A, Venizelos N, Kolisis F. Gene Expression Analysis of Fibroblasts from Patients with Bipolar Disorder. *J Neuropsychopharmacol Mental Health* 2015; **1**(103): 2.
280. Israsena N, Hu M, Fu W, Kan L, Kessler JA. The presence of FGF2 signaling determines whether β -catenin exerts effects on proliferation or neuronal differentiation of neural stem cells. *Developmental Biology* 2004; **268**(1): 220-231.
281. Kléber M, Lee H-Y, Wurdak H, Buchstaller J, Riccomagno MM, Ittner LM, *et al.* Neural crest stem cell maintenance by combinatorial Wnt and BMP signaling. *The Journal of Cell Biology* 2005; **169**(2): 309-320.
282. Evans SJ, Choudary PV, Neal CR, Li JZ, Vawter MP, Tomita H, *et al.* Dysregulation of the fibroblast growth factor system in major depression. *Proceedings of the National Academy of Sciences of the United States of America* 2004; **101**(43): 15506-15511.
283. Ordway GA, Szebeni A, Chandley MJ, Stockmeier CA, Xiang L, Newton SS, *et al.* Low gene expression of bone morphogenetic protein 7 in brainstem astrocytes in major depression. *International Journal of Neuropsychopharmacology* 2012; **15**(7): 855-868.
284. Fuentealba Luis C, Obernier K, Alvarez-Buylla A. Adult Neural Stem Cells Bridge Their Niche. *Cell Stem Cell* 2012; **10**(6): 698-708.
285. Quesseveur G, David D, Gaillard M, Pla P, Wu M, Nguyen H, *et al.* BDNF overexpression in mouse hippocampal astrocytes promotes local neurogenesis and elicits anxiolytic-like activities. *Translational psychiatry* 2013; **3**(4): e253.
286. Inestrosa NC, Arenas E. Emerging roles of Wnts in the adult nervous system. *Nature Reviews Neuroscience* 2010; **11**(2): 77-86.

287. Kuwabara T, Hsieh J, Muotri A, Yeo G, Warashina M, Lie DC, *et al.* Wnt-mediated activation of NeuroD1 and retro-elements during adult neurogenesis. *Nature neuroscience* 2009; **12**(9): 1097-1105.
288. Vanderhaeghen P. Wnts blow on NeuroD1 to promote adult neuron production and diversity. *Nature neuroscience* 2009; **12**(9): 1079-1081.
289. Bayatti N, Sarma S, Shaw C, Eyre JA, Vouyiouklis DA, Lindsay S, *et al.* Progressive loss of PAX6, TBR2, NEUROD and TBR1 mRNA gradients correlates with translocation of EMX2 to the cortical plate during human cortical development. *European Journal of Neuroscience* 2008; **28**(8): 1449-1456.
290. Couillard-Despres S, Winner B, Schaubeck S, Aigner R, Vroemen M, Weidner N, *et al.* Doublecortin expression levels in adult brain reflect neurogenesis. *European Journal of Neuroscience* 2005; **21**(1): 1-14.
291. Duncan RN, Xie Y, McPherson AD, Taibi AV, Bonkowsky JL, Douglass AD, *et al.* Hypothalamic radial glia function as self-renewing neural progenitors in the absence of Wnt/ β -catenin signaling. *Development* 2016; **143**(1): 45-53.
292. Clevers H, Loh KM, Nusse R. An integral program for tissue renewal and regeneration: Wnt signaling and stem cell control. *Science* 2014; **346**(6205): 1-7.
293. Bengoa-Vergniory N, Kypta RM. Canonical and noncanonical Wnt signaling in neural stem/progenitor cells. *Cell Mol Life Sci* 2015; **72**(21): 4157-4172.
294. Halleskog C, Mulder J, Dahlström J, Mackie K, Hortobágyi T, Tanila H, *et al.* WNT signaling in activated microglia is proinflammatory. *Glia* 2011; **59**(1): 119-131.
295. Prinz M, Priller J. Microglia and brain macrophages in the molecular age: from origin to neuropsychiatric disease. *Nature Reviews Neuroscience* 2014; **15**(5): 300-312.
296. Coullery RP, Ferrari ME, Rosso SB. Neuronal development and axon growth are altered by glyphosate through a WNT non-canonical signaling pathway. *NeuroToxicology* 2016; **52**: 150-161.
297. Lie D-C, Colamarino SA, Song H-J, Desire L, Mira H, Consiglio A, *et al.* Wnt signalling regulates adult hippocampal neurogenesis. *Nature* 2005; **437**(7063): 1370-1375.
298. Ikeya M, Lee SMK, Johnson JE, McMahon AP, Takada S. Wnt signalling required for expansion of neural crest and CNS progenitors. *Nature* 1997; **389**(6654): 966-970.

References

299. Sahores M, Gibb A, Salinas PC. Frizzled-5, a receptor for the synaptic organizer Wnt7a, regulates activity-mediated synaptogenesis. *Development* 2010; **137**(13): 2215-2225.
300. Varela-Nallar L, Grabowski CP, Alfaro IE, Alvarez AR, Inestrosa NC. Role of the Wnt receptor Frizzled-1 in presynaptic differentiation and function. *Neural Dev* 2009; **4**(1): 41.
301. Jessberger S, Clark RE, Broadbent NJ, Clemenson GD, Consiglio A, Lie DC, *et al.* Dentate gyrus-specific knockdown of adult neurogenesis impairs spatial and object recognition memory in adult rats. *Learning & Memory* 2009; **16**(2): 147-154.
302. Okamoto H, Voleti B, Banasr M, Sarhan M, Duric V, Girgenti MJ, *et al.* Wnt2 expression and signaling is increased by different classes of antidepressant treatments. *Biological psychiatry* 2010; **68**(6): 521-527.
303. Eom T-Y, Jope RS. Blocked inhibitory serine-phosphorylation of glycogen synthase kinase-3 α/β impairs in vivo neural precursor cell proliferation. *Biological psychiatry* 2009; **66**(5): 494-502.
304. Machado-Vieira R, Salvadore G, DiazGranados N, Zarate CA. Ketamine and the next generation of antidepressants with a rapid onset of action. *Pharmacology & therapeutics* 2009; **123**(2): 143-150.
305. Sidharthan NP, Butcher NJ, Mitchell DJ, Minchin RF. Expression of the orphan cytosolic sulfotransferase SULT4A1 and its major splice variant in human tissues and cells: dimerization, degradation and polyubiquitination. *PloS one* 2014; **9**(7): e101520.
306. Minchin RF, Lewis A, Mitchell D, Kadlubar FF, McManus ME. Sulfotransferase 4A1. *The international journal of biochemistry & cell biology* 2008; **40**(12): 2686-2691.
307. Alnouti Y, Klaassen CD. Tissue distribution and ontogeny of sulfotransferase enzymes in mice. *Toxicological Sciences* 2006; **93**(2): 242-255.
308. Meltzer HY, Brennan MD, Woodward ND, Jayathilake K. Association of Sult4A1 SNPs with psychopathology and cognition in patients with schizophrenia or schizoaffective disorder. *Schizophrenia research* 2008; **106**(2): 258-264.
309. Alnouti Y, Klaassen CD. Mechanisms of gender-specific regulation of mouse sulfotransferases (Sults). *Xenobiotica* 2011; **41**(3): 187-197.
310. Butcher NJ, Mitchell DJ, Burow R, Minchin RF. Regulation of mouse brain-selective sulfotransferase sult4a1 by cAMP response element-binding protein and activating transcription factor-2. *Molecular pharmacology* 2010; **78**(3): 503-510.
311. Gass P, Riva MA. CREB, neurogenesis and depression. *Bioessays* 2007; **29**(10): 957-961.

312. Pandey GN, Dwivedi Y, Ren X, Rizavi HS, Roberts RC, Conley RR. Cyclic AMP response element-binding protein in post-mortem brain of teenage suicide victims: specific decrease in the prefrontal cortex but not the hippocampus. *The International Journal of Neuropsychopharmacology* 2007; **10**(05): 621-629.
313. Lim S-W, Kim S, Carroll BJ, Kim DK. T-lymphocyte CREB as a potential biomarker of response to antidepressant drugs. *The International Journal of Neuropsychopharmacology* 2013; **16**(05): 967-974.
314. Zeigler-Johnson C, Friebel T, Walker AH, Wang Y, Spangler E, Panossian S, *et al.* CYP3A4, CYP3A5, and CYP3A43 genotypes and haplotypes in the etiology and severity of prostate cancer. *Cancer research* 2004; **64**(22): 8461-8467.
315. Westlind A, Malmebo S, Johansson I, Otter C, Andersson TB, Ingelman-Sundberg M, *et al.* Cloning and tissue distribution of a novel human cytochrome p450 of the CYP3A subfamily, CYP3A43. *Biochemical and biophysical research communications* 2001; **281**(5): 1349-1355.
316. Bojanic DD, Tarr PT, Gale GD, Smith DJ, Bok D, Chen B, *et al.* Differential expression and function of ABCG1 and ABCG4 during development and aging. *Journal of lipid research* 2010; **51**(1): 169-181.
317. Uehara Y, Yamada T, Baba Y, Miura S-i, Abe S, Kitajima K, *et al.* ATP-binding cassette transporter G4 is highly expressed in microglia in Alzheimer's brain. *Brain research* 2008; **1217**: 239-246.
318. Bilici M, Efe H, Koroğlu MA, Uydu HA, Bekaroğlu M, Değer O. Antioxidative enzyme activities and lipid peroxidation in major depression: alterations by antidepressant treatments. *Journal of affective disorders* 2001; **64**(1): 43-51.
319. Maes M, Smith R, Christophe A, Cosyns P, Desnyder R, Meltzer H. Fatty acid composition in major depression: decreased ω 3 fractions in cholesteryl esters and increased C20:4 ω 6C20:5 ω 3 ratio in cholesteryl esters and phospholipids. *Journal of affective disorders* 1996; **38**(1): 35-46.
320. Kushihara H, Suzuki H, Sugiyama Y. The role of P-Glycoprotein and canalicular multispecific organic anion transporter in the hepatobiliary excretion of drugs. *Journal of pharmaceutical sciences* 1998; **87**(9): 1025-1040.
321. Chiou WL, Chung SM, Wu TC. Potential role of P-glycoprotein in affecting hepatic metabolism of drugs. *Pharmaceutical research* 2000; **17**(8): 903-905.
322. van Asperen J, van Tellingen OH, Beijnen JH. The pharmacological role of P-glycoprotein in the intestinal epithelium. *Pharmacological research* 1998; **37**(6): 429-435.

References

323. Herman J, McKlveen J, Solomon M, Carvalho-Netto E, Myers B. Neural regulation of the stress response: glucocorticoid feedback mechanisms. *Brazilian journal of medical and biological research* 2012; **45**(4): 292-298.
324. Fitzsimons C, Van Hooijdonk L, Schouten M, Zalachoras I, Brinks V, Zheng T, *et al.* Knockdown of the glucocorticoid receptor alters functional integration of newborn neurons in the adult hippocampus and impairs fear-motivated behavior. *Molecular psychiatry* 2013; **18**(9): 993-1005.
325. Uhr M, Grauer MT, Holsboer F. Differential enhancement of antidepressant penetration into the brain in mice with *abcb1ab* (*mdr1ab*) P-glycoprotein gene disruption. *Biological psychiatry* 2003; **54**(8): 840-846.
326. Wang J-S, Zhu H-J, Gibson BB, Markowitz JS, Donovan JL, DeVane CL. Sertraline and its metabolite desmethylsertraline, but not bupropion or its three major metabolites, have high affinity for P-glycoprotein. *Biological & pharmaceutical bulletin* 2008; **31**(2): 231.
327. Ejsing TB, Hasselstrøm J, Linnet K. The influence of P-glycoprotein on cerebral and hepatic concentrations of nortriptyline and its metabolites. *Drug metabolism and drug interactions* 2006; **21**(3-4): 139-162.
328. Karlsson L, Carlsson B, Hiemke C, Ahlner J, Bengtsson F, Schmitt U, *et al.* Altered brain concentrations of citalopram and escitalopram in P-glycoprotein deficient mice after acute and chronic treatment. *European Neuropsychopharmacology* 2013; **23**(11): 1636-1644.
329. Löscher W, Potschka H. Drug resistance in brain diseases and the role of drug efflux transporters. *Nature Reviews Neuroscience* 2005; **6**(8): 591-602.
330. Gex-Fabry M, Eap CB, Oneda B, Gervasoni N, Aubry J-M, Bondolfi G, *et al.* CYP2D6 and ABCB1 genetic variability: influence on paroxetine plasma level and therapeutic response. *Therapeutic drug monitoring* 2008; **30**(4): 474-482.
331. Kato M, Fukuda T, Serretti A, Wakeno M, Okugawa G, Ikenaga Y, *et al.* ABCB1 (MDR1) gene polymorphisms are associated with the clinical response to paroxetine in patients with major depressive disorder. *Progress in Neuro-Psychopharmacology and Biological Psychiatry* 2008; **32**(2): 398-404.
332. Nikisch G, Eap CB, Baumann P. Citalopram enantiomers in plasma and cerebrospinal fluid of ABCB1 genotyped depressive patients and clinical response: a pilot study. *Pharmacological research* 2008; **58**(5): 344-347.
333. Fukui N, Suzuki Y, Sawamura K, Sugai T, Watanabe J, Inoue Y, *et al.* Dose-dependent effects of the 3435 C> T genotype of ABCB1 gene on the steady-state plasma concentration of fluvoxamine in psychiatric patients. *Therapeutic drug monitoring* 2007; **29**(2): 185-189.

334. Sarginson JE, Lazzeroni LC, Ryan HS, Ershoff BD, Schatzberg AF, Murphy Jr GM. ABCB1 (MDR1) polymorphisms and antidepressant response in geriatric depression. *Pharmacogenetics and genomics* 2010; **20**(8): 467-475.
335. Lin K-M, Chiu Y-F, Tsai I-J, Chen C-H, Shen WW, Liu SC, *et al.* ABCB1 gene polymorphisms are associated with the severity of major depressive disorder and its response to escitalopram treatment. *Pharmacogenetics and Genomics* 2011; **21**(4): 163-170.
336. Singh A, Bousman C, Ng C, Byron K, Berk M. ABCB1 polymorphism predicts escitalopram dose needed for remission in major depression. *Translational psychiatry* 2012; **2**(11): e198.
337. Uhr M, Steckler T, Yassouridis A, Holsboer F. Penetration of amitriptyline, but not of fluoxetine, into brain is enhanced in mice with blood-brain barrier deficiency due to *mdr1a* P-glycoprotein gene disruption. *Neuropsychopharmacology* 2000; **22**(4): 380-387.
338. Doran A, Obach RS, Smith BJ, Hosea NA, Becker S, Callegari E, *et al.* The impact of P-glycoprotein on the disposition of drugs targeted for indications of the central nervous system: evaluation using the MDR1A/1B knockout mouse model. *Drug Metabolism and Disposition* 2005; **33**(1): 165-174.
339. Xie W-W, Zhang L, Wu R-R, Yu Y, Zhao J-P, Li L-H. Case-control association study of ABCB1 gene and major depressive disorder in a local Chinese Han population. *Neuropsychiatric Disease and Treatment* 2015; **11**: 1967-1971.
340. De Klerk O, Nolte I, Bet P, Bosker F, Snieder H, den Boer J, *et al.* ABCB1 gene variants influence tolerance to selective serotonin reuptake inhibitors in a large sample of Dutch cases with major depressive disorder. *The pharmacogenomics journal* 2013; **13**(4): 349-353.
341. Singh AB, Bousman CA, Ng CH, Byron K, Berk M. ABCB1 polymorphism predicts escitalopram dose needed for remission in major depression. *Transl Psychiatry* 2012; **2**: e198.
342. Guey LT, Kravic J, Melander O, Burt NP, Laramie JM, Lyssenko V, *et al.* Power in the phenotypic extremes: a simulation study of power in discovery and replication of rare variants. *Genetic epidemiology* 2011; **35**(4): 236-246.
343. Dolan ME, Newbold KG, Nagasubramanian R, Wu X, Ratain MJ, Cook EH, *et al.* Heritability and linkage analysis of sensitivity to cisplatin-induced cytotoxicity. *Cancer research* 2004; **64**(12): 4353-4356.
344. Hartford CM, Duan S, Delaney SM, Mi S, Kistner EO, Lamba JK, *et al.* Population-specific genetic variants important in susceptibility to cytarabine arabinoside cytotoxicity. *Blood* 2009; **113**(10): 2145-2153.

References

345. Bleibel WK, Duan S, Huang RS, Kistner EO, Shukla SJ, Wu X, *et al.* Identification of genomic regions contributing to etoposide-induced cytotoxicity. *Human genetics* 2009; **125**(2): 173-180.
346. Thase ME. Evaluating antidepressant therapies: remission as the optimal outcome. *J Clin Psychiatry* 2003; **64**(13): 1,478-425.
347. Judd LL. Major depressive disorder: longitudinal symptomatic structure, relapse and recovery. *Acta Psychiatrica Scandinavica* 2001; **104**(2): 81-83.
348. Kennedy BL, Schwab JJ, Morris RL, Beldia G. Assessment of state and trait anxiety in subjects with anxiety and depressive disorders. *Psychiatric Quarterly* 2001; **72**(3): 263-276.
349. Julian LJ. Measures of anxiety: State-Trait Anxiety Inventory (STAI), Beck Anxiety Inventory (BAI), and Hospital Anxiety and Depression Scale-Anxiety (HADS-A). *Arthritis care & research* 2011; **63**(S11): S467-S472.
350. Trajković G, Starčević V, Latas M, Leštarević M, Ille T, Bukumirić Z, *et al.* Reliability of the Hamilton Rating Scale for Depression: A meta-analysis over a period of 49years. *Psychiatry research* 2011; **189**(1): 1-9.
351. Smith R. The macrophage theory of depression. *Medical hypotheses* 1991; **35**(4): 298-306.
352. Maes M, Smith R, Simon S. The monocyte-T-lymphocyte hypothesis of major depression. *Psychoneuroendocrinology* 1995; **20**(2): 111-116.
353. Owen B, Eccleston D, Ferrier I, Young H. Raised levels of plasma interleukin-1 β in major and postviral depression. *Acta Psychiatrica Scandinavica* 2001; **103**(3): 226-228.
354. Penninx BW, Kritchovsky SB, Yaffe K, Newman AB, Simonsick EM, Rubin S, *et al.* Inflammatory markers and depressed mood in older persons: results from the Health, Aging and Body Composition study. *Biological psychiatry* 2003; **54**(5): 566-572.
355. Harrison NA, Brydon L, Walker C, Gray MA, Steptoe A, Critchley HD. Inflammation causes mood changes through alterations in subgenual cingulate activity and mesolimbic connectivity. *Biological psychiatry* 2009; **66**(5): 407-414.
356. Frenois F, Moreau M, O'Connor J, Lawson M, Micon C, Lestage J, *et al.* Lipopolysaccharide induces delayed FosB/DeltaFosB immunostaining within the mouse extended amygdala, hippocampus and hypothalamus, that parallel the expression of depressive-like behavior. *Psychoneuroendocrinology* 2007; **32**(5): 516-531.

357. Blackford JU, Avery SN, Cowan RL, Shelton RC, Zald DH. Sustained amygdala response to both novel and newly familiar faces characterizes inhibited temperament. *Social Cognitive and Affective Neuroscience* 2010; **6**(5): 621-629.
358. Inagaki TK, Muscatell KA, Irwin MR, Cole SW, Eisenberger NI. Inflammation selectively enhances amygdala activity to socially threatening images. *Neuroimage* 2012; **59**(4): 3222-3226.
359. Blair K, Shaywitz J, Smith BW, Rhodes R, Geraci M, Jones M, *et al.* Response to emotional expressions in generalized social phobia and generalized anxiety disorder: evidence for separate disorders. *American Journal of Psychiatry* 2008; **165**(9): 1193-1202.
360. Godbout JP, Moreau M, Lestage J, Chen J, Sparkman NL, O'Connor J, *et al.* Aging exacerbates depressive-like behavior in mice in response to activation of the peripheral innate immune system. *Neuropsychopharmacology* 2008; **33**(10): 2341-2351.
361. van den Biggelaar AH, Gussekloo J, de Craen AJ, Frölich M, Stek ML, van der Mast RC, *et al.* Inflammation and interleukin-1 signaling network contribute to depressive symptoms but not cognitive decline in old age. *Experimental gerontology* 2007; **42**(7): 693-701.
362. Lanquillon S, Krieg J, Bening-Abu-Shach U, Vedder H. Cytokine production and treatment response in major depressive disorder. *Neuropsychopharmacology* 2000; **22**(4): 370-379.
363. Nemeroff CB, Vale WW. The neurobiology of depression: inroads to treatment and new drug discovery. *Journal of Clinical Psychiatry* 2005; **66**: 5.
364. Miller A. Cytokine targets in the brain: impact on neurotransmitters and neurocircuits. *The FASEB Journal* 2014; **28**(1): 844.
365. Bluthé R-M, Walter V, Parnet P, Layé S, Lestage J, Verrier D, *et al.* Lipopolysaccharide induces sickness behaviour in rats by a vagal mediated mechanism. *Comptes rendus de l'Academie des sciences Serie III, Sciences de la vie* 1994; **317**(6): 499-503.
366. Luheshi GN, Bluthé R-M, Rushforth D, Mulcahy N, Konsman J-P, Goldbach M, *et al.* Vagotomy attenuates the behavioural but not the pyrogenic effects of interleukin-1 in rats. *Autonomic Neuroscience* 2000; **85**(1): 127-132.
367. Cottrell GT, Ferguson AV. Sensory circumventricular organs: central roles in integrated autonomic regulation. *Regulatory peptides* 2004; **117**(1): 11-23.
368. Vitkovic L, Konsman J, Bockaert J, Dantzer R, Homburger V, Jacque C. Cytokine signals propagate through the brain. *Molecular psychiatry* 2000; **5**(6): 604-615.

References

369. Banks WA. The blood–brain barrier in psychoneuroimmunology. *Immunology and allergy clinics of North America* 2009; **29**(2): 223-228.
370. Banks WA. Blood-brain barrier transport of cytokines: a mechanism for neuropathology. *Current pharmaceutical design* 2005; **11**(8): 973-984.
371. O'connor J, Lawson M, Andre C, Moreau M, Lestage J, Castanon N, *et al.* Lipopolysaccharide-induced depressive-like behavior is mediated by indoleamine 2, 3-dioxygenase activation in mice. *Molecular psychiatry* 2009; **14**(5): 511-522.
372. O'Connor JC, Lawson MA, André C, Briley EM, Szegedi SS, Lestage J, *et al.* Induction of IDO by bacille Calmette-Guerin is responsible for development of murine depressive-like behavior. *The Journal of Immunology* 2009; **182**(5): 3202-3212.
373. Zhu C-B, Blakely RD, Hewlett WA. The proinflammatory cytokines interleukin-1beta and tumor necrosis factor-alpha activate serotonin transporters. *Neuropsychopharmacology* 2006; **31**(10): 2121-2131.
374. Zhu C-B, Carneiro AM, Dostmann WR, Hewlett WA, Blakely RD. p38 MAPK activation elevates serotonin transport activity via a trafficking-independent, protein phosphatase 2A-dependent process. *Journal of Biological Chemistry* 2005; **280**(16): 15649-15658.
375. Morón JA, Zakharova I, Ferrer JV, Merrill GA, Hope B, Lafer EM, *et al.* Mitogen-activated protein kinase regulates dopamine transporter surface expression and dopamine transport capacity. *The Journal of neuroscience* 2003; **23**(24): 8480-8488.
376. Bierhaus A, Wolf J, Andrassy M, Rohleder N, Humpert PM, Petrov D, *et al.* A mechanism converting psychosocial stress into mononuclear cell activation. *Proceedings of the National Academy of Sciences* 2003; **100**(4): 1920-1925.
377. Müller N, Schwarz M, Dehning S, Douhe A, Cerovecki A, Goldstein-Müller B, *et al.* The cyclooxygenase-2 inhibitor celecoxib has therapeutic effects in major depression: results of a double-blind, randomized, placebo controlled, add-on pilot study to reboxetine. *Molecular psychiatry* 2006; **11**(7): 680-684.
378. Tying S, Gottlieb A, Papp K, Gordon K, Leonardi C, Wang A, *et al.* Etanercept and clinical outcomes, fatigue, and depression in psoriasis: double-blind placebo-controlled randomised phase III trial. *The Lancet* 2006; **367**(9504): 29-35.
379. Raison CL, Rutherford RE, Woolwine BJ, Shuo C, Schettler P, Drake DF, *et al.* A randomized controlled trial of the tumor necrosis factor antagonist infliximab for treatment-resistant depression: the role of baseline inflammatory biomarkers. *JAMA psychiatry* 2013; **70**(1): 31-41.

380. Brunello N, Alboni S, Capone G, Benatti C, Blom JM, Tascedda F, *et al.* Acetylsalicylic acid accelerates the antidepressant effect of fluoxetine in the chronic escape deficit model of depression. *International clinical psychopharmacology* 2006; **21**(4): 219-225.
381. Mendlewicz J, Kriwin P, Oswald P, Souery D, Alboni S, Brunello N. Shortened onset of action of antidepressants in major depression using acetylsalicylic acid augmentation: a pilot open-label study. *International clinical psychopharmacology* 2006; **21**(4): 227-231.
382. Merali Z, Brennan K, Brau P, Anisman H. Dissociating anorexia and anhedonia elicited by interleukin-1 β : antidepressant and gender effects on responding for "free chow" and "earned" sucrose intake. *Psychopharmacology* 2003; **165**(4): 413-418.
383. Simmons DA, Broderick PA. Cytokines, stressors, and clinical depression: augmented adaptation responses underlie depression pathogenesis. *Progress in Neuro-Psychopharmacology and Biological Psychiatry* 2005; **29**(5): 793-807.
384. Dunn AJ, Swiergiel AH, de Beaurepaire R. Cytokines as mediators of depression: what can we learn from animal studies? *Neuroscience & Biobehavioral Reviews* 2005; **29**(4): 891-909.
385. Capuron L, Raison CL, Musselman DL, Lawson DH, Nemeroff CB, Miller AH. Association of exaggerated HPA axis response to the initial injection of interferon-alpha with development of depression during interferon-alpha therapy. *American Journal of Psychiatry* 2003.
386. Pariante CM. Depression, stress and the adrenal axis. *Journal of neuroendocrinology* 2003; **15**(8): 811-812.
387. Swaab DF, Bao A-M, Lucassen PJ. The stress system in the human brain in depression and neurodegeneration. *Ageing research reviews* 2005; **4**(2): 141-194.
388. Holsboer F. Corticotropin-releasing hormone modulators and depression. *Current opinion in investigational drugs* 2003; **4**(1): 46-50.
389. Abler B, Seeringer A, Hartmann A, Grön G, Metzger C, Walter M, *et al.* Neural correlates of antidepressant-related sexual dysfunction: a placebo-controlled fMRI study on healthy males under subchronic paroxetine and bupropion. *Neuropsychopharmacology* 2011; **36**(9): 1837-1847.
390. Wang DJ, Chen Y, Fernández-Seara MA, Detre JA. Potentials and challenges for arterial spin labeling in pharmacological magnetic resonance imaging. *Journal of Pharmacology and Experimental Therapeutics* 2011; **337**(2): 359-366.
391. Sheline YI, Barch DM, Donnelly JM, Ollinger JM, Snyder AZ, Mintun MA. Increased amygdala response to masked emotional faces in depressed subjects resolves with antidepressant treatment: an fMRI study. *Biological psychiatry* 2001; **50**(9): 651-658.

References

392. Addington J, Saeedi H, Addington D. Facial affect recognition: a mediator between cognitive and social functioning in psychosis? *Schizophrenia research* 2006; **85**(1): 142-150.
393. Philippot P, Kornreich C, Blairy S, Baert I, Dulk AD, Bon OL, *et al.* Alcoholics' deficits in the decoding of emotional facial expression. *Alcoholism: Clinical and Experimental Research* 1999; **23**(6): 1031-1038.
394. Celani G, Battacchi MW, Arcidiacono L. The understanding of the emotional meaning of facial expressions in people with autism. *Journal of autism and developmental disorders* 1999; **29**(1): 57-66.
395. Button K, Lewis G, Penton-Voak I, Munafò M. Social anxiety is associated with general but not specific biases in emotion recognition. *Psychiatry research* 2013; **210**(1): 199-207.
396. Derntl B, Seidel EM, Kryspin-Exner I, Hasmann A, Dobmeier M. Facial emotion recognition in patients with bipolar I and bipolar II disorder. *British Journal of Clinical Psychology* 2009; **48**(4): 363-375.
397. Rubinow DR, Post RM. Impaired recognition of affect in facial expression in depressed patients. *Biological psychiatry* 1992; **31**(9): 947-953.
398. Carton JS, Kessler EA, Pape CL. Nonverbal decoding skills and relationship well-being in adults. *Journal of Nonverbal Behavior* 1999; **23**(1): 91-100.
399. Platt B, Kadosh KC, Lau JY. The role of peer rejection in adolescent depression. *Depression and anxiety* 2013; **30**(9): 809-821.
400. Bourke C, Douglas K, Porter R. Processing of facial emotion expression in major depression: a review. *Australian and New Zealand Journal of Psychiatry* 2010; **44**(8): 681-696.
401. Whalen PJ, Shin LM, Somerville LH, McLean AA, Kim H. Functional neuroimaging studies of the amygdala in depression. *Seminars in clinical neuropsychiatry* 2002; **7**(4): 234-242.
402. O'Connor M-F, Irwin MR, Wellisch DK. When grief heats up: pro-inflammatory cytokines predict regional brain activation. *Neuroimage* 2009; **47**(3): 891-896.
403. Demenescu LR, Kortekaas R, den Boer JA, Aleman A. Impaired attribution of emotion to facial expressions in anxiety and major depression. *PLoS One* 2010; **5**(12): e15058.
404. Kohler CG, Hoffman LJ, Eastman LB, Healey K, Moberg PJ. Facial emotion perception in depression and bipolar disorder: a quantitative review. *Psychiatry research* 2011; **188**(3): 303-309.

405. Dalili M, Penton-Voak I, Harmer C, Munafò M. Meta-analysis of emotion recognition deficits in major depressive disorder. *Psychological medicine* 2015; **45**(06): 1135-1144.
406. Frodl T, Scheuerecker J, Albrecht J, Kleemann AM, Müller-Schunk S, Koutsouleris N, *et al.* Neuronal correlates of emotional processing in patients with major depression. *The World Journal of Biological Psychiatry* 2009; **10**(3): 202-208.
407. Murphy SE, Norbury R, O'Sullivan U, Cowen PJ, Harmer CJ. Effect of a single dose of citalopram on amygdala response to emotional faces. *The British Journal of Psychiatry* 2009; **194**(6): 535-540.
408. Anand A, Li Y, Wang Y, Gardner K, Lowe MJ. Reciprocal effects of antidepressant treatment on activity and connectivity of the mood regulating circuit: an FMRI study. *The Journal of neuropsychiatry and clinical neurosciences* 2007; **19**(3): 274-282.
409. Fu CH, Williams SC, Cleare AJ, Brammer MJ, Walsh ND, Kim J, *et al.* Attenuation of the neural response to sad faces in major depression by antidepressant treatment: a prospective, event-related functional magnetic resonance imaging study. *Archives of general psychiatry* 2004; **61**(9): 877-889.
410. Arnone D, McKie S, Elliott R, Thomas EJ, Downey D, Juhasz G, *et al.* Increased amygdala responses to sad but not fearful faces in major depression: relation to mood state and pharmacological treatment. *American Journal of Psychiatry* 2012; **169**(8): 841-850.
411. Tao R, Calley CS, Hart J, Mayes TL, Nakonezny PA, Lu H, *et al.* Brain activity in adolescent major depressive disorder before and after fluoxetine treatment. *American Journal of Psychiatry* 2012; **169**(4): 381-388.
412. Godlewska B, Norbury R, Selvaraj S, Cowen P, Harmer C. Short-term SSRI treatment normalises amygdala hyperactivity in depressed patients. *Psychological medicine* 2012; **42**(12): 2609-2617.
413. Harmer CJ, de Bodinat C, Dawson GR, Dourish CT, Waldenmaier L, Adams S, *et al.* Agomelatine facilitates positive versus negative affective processing in healthy volunteer models. *Journal of Psychopharmacology* 2011; **25**(9): 1159-1167.
414. Harmer CJ, Dawson GR, Dourish CT, Favaron E, Parsons E, Fiore M, *et al.* Combined NK1 antagonism and serotonin reuptake inhibition: effects on emotional processing in humans. *Journal of Psychopharmacology* 2013; **27**(5): 435-443.
415. Pringle A, McCabe C, Cowen P, Harmer C. Antidepressant treatment and emotional processing: can we dissociate the roles of serotonin and noradrenaline? *Journal of Psychopharmacology* 2013; **27**(8): 719-731.

References

416. Domschke K, Dannlowski U, Hohoff C, Ohrmann P, Bauer J, Kugel H, *et al.* Neuropeptide Y (NPY) gene: impact on emotional processing and treatment response in anxious depression. *European Neuropsychopharmacology* 2010; **20**(5): 301-309.
417. Domschke K, Dannlowski U, Ohrmann P, Lawford B, Bauer J, Kugel H, *et al.* Cannabinoid receptor 1 (CNR1) gene: impact on antidepressant treatment response and emotion processing in major depression. *European Neuropsychopharmacology* 2008; **18**(10): 751-759.
418. Rosenblau G, Sterzer P, Stoy M, Park S, Friedel E, Heinz A, *et al.* Functional neuroanatomy of emotion processing in major depressive disorder is altered after successful antidepressant therapy. *Journal of Psychopharmacology* 2012; **26**(11): 1424-1433.
419. Dayan P, Balleine BW. Reward, motivation, and reinforcement learning. *Neuron* 2002; **36**(2): 285-298.
420. Takahashi YK, Roesch MR, Wilson RC, Toreson K, O'Donnell P, Niv Y, *et al.* Expectancy-related changes in firing of dopamine neurons depend on orbitofrontal cortex. *Nature neuroscience* 2011; **14**(12): 1590-1597.
421. Pedroni A, Koeneke S, Velickaite A, Jäncke L. Differential magnitude coding of gains and omitted rewards in the ventral striatum. *Brain research* 2011; **1411**: 76-86.
422. Haber SN, Knutson B. The reward circuit: linking primate anatomy and human imaging. *Neuropsychopharmacology* 2010; **35**(1): 4-26.
423. Grabenhorst F, Rolls ET. Value, pleasure and choice in the ventral prefrontal cortex. *Trends in cognitive sciences* 2011; **15**(2): 56-67.
424. Keedwell PA, Andrew C, Williams SC, Brammer MJ, Phillips ML. A double dissociation of ventromedial prefrontal cortical responses to sad and happy stimuli in depressed and healthy individuals. *Biological psychiatry* 2005; **58**(6): 495-503.
425. Kumar P, Waiter G, Ahearn T, Milders M, Reid I, Steele J. Abnormal temporal difference reward-learning signals in major depression. *Brain* 2008; **131**(8): 2084-2093.
426. Knutson B, Bhanji JP, Cooney RE, Atlas LY, Gotlib IH. Neural responses to monetary incentives in major depression. *Biological psychiatry* 2008; **63**(7): 686-692.
427. Pizzagalli DA, Holmes AJ, Dillon DG, Goetz EL, Birk JL, Ryan Bogdan A, *et al.* Reduced caudate and nucleus accumbens response to rewards in unmedicated individuals with major depressive disorder. *American Journal of Psychiatry* 2009; **166**(6): 702-710.

428. Gradin VB, Kumar P, Waiter G, Ahearn T, Stickle C, Milders M, *et al.* Expected value and prediction error abnormalities in depression and schizophrenia. *Brain* 2011; **134**(6): 1751-1764.
429. Surguladze S, Brammer MJ, Keedwell P, Giampietro V, Young AW, Travis MJ, *et al.* A differential pattern of neural response toward sad versus happy facial expressions in major depressive disorder. *Biological psychiatry* 2005; **57**(3): 201-209.
430. Robinson OJ, Cools R, Carlisi CO, Sahakian BJ, Drevets WC. Ventral striatum response during reward and punishment reversal learning in unmedicated major depressive disorder. *American Journal of Psychiatry* 2012; **169**(2): 152-159.
431. Tremblay LK, Naranjo CA, Graham SJ, Herrmann N, Mayberg HS, Hevenor S, *et al.* Functional neuroanatomical substrates of altered reward processing in major depressive disorder revealed by a dopaminergic probe. *Archives of general psychiatry* 2005; **62**(11): 1228-1236.
432. Pessiglione M, Seymour B, Flandin G, Dolan RJ, Frith CD. Dopamine-dependent prediction errors underpin reward-seeking behaviour in humans. *Nature* 2006; **442**(7106): 1042-1045.
433. Ossewaarde L, Verkes RJ, Hermans EJ, Kooijman SC, Urner M, Tendolkar I, *et al.* Two-week administration of the combined serotonin-noradrenaline reuptake inhibitor duloxetine augments functioning of mesolimbic incentive processing circuits. *Biological psychiatry* 2011; **70**(6): 568-574.
434. Dichter GS, Felder JN, Petty C, Bizzell J, Ernst M, Smoski MJ. The effects of psychotherapy on neural responses to rewards in major depression. *Biological psychiatry* 2009; **66**(9): 886-897.
435. Capuron L, Pagnoni G, Demetrashvili MF, Lawson DH, Fornwalt FB, Woolwine B, *et al.* Basal ganglia hypermetabolism and symptoms of fatigue during interferon- α therapy. *Neuropsychopharmacology* 2007; **32**(11): 2384-2392.
436. Capuron L, Pagnoni G, Drake DF, Woolwine BJ, Spivey JR, Crowe RJ, *et al.* Dopaminergic mechanisms of reduced basal ganglia responses to hedonic reward during interferon alfa administration. *Archives of general psychiatry* 2012; **69**(10): 1044-1053.
437. Eisenberger NI, Berkman ET, Inagaki TK, Rameson LT, Mashal NM, Irwin MR. Inflammation-induced anhedonia: endotoxin reduces ventral striatum responses to reward. *Biological psychiatry* 2010; **68**(8): 748-754.
438. Keedwell PA, Andrew C, Williams SC, Brammer MJ, Phillips ML. The neural correlates of anhedonia in major depressive disorder. *Biological psychiatry* 2005; **58**(11): 843-853.

References

439. Collins PY, Patel V, Joestl SS, March D, Insel TR, Daar AS, *et al.* Grand challenges in global mental health. *Nature* 2011; **475**(7354): 27-30.
440. Rook GA, Raison CL, Lowry CA. Can we vaccinate against depression? *Drug discovery today* 2012; **17**(9): 451-458.
441. McMahon FJ, Insel TR. Pharmacogenomics and personalized medicine in neuropsychiatry. *Neuron* 2012; **74**(5): 773-776.
442. Choi SM, Liu H, Chaudhari P, Kim Y, Cheng L, Feng J, *et al.* Reprogramming of EBV-immortalized B-lymphocyte cell lines into induced pluripotent stem cells. *Blood* 2011; **118**(7): 1801-1805.
443. Rajesh D, Dickerson SJ, Yu J, Brown ME, Thomson JA, Seay NJ. Human lymphoblastoid B-cell lines reprogrammed to EBV-free induced pluripotent stem cells. *Blood* 2011; **118**(7): 1797-1800.
444. Bennett CM, Miller MB. How reliable are the results from functional magnetic resonance imaging? *Annals of the New York Academy of Sciences* 2010; **1191**(1): 133-155.
445. Plichta MM, Schwarz AJ, Grimm O, Morgen K, Mier D, Haddad L, *et al.* Test–retest reliability of evoked BOLD signals from a cognitive–emotive fMRI test battery. *Neuroimage* 2012; **60**(3): 1746-1758.
446. Mori S, Zhang J. Principles of diffusion tensor imaging and its applications to basic neuroscience research. *Neuron* 2006; **51**(5): 527-539.
447. Tost H, Bilek E, Meyer-Lindenberg A. Brain connectivity in psychiatric imaging genetics. *Neuroimage* 2012; **62**(4): 2250-2260.
448. Vogt N. Neuroscience: fMRI goes individual. *Nature Methods* 2015; **12**(12): 1112-1113.
449. Finn ES, Shen X, Scheinost D, Rosenberg MD, Huang J, Chun MM, *et al.* Functional connectome fingerprinting: identifying individuals using patterns of brain connectivity. *Nature neuroscience* 2015; **18**(11): 1664-1671.

Appendix

Lab Equipment

Centrifuge 5415 D	Eppendorf, Germany
Centrifuge 5415 R	Eppendorf, Germany
Centrifuge 5702	Eppendorf, Germany
Centrifuge 5804	Eppendorf, Germany
Centrifuge 5810 R	Eppendorf, Germany
CO2 incubator	Binder, Germany
FACSCalibur	BD Biosciences, Germany
Hybridization oven	Agilent Technologies, USA
Inverse light microscope Axiovert 40C	Zeiss, Germany
Laminar flow cabinet HERAsafe	Heraeus, Germany
LightCycler® 480	Roche, Germany
LightCycler® 480 II	Roche, Germany
Mastercycler gradient	Eppendorf, Germany
Micropipettes	Eppendorf, Germany
MixMate plate stirrer	Eppendorf, Germany
MS3 Basic shaker	IKA®, Germany
Multipette® plus	Eppendorf, Germany
NanoDrop 1000 spectrophotometer	Thermo Scientific
Pipetboy	Integra, Switzerland
Safire ² microplate reader	Tecan, Switzerland
SureScan Microarray Scanner	Agilent Technologies, USA
TC20™ cell counter	BIO RAD, USA
Water bath	GFL, Germany

Appendix

Lab disposables / Labware

Pipette tips, sterile with filter	Sarstedt, Germany
Flat-bottom 96-well sterile plates	Becton Dickinson, USA
Cell culture flasks T25, T75	Sarstedt, Germany
Combitips plus	Eppendorf, Germany
Cryo Tube vials	Nunc, Denmark
DMSO safe Acrodisc syringe filters	PALL, Germany
FACS tubes	VWR, Germany
Glass vials, brown	Agilent Technologies, Germany
LightCycler 480 multiwell plate 96, white	Roche, Germany
Microtubes 1.5 ml	Thermo Scientific, USA
Microtubes 0.2 ml	Thermo Scientific, USA
Mr. Frosty™ Freezing Container	Thermo Scientific, USA
Pipettes (5-50 ml), sterile	Sarstedt, Germany
Polystyrene round-bottom tube (5 ml)	Becton Dickinson Falcon, Germany
Syringes Omnifix 3 ml	B. Braun, Melsungen, Germany
Tissue culture flasks T25	TPP, Switzerland
Tissue culture flasks T75	TPP, Switzerland
Tissue culture test plates 12 wells	TPP, Switzerland

Chemicals, drugs, solutions and media

Agarose standard	Roth, Germany
2-Mercaptoethanol	Sigma Aldrich, USA
Biocoll Separating Solution	Biochrom, Germany
Citalopram hydrobromide	Sigma Aldrich, USA
Cyclosporine A	Sigma Aldrich, USA
DMSO	Sigma-Aldrich, USA
DNA loading dye (6 x)	Thermo Scientific, Germany

Dulbecco's PBS (1x)	PAA, Germany
Ethanol 96%	Merck, Germany
Ethidium bromide	Sigma Aldrich, USA
FACS Flow	BD Bioscience, Germany
FACS Clean	BD Bioscience, Germany
FACS Rinse	BD Bioscience, Germany
Fetal Bovine Serum	Biochrom, Germany
Fluoxetine hydrochloride	Sigma Aldrich, USA
Gene Ruler 50 bp DNA Ladder	Thermo Scientific, USA
Imipramine hydrochloride	Sigma Aldrich, USA
Interferon beta 1a (Rebif®)	Merck, Germany
L-glutamine	Biowest, France
Penicillin/Streptomycin	Biowest, France
RPMI 1640	Biowest, France
Sodium chloride	Carl Roth GmbH, Germany

Kits

AllPrep RNA/DNA Mini Kit	Qiagen, Germany
Click-iT® EdU Alexa Fluor® 647 Flow Cytometry Assay Kit	Life technologies, USA
MycoAlert™ Plus Mycoplasma Detection Kit	Lonza, USA
QiaShredder	Qiagen, Germany
QuantiTect SYBR® Green PCR Kit	Qiagen, Germany
SurePrint G3 Human Gene Expression 8x60K Microarray Kit	Agilent Technologies, USA
Transcriptor First Strand cDNA Synthesis Kit	Roche, Germany
Tritest™ Kit	Becton Dickinson, Germany

STAR*D cell lines

	cell line	anxious depression	sex	age	citalopram dose [mg]	QJDS						
						week 0	week 2	week 4	week 6	week 9	week 12	week 14
Non-Responder	396613	Yes	f	47	10	21	13	13	16			
	482572	Yes	m	43	20	24	23	22	10	18		
	14951	Yes	m	53	20	19	15	19		10	14	
	15100	No	m	38	10	17	15	14	10		10	
	14754	No	f	49	20	23	11	13	13	5	8	
	15920	Yes	m	61	20	22	19	21	18	19	18	
	566271	No	f	38	20	16	13	15	11	13		
	18132	No	m	32	20	15	17	17	17			
	232816	Yes	m	63	10	17	16	14	18	19	21	
	407004	Yes	m	56	20	14	13	15	15			
	279249	No	m	52	20	19	15	18	15	17		
	17326	Yes	m	43	20	21	11	11	8			
	14605	No	m	52	20	19	20	20	16	20		
	402264	Yes	f	24	20	22	17	19				
	521742	Yes	f	42	20	18		18	6	16	10	9
	368252	No	f	55	40	15		6	21			
	301611	No	f	52	20	14	18	17	12			
	592780	Yes	m	55	20	16	13	14	14		16	
	613529	Yes	f	52	20	19	19	19	19	19		
	635406	Yes	m	56	20	21	19	7	14			
478406	No	f	55	10	18	12	15	17				
437434	No	m	42	20	16	17	15	18				
572045	Yes	m	57	20	20	13	15	8	13			
578879	Yes	f	60	20	22	14	13	14	14			
684462	Yes	f	43	20	24	20						
Responder	367664	Yes	f	27	20	19	17	13	6	0	0	
	375024	Yes	m	53	10	15	14	17	9	7	4	
	14132	No	m	28	20	16	3	6	2	1	2	
	755591	Yes	f	54	20	21	19	14	2	2	15	1
	443508	Yes	m	42	20	23	22	12	6	5		2
	311634	No	m	70	20	15	8	5	2			
	15269	Yes	f	66	20	16	3	10	4	3	4	5
	14267	Yes	f	53	20	16	13	9	1	2	0	
	17853	Yes	m	32	20	20	9	6	9	7	2	
	362372	No	f	42	5	17	6	10	11		1	
	17827	Yes	m	55	20	13		8		4	6	
	234078	Yes	f	48	10	17	12	6	3	3		
	16718	Yes	f	38	20	20	12	9	6	4	2	
	14451	Yes	f	26	10	12	11	8	6	2	1	
	466830	No	f	68	10	16	9	7	5	2	1	
	330833	No	m	44	20	15	16	3	3	4	0	
	352423	No	f	48	20	17	8		3	3		1
	409700	No	f	65	10	12	8	5	5	2	1	
	323701	No	m	28	20	16	8	9	7	4	4	
	510496	Yes	f	60	20	18	19	9	8	4		
400643	No	f	35	20	15	12	10	4	3	4		
411724	Yes	m	69	10	19	13	6	7	4	5		
17563	No	m	53	20	13	11	13	13	10		7	
546797	Yes	f	49	20	18	14	9	11	8	3		
550878	Yes	f	54	20	23	21	16	7	5	3		

List of Publications

Research articles

J Breitfeld, C Scholl, M Steffens, Gonzalo Laje, Julia Stingl (2017): „Gene expression and proliferation biomarkers for antidepressant treatment resistance.” *Translational Psychiatry* (accepted)

J Breitfeld, C Scholl, M Steffens, K Brandenburg, K Probst-Schendzielorz, O Efimkina, D Gurwitz, M Ising, F Holsboer, S Lucae, J Stingl (2016): “Proliferation rates and gene expression profiles in human lymphoblastoid cell lines from patients with depression characterized in response to antidepressant drug therapy.” *Translational Psychiatry* - 6.11, e950

Congress talks

J Breitfeld, C Scholl, J Stingl (2014): “Antidepressant-mediated modulation of cell proliferation.” *Retreat on Biomedical Research of the Paul Ehrlich Institute* (Heidelberg, Germany)

Poster presentations

J Breitfeld, M Steffens, M Coenen, G Hartmann, R Viviani, J Stingl, C Coch (2016): “Functional magnetic resonance imaging depicts interferon beta induced sickness behaviour in healthy volunteers.” *Annual Meeting of the Organization for Human Brain Mapping (OHBM)* (Geneva, Switzerland)

R Viviani, L Dommès, J Breitfeld, A Paul, M Steffens, K Kaumanns, J Stingl, P Beschoner (2016): “Dissociation of neural substrates of temporal difference and mean reward rates in a foraging task.” *Annual Meeting of the Organization for Human Brain Mapping (OHBM)* (Geneva, Switzerland)

L Dommès, M Steffens, J Breitfeld, A Paul, K Kaumanns, J Stingl, P Beschoner, R Viviani (2016): “The neural correlates of reward cues and mean reward rates in the human brain: motivational and

attentional effects in a foraging task” *Meeting of the Austrian Psychological Society* (Innsbruck, Austria)

J Breitfeld, C Scholl, J Stingl (2015): “Antidepressant-mediated modulation of lymphoblastoid cell line proliferation reveals potential expression biomarkers.” *Annual Meeting of the German Society of Neurogenetics* (Bonn, Germany)

R Viviani, L Dommes, M Steffens, J Breitfeld, A Paul, J Stingl, P Beschoner (2015): “Dissociation of signals of changes in the expectation of reward and mean reward rates from the temporal difference learning model in the human brain.” *International Conference on Brain Informatics & Health (BIH)* (London, United Kingdom)

J Breitfeld, A Paul, R Viviani, J Stingl (2015): “Use of functional Magnetic Resonance Imaging in pharmacogenomics to study affective disorders: A pilot study” *Retreat on Biomedical Research of the Paul Ehrlich Institute* (Heidelberg, Germany)

Acknowledgements

I would like to express my sincere gratitude to Prof. Julia Stingl for accepting me into her working group to carry out my PhD studies. I thank her very much for the guidance and her expertise during the last years.

I would also like to thank Prof. Klaus Mohr for being the second member of the examining committee of my thesis as well as Prof. Gerd Bendas and Prof. Tony Stöcker for completing the examining committee.

I extend my appreciation to Dr. Catharina Scholl for her manifold support and the constructive ideas towards my work. Many thanks also to Dr. Roberto Viviani for the introduction to MRI and his help in analyzing the fMRI data. My sincere appreciation is extended to Dr. Michael Steffens and Dr. Florian Engel for their expertise in statistical and microarray question, respectively.

I would also like to thank our cooperation partners from the Institute of Clinical Chemistry and Clinical Pharmacology for the opportunity to collaborating in this interesting clinical study. Furthermore, I wish to express my gratitude to the colleagues from the German Centre for Neurodegenerative Diseases (DZNE) for the training on MRI and their support during this study. Additionally, I would like to thank the members of the PADRE ERA-NET project.

My deepest gratitude is extended to all members of the Research Department of the German Federal Institute for Drugs and Medical Devices for the enjoyable working atmosphere and the frequent challenging extracurricular activities. Especially, I would like to highlight my office colleague and friend Vivien Hichert for her ongoing optimism and encouragement which always brightened my days.

I would also like to extend my heartfelt thanks to my fiancée Plamena Yordanova, who was a great support in any situation during the last years.

Selbstständigkeitserklärung

Hiermit versichere ich an Eides statt, die vorliegende Dissertation mit dem Thema „**Identification of Potential Biomarkers for Depressive Disorders**“ persönlich, selbständig und ohne Benutzung anderer als der angegebenen Hilfsmittel angefertigt zu haben. Die aus anderen Quellen direkt oder indirekt stammenden Daten und Konzepte wurden unter Angabe der Quelle kenntlich gemacht. Ich habe keine anderen als die im Literaturverzeichnis angeführten Quellen benutzt und sämtliche Textstellen oder Bilder, die aus veröffentlichten Schriften entnommen wurden, als solche gekennzeichnet. Ebenfalls versichere ich, dass für die Erstellung der vorgelegten Arbeit keine fremde, entgeltliche Hilfe in Anspruch genommen wurde.

Jörg Breitfeld